ISSN 0021-3438 (Print)
ISSN 2412-8783 (Online)

IZVESTIYA
NON-FERROUS METALLURGY

Vol. 31, No. 3, 2025

Scientific and Technical Journal
Founded in 1958
4 Issues per year

ИЗВЕСТИЯ ВУЗОВ
ЦВЕТНАЯ МЕТАЛЛУРГИЯ

Том 31, № 3, 2025

Научно-технический журнал
Основан в 1958 г.
Выходит 4 раза в год

ISSN 0021-3438 (Print)
ISSN 2412-8783 (Online)

IZVESTIYA NON-FERROUS METALLURGY

Vol. 31, No. 3
2025

Scientific and Technical Journal Founded in 1958 4 Issues per year http://cvmet.misis.ru

Journal is included into the List of the peer-reviewed scientific publications recommended by the Highest Attestation Commission of the Ministry of Education and Science of the Russian Federation for publishing the results of doctoral and candidate dissertations

Abstracting/Indexing: Russian Science Citation Index (RSCI), Chemical Abstracts (Online), INIS, OCLC ArticleFirst, Ulrich's Periodicals Directory, VINITI Database (Abstract Journal)

Founder

National University of Science and Technology "MISIS"
Address: 1 Bld, 4 Leninskiy Prosp., Moscow 119049, Russia
http://www.misis.ru

Editorial Staff

Address: NUST MISIS, 1 Bld, 4 Leninskiy Prosp., Moscow 119049, Russia
Phone: +7 (495) 638-45-35
E-mail: izv.vuz@misis.ru

Certificate of registration No. 015842 (13.03.1997)
Re-registration PI No. ФС77-79229 (25.09.2020)

Subscription: Ural-Press Agency

Leading Editor – O.V. Sosnina
Executive Editor – A.A. Kudinova
Layout Designer – E.A. Legkaya

Signed print 29.09.2025. Format 60×90 1/8.
Offset paper No. 1. Digital printing. Quires 10,5
Order 23091. Free price

Printed in the printing house of the MISIS Publish House
1 Bld, 4 Leninskiy Prosp., Moscow 119049, Russia. Phone/fax: +7 (499) 236-76-17

ISSN 0021-3438 (Print)
ISSN 2412-8783 (Online)

ИЗВЕСТИЯ ВУЗОВ
ЦВЕТНАЯ МЕТАЛЛУРГИЯ

Том 31, № 3
2025

Научно-технический журнал Основан в 1958 г. Выходит 4 раза в год http://cvmet.misis.ru

Журнал включен в Перечень рецензируемых научных изданий, рекомендованных ВАК Минобрнауки РФ для публикации результатов диссертаций на соискание ученых степеней

Журнал включен в базы данных: Russian Science Citation Index (RSCI), Chemical Abstracts (Online), INIS, OCLC ArticleFirst, Ulrich's Periodicals Directory, РИНЦ, БД/РЖ ВИНИТИ

Учредитель

ФГАОУ ВО Национальный исследовательский технологический университет «МИСИС»
Адрес: 119049, г. Москва, Ленинский пр-т, 4, стр. 1
http://www.misis.ru

Редакция журнала

Адрес: 119049, г. Москва, Ленинский пр-т, 4, стр. 1, НИТУ МИСИС
Тел.: +7 (495) 638-45-35
E-mail: izv.vuz@misis.ru

Свидетельство о регистрации № 015842 от 13.03.1997 г.
Перерегистрация ПИ № ФС77-79229 от 25.09.2020 г.

Подписка: Агентство «Урал-пресс»

Ведущий редактор – О.В. Соснина
Выпускающий редактор – А.А. Кудинова
Дизайн и верстка – Е.А. Легкая

Подписано в печать 29.09.2025. Формат 60×90 1/8.
Бум. офсетная № 1. Печать цифровая. Усл. печ. л. 10,5
Заказ 23091. Цена свободная

Отпечатано в типографии Издательского Дома МИСИС
119049, г. Москва, Ленинский пр-т, 4, стр. 1. Тел./факс: +7 (499) 236-76-17

CONTENTS

СОДЕРЖАНИЕ

95 Years of the Department of Non-Ferrous Metallurgy at UrFU

The Department of Non-Ferrous Metallurgy of Ural Federal University celebrates its 95th anniversary in 2025. Founded in 1930 by Vasily Ivanovich Smirnov (1899–1972), later Professor, Doctor of Technical Sciences, and Academician of the Academy of Sciences of the Kazakh SSR, the department has become one of Russia's leading centers of research and education in metallurgy. Over its history, it has trained more than 2000 engineers, bachelors, and masters (including over 100 international graduates), along with 140 Candidates and 24 Doctors of Technical Sciences.

Research and scientific legacy

Since the 1930s, the department has developed a strong research tradition in the field of "Complex Utilization of Raw Materials". Its studies have focused on the metallurgy of copper, nickel, cobalt, zinc, as well as precious and rare metals, with many research outcomes successfully implemented in industrial practice.

Professor V.I. Smirnov led the department for 40 years. A prominent scientist, engineer, and educator, he authored more than 350 articles, about 40 monographs and textbooks, and mentored hundreds of engineers and dozens of postgraduate researchers. His contributions earned him election as a full member of the Academy of Sciences of the Kazakh SSR and the honorary title Honored Scientist and Engineer of the RSFSR.

Period of expansion (1971–1988)

From 1971 to 1988, the department was chaired by Professor I.F. Khudyakov, a 1944 graduate and veteran of the World War II. Under his leadership, laboratories in pyrometallurgy and hydrometallurgy were modernized, new instrumental analysis methods and computing technologies were introduced, and student research activity intensified. Research into the processing of secondary raw materials expanded significantly. Notable academic contributions of this period include Hydrometallurgy of Copper (1974), Metallurgy of Copper, Nickel, and Cobalt (2nd edition, 1977), Technology of Secondary Metals (1981), Thermodynamics and Kinetics of Hydrometallurgical Processes (1986), and Metallurgy of Secondary Heavy Non-Ferrous Metals (1987).

Professor Khudyakov also served as Vice-Rector for Research (1968–1978), was awarded the title Honored Scientist and Engineer of the RSFSR (1977), and received the USSR Council of Ministers Prize (1985).

Leadership of Professor S.S. Naboychenko (1988–2018)

From 1988 to 2018, the department was led by Professor Sergey Sergeyevich Naboychenko, a 1963 graduate, Doctor of Technical Sciences, and Corresponding Member of the Russian Academy of Sciences in the field of "Physical Chemistry and Technology of Inorganic Materials" (2000).

Professor Naboychenko is a two-time government laureate of the Russian Federation Prize in Education (2000, 2005), Honored Scientist and Engineer of the Russian Federation (1992), and Honorary Worker of Science and Higher Education (Mongolia, 1988). His international recognition includes honorary doctorates from Mongolian Technical University (1992) and Orenburg State Technical University (1998), as well as membership in the American Society for Metals Engineers since 1995. He has also received the RAS I.P. Bardin Prize (2016), the Governor of Sverdlovsk Region Prize (2016), and numerous state and professional honors, including the Orders "For Services to the Fatherland" (III and IV Class).

Alongside his scientific work, Professor Naboychenko played a major role in academic governance, serving as Rector of USTU-UPI (1986–2007), Chairman of the Council of Rectors of Sverdlovsk Region and the Ural Federal District, and Vice-President of the Russian Union of Rectors.

Scientific school and research areas

The Department of Non-Ferrous Metallurgy has established a recognized scientific school, "Metallurgy of Non-Ferrous Metals", dedicated to solving problems of extracting and processing non-ferrous metals from both ore and technogenic raw materials:

— pyrometallurgical and autogenous technologies;
— autoclave processes;
— sorption technologies.

The department maintains postgraduate and doctoral programs in specialty 2.6.2 "Metallurgy of Ferrous, Non-Ferrous, and Rare Metals". In the last de-

cade alone, 44 full-time doctoral students and 8 external candidates have been trained, resulting in 7 doctoral and 30 candidate defenses.

Academic and industrial contributions

The department houses advanced laboratories in hydrometallurgy, pyrometallurgy, autoclave and sorption processes, secondary and technogenic raw material processing, physicochemical analysis, computer modeling, and mineral beneficiation.

Over its history, the department has published more than 80 textbooks and monographs, and over 1000 scientific articles. For their comprehensive contributions to metallurgy education, faculty members (S.S. Naboychenko, I.F. Khudyakov, S.V. Karelov, A.P. Doroshkevich, N.G. Ageev, and S.E. Klein) received the Government of the Russian Federation Prize in Education. Staff have carried out more than 300 research projects and obtained over 170 USSR author's certificates and Russian patents, participating in more than 10 state scientific and technical programs.

Today and the future

The department continues to uphold the traditions established by Professors Smirnov, Khudyakov, and Naboychenko: dedication, responsibility, strong ties with industry, and the pursuit of advanced scientific directions. Collaborations with universities in Kazakhstan, Kyrgyzstan, Mongolia, and Uzbekistan are being strengthened.

With the Urals remaining a global leader in non-ferrous metallurgy and possessing significant reserves of both ore and secondary raw materials, the department looks to the future with a focus on training highly qualified scientific personnel, conducting fundamental research, and deepening its industrial partnerships.

The pride of the Department remains its graduates.

Happy Anniversary to the Department of Non-Ferrous Metallurgy, UrFU!

Head of the Department S.V. Mamyachenkov

UDC 621.365.2:669.2/8
https://doi.org/10.17073/0021-3438-2025-3-7-15

Research article
Научная статья

Influence of high-temperature oxidation kinetics of copper on the electrical properties of the melt

S.I. Kholod[1,3], **V.P. Zhukov**[2], **S.V. Mamyachenkov**[3], **V.V. Rogachev**[3]

[1] **Technical University of UMMC**
3 Uspenskiy Prosp., Sverdlovsk reg., Verkhnyaya Pyshma 624091, Russia

[2] **JSC "Uralmekhanobr"**
87 Khokhryakova Str., Ekaterinburg 620144, Russia

[3] **Ural Federal University n.a. the First President of Russia B.N. Yeltsin**
19 Mira Str., Ekaterinburg 620002, Russia

✉ Sergey I. Kholod (hsi503@yandex.ru)

Abstract: The kinetics of high-temperature oxidation of copper of various chemical compositions by gaseous oxygen follows a parabolic rate law within the temperature range of 350–1050 °C. For specialists engaged in the theory and practice of fire refining, of particular interest is the kinetics of copper oxidation over a broader temperature interval of 350–1160 °C. Within this range, the processes include oxidation of solid copper and its melting, oxidation of liquid copper by oxygen introduced into the melt, oxygen solubility in copper, and slag formation. The duration of high-temperature interaction between copper and oxygen has a considerable effect on both the technical and economic indicators of anode smelting and the electrical properties of copper. Therefore, investigating the kinetics of high-temperature oxidation of copper and its influence on the electrical properties of the metal is essential for the optimal organization of fire refining. In the temperature range of 1100–1200 °C, copper oxidation occurs predominantly due to oxygen introduced into the melt with air. The copper(I) oxide formed migrates from the zone of direct contact with gaseous oxygen into the depth of the melt with lower oxygen concentration, where it dissociates into copper and oxygen, thus increasing oxygen concentration in the melt. Overoxidation of copper and excessive saturation of the anode metal with gases lead to its transfer into slag in the form of oxides, to excessive consumption of resources and refractory materials, and to a deterioration of the electrical properties of the metal. To identify optimal oxidation modes and to assess the influence of copper oxidation kinetics on the electrical properties of the melt, a comparative analysis was conducted of the kinetic patterns of oxidation of solid and liquid copper of various chemical compositions under identical experimental conditions, using differential thermogravimetric analysis (DTA) and by surface blowing of the copper melt with an air mixture. The results show that copper samples oxidize at nearly the same rate and that the presence of impurities does not affect the process. All oxygen intended for copper (I) oxide formation dissolves in copper up to the thermodynamic limit (up to 12 % Cu_2O). It was established that oxygen concentrations in the melt above 0.06% adversely affect the electrical properties of copper.

Keywords: kinetics of high-temperature oxidation, blister copper, anode copper, fire refining of copper, oxygen concentration, electrical resistivity of the melt.

For citation: Kholod S.I., Zhukov V.P., Mamyachenkov S.V., Rogachev V.V. Influence of high-temperature oxidation kinetics of copper on the electrical properties of the melt. *Izvestiya. Non-Ferrous Metallurgy.* 2025;31(3):7–15. https://doi.org/10.17073/0021-3438-2025-3-7-15

Влияние кинетики высокотемпературного окисления меди на электротехнические свойства расплава

С.И. Холод[1,3], **В.П. Жуков**[2], **С.В. Мамяченков**[3], **В.В. Рогачев**[3]

[1] **Технический университет УГМК**
Россия, 624091, Свердловская обл., г. Верхняя Пышма, Успенский пр-т, 3

[2] **АО «Уралмеханобр»**
Россия, 620144, г. Екатеринбург, ул. Хохрякова, 87

[3] **Уральский федеральный университет имени первого Президента России Б.Н. Ельцина**
Россия, 620002, г. Екатеринбург, ул. Мира, 19

✉ Сергей Иванович Холод (hsi503@yandex.ru)

Аннотация: Кинетика высокотемпературного окисления меди различного химического состава кислородом газовой фазы протекает по параболическому закону окисления в температурном интервале 350–1050 °С. Для специалистов, занимающихся теорий и практикой огневого рафинирования, интересна кинетика высокотемпературного окисления меди в более широком температурном диапазоне 350–1160 °С, в пределах которого осуществляются окисление твердой меди и ее плавление, окисление жидкой меди кислородом воздуха, вводимого в расплав, растворимость в ней кислорода, процесс шлакообразования. Продолжительность высокотемпературного взаимодействия меди с кислородом оказывает большое влияние на технико-экономические показатели анодной плавки и электротехнические свойства меди. Поэтому исследование кинетики высокотемпературного окисления меди и влияния ее на электротехнические свойства металла имеет принципиальное значение для оптимальной организации огневого рафинирования. В температурном интервале 1100–1200 °С окисление меди осуществляется преимущественно за счет кислорода воздуха, вводимого в расплав. Образовавшийся оксид меди (I) перемещается из зоны непосредственного контакта с газообразным кислородом в глубину расплава с низкой концентрацией кислорода и диссоциирует на медь и кислород, что способствует повышению концентрации кислорода в расплаве. Переокисление меди и чрезмерное насыщение анодного металла газами приводят к переводу ее в шлак в виде оксидов, перерасходу материальных ресурсов и огнеупорных материалов и оказывают отрицательное влияние на электротехнические свойства металла. Для поиска оптимальных режимов окисления и оценки влияния кинетики окисления меди на электротехнические свойства расплава проведен сопоставимый анализ кинетических закономерностей окисления твердой и жидкой меди различного химического состава, полученной в одинаковых условиях эксперимента, методом дифференциально-термогравиметрического анализа (ДТА) и путем поверхностного обдува воздушной смесью медного расплава. Проведенные исследования показали, что образцы меди окисляются практически с одинаковой скоростью и наличие примесей не влияет на этот процесс. Весь кислород, предназначенный для образования оксида меди (I), растворяется в нем до предела термодинамического ограничения (до 12 % Cu_2O). Установлено, что наличие кислорода в расплаве больше 0,06 % отрицательно влияет на электротехнические свойства меди.

Ключевые слова: кинетика высокотемпературного окисления, черновая медь, анодная медь, огневое рафинирование меди, концентрация кислорода, электросопротивление расплава.

Для цитирования: Холод С.И., Жуков В.П., Мамяченков С.В., Рогачев В.В. Влияние кинетики высокотемпературного окисления меди на электротехнические свойства расплава. *Известия вузов. Цветная металлургия*. 2025;31(3):7–15.

https://doi.org/10.17073/0021-3438-2025-3-7-15

Introduction

The kinetics of high-temperature oxidation of copper by gaseous oxygen was the subject of extensive theoretical and practical research in the second half of the 20th century. Domestic and international studies examined in detail the mechanisms of oxidation of copper of various chemical compositions. A parabolic rate law for oxidation was established in the temperature interval of 350—1050 °C, conventionally divided into three ranges: low-temperature (350—550 °C), intermediate (550—850 °C), and high-temperature (850—1050 °C) [1]. For specialists engaged in the theory and practice of fire refining, the oxidation kinetics of copper in the wider temperature interval of 350—1170 °C are of particular interest. Within this range, the fol-

lowing processes occur: oxidation of solid copper (in a furnace oxidizing atmosphere with an oxidizer excess coefficient $\alpha = 1.1 \div 1.15$), melting of copper, oxidation of liquid copper by oxygen from the air introduced into the melt, dissolution of oxygen in the melt, and slag formation.

The duration of high-temperature interaction between copper and oxygen has a considerable effect on the technical and economic indicators of anode smelting and on the electrical properties of the metal. Therefore, investigation of the kinetics of this process and its effect on the electrical properties of copper is of fundamental importance for the optimal organization of fire refining.

Studies [1; 2] have shown that impurities in copper exert different effects on the oxidation rate. These effects are present in the low- and intermediate-temperature ranges, while in the high-temperature range the oxidation rates of copper of different purities are practically identical [1]. In general, the kinetic behavior of the process depends on the formation of a copper (I) oxide film on the surface of solid copper. In the high-temperature interval (600—1050 °C), it is mainly governed by the growth of the copper(I) oxide phase, limited by the oxygen partial pressure (P_{O_2}).

At 1100—1200 °C, copper oxidation proceeds predominantly by oxygen from the air introduced into the melt:

$$4Cu + O_2 = 2Cu_2O.$$

The Cu_2O formed migrates from the zone of direct contact with gaseous oxygen into the deeper layers of the melt, where the oxygen concentration is lower. The direction of reaction (1) then reverses: Cu_2O dissolves in the copper melt, thereby increasing the concentration of O_2 in the melt. In this case, the kinetic patterns of high-temperature oxidation of copper are limited by the transfer of copper into slag when the melt is saturated with oxygen (1.4 %) up to 12.4 % Cu_2O.

Overoxidation of copper and excessive oxygen saturation of the melt result in transfer of the metal into slag in the form of oxides, leading to excessive consumption of materials and refractories and to deterioration of the electrical properties of the metal.

The aim of the present study was to carry out a comparative analysis of the kinetic patterns of oxidation of solid and liquid copper of different chemical compositions, obtained under identical experimental conditions and by surface blowing of the copper melt with an air mixture, as well as to evaluate the degree of oxygen solubility in liquid copper and its influence on the electrical properties of the melt, particularly at oxygen concentrations above 0.08 wt. %.

Methods

The comparison of the kinetic patterns of copper oxidation was carried out using simultaneous thermogravimetric and differential scanning calorimetry (TG—DSC) on a NETZSCH STA 449 F3 thermal analyzer (Germany), coupled with a Tensor 27 Fourier-transform infrared (FTIR) spectrometer (Bruker, USA). The instrument simultaneously recorded changes in sample mass (Δm_i) and heat release/absorption (DSC) during continuous heating at a rate of 10 °C/min up to 1150 °C.

The objects of study were solid copper samples: 49.5 mg of pure copper (99.98 % Cu) and 48.47 mg of blister copper (98.7 % Cu). The samples were placed in a crucible with an inner diameter of 6 mm and a height of 4 mm. During the tests, the working space above the crucible surface was blown with air at a flow rate of 250 mL/min. In the experiment with pure copper, the change in sample mass (Δm_i) was interpreted as the oxygen mass $m_{[O]}$ incorporated into copper oxides of the Cu—O system. For blister copper, Δm_i was taken as the integral amount of oxygen incorporated into oxides of the Cu—Mei—O system.

To assess the degree of oxygen solubility and evaluate its effect on the electrical properties of copper, surface oxidation of blister and pure (anode) copper melt samples was performed using an air mixture. The experiments were carried out under laboratory conditions with the following equipment:

— an electric furnace with silicon carbide heaters and a temperature control unit, operating at approximately 1170 °C;

— a crucible with batch loading of blister and anode copper chips, with a melt surface area S of approximately 7539 mm^2;

— a laboratory compressor with a capacity of 7 m^3/h and an air-blowing rate of 1.75—2.45 m^3/h.

Three samples of blister copper and three samples of anode copper of different chemical compositions, each weighing approximately 5000 g, were selected for study. All samples were melted under a charcoal layer. After the copper melted, slag was removed from the crucible surface, and oxidation was carried out by blowing with an air mixture or approximately 12—18 min.

The degree of oxygen solubility was determined by periodic sampling (one sample per measurement), fol-

lowed by analysis on an ELTRA CS-2000 (Germany) carbon/sulfur analyzer, a SPECTROLAB S (Germany) optical emission spectrometer for copper composition, and an ELTRA ON-900 (Germany) oxygen/nitrogen analyzer. The effect of copper oxidation kinetics on its electrical properties was studied by measuring the electrical resistivity of the anode copper melt [3].

Results and discussion

The TG—DSC curves obtained during 120 min of heating pure and blister copper samples to 1150 °C were plotted on the same coordinate system for clarity (Fig. 1). The numerical values of Δm_i, τ, and t_i at the most characteristic points are shown separately in the diagram field [4].

The kinetic dependences of sample mass change on oxidation time in the temperature interval of 300—1050 °C exhibit a complex rate law close to parabolic, consistent with most previous studies (Fig. 1, curve 2*a* — pure copper, curve 2*b* — blister copper) [5].

The complex oxidation behavior can be explained by thermodynamically probable reactions in the Cu—O system: oxidation of copper to Cu_2O by atomic and molecular oxygen, and recombination reduction of CuO to Cu_2O.

At temperatures of approximately 650 °C and above, bulk diffusion of copper cations within the Cu_2O crystal lattice begins to dominate over grain-boundary diffusion. As a result of grain growth, both the size and the mass fraction of Cu_2O in the oxide layer increase, ensuring complete oxidation of copper to Cu_2O [6—15]. The oxygen diffusion rate also rises, which is reflected in the increase in sample mass and confirms the parabolic rate law (Fig. 1).

A comparison of the Cu_2O masses formed during oxidation of pure and blister copper shows close agreement (3.55 and 3.01 mg, respectively). This indicates that the samples oxidize at nearly the same rate and that the presence of impurities has little effect on the process.

The oxygen required for Cu_2O formation during oxidation of pure and blister copper was calculated based on the mass change. It was established that, to obtain 3.55 mg of Cu_2O in the pure-copper experiment, 0.267 mL of oxygen is required, whereas in the blister-copper experiment 0.234 mL is required; this corresponds to 0.00355 at. % ($8.8 \cdot 10^{-4}$ wt. %) and 0.00301 at.% ($7.5 \cdot 10^{-4}$ wt. %), respectively.

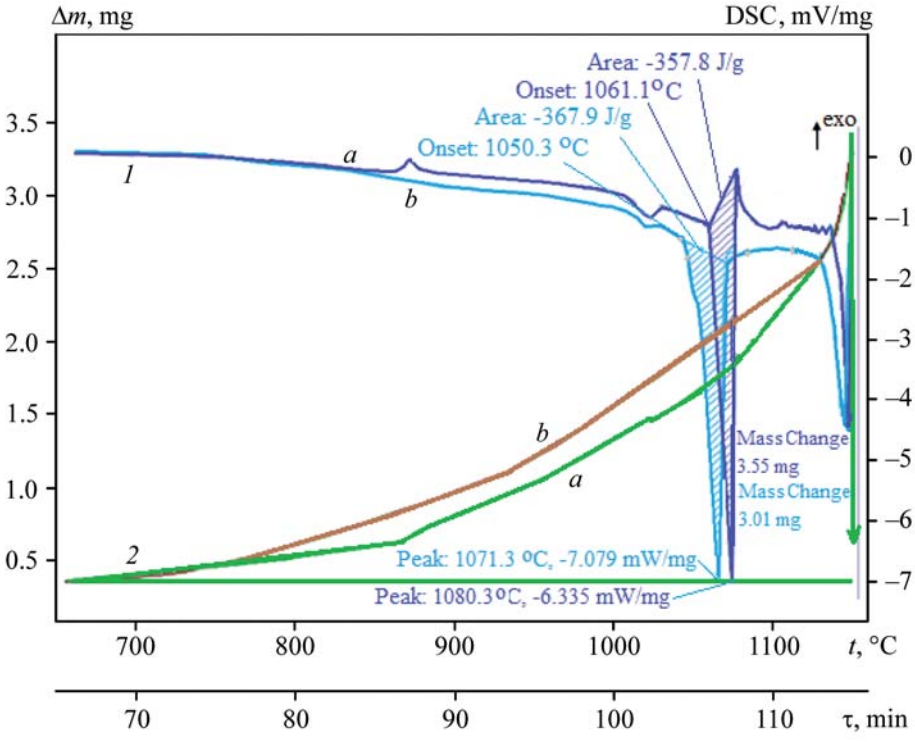

Fig. 1. TG—DSC curves of copper oxidation: pure copper (***a***), blister copper (***b***)
1 – DSC signal, ***2*** – sample mass change, mg

Рис. 1. Кривые ДТА окисления чистой (***a***) и черновой (***b***) меди
1 – ДСК, ***2*** – изменение массы навески, мг

The maximum solubility of oxygen in copper (at. %) at 750—1030 °C is determined according to the following equation [11; 12]

$$\lg[\%O]_{max} = -\frac{6600}{t} + 3{,}41.$$

At 1030 °C, the solubility limit of oxygen in solid copper is 0.02215 at. % (0.0055 wt. %). This indicates that at the given temperature all oxygen intended for copper (I) oxide formation dissolves in the metal, and a continuous oxide layer does not form at the Cu—Cu_2O interface.

During fire refining in the temperature range of 1100—1200 °C, copper is oxidized primarily by atomic oxygen from the air introduced into the melt [16]. The maximum solubility of oxygen in copper in this interval is determined as follows:

$$\lg[\%O]_{max} = -\frac{9260}{t} + 7{,}15.$$

At 1170 °C, the solubility limit of oxygen in liquid copper is 5.4 at. % (1.41 wt. %).

To assess the degree of oxygen solubility and to evaluate its effect on the electrical properties of blister copper, three samples with an average chemical composition were used (Table 1).

The kinetic oxidation curves of blister copper samples with different chemical compositions at 1170 °C are shown in Fig. 2.

Analysis of the empirical curves (Fig. 2) shows that blister copper samples of different chemical compositions exhibit complex oxidation behavior. At the initial stage (up to 6 min), deviations from linear oxidation kinetics are observed. This is explained by the fact that most of the oxygen is consumed in oxidizing impurities (Zn, Fe, Ni, S) and transferring them into the slag and gas phase. The deviation from linearity is most pronounced for curve *2* (Fig. 2). After 3 min of blowing, the oxygen concentration decreases from 0.06 to 0.047 % before starting to rise again. This behavior is attributed to the relatively high sulfur content in this blister copper sample (0.23 %) compared with the other

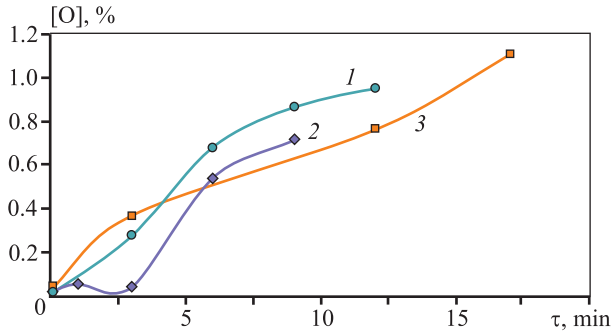

Fig. 2. Empirical dependence of oxygen concentration in copper melt on oxidation time

1–3 – blister copper samples of different chemical compositions (see Table 1)

Рис. 2. Эмпирическая зависимость концентрации кислорода в расплаве меди от продолжительности окисления

1–3 – образцы черновой меди различного химического состава (см. табл. 1)

samples (0.019 and 0.083 %). Since the experiments were conducted under isothermal conditions, 1 min of air blowing was sufficient to saturate the melt with oxygen (from 0.02 to 0.06 %) and to oxidize Zn and Fe. However, this time was insufficient for complete degassing of the copper melt as SO_2, so sulfur largely remained in the melt as dissolved SO_2 bubbles. Prolonged air blowing subsequently removed SO_2 from the melt, while simultaneously reducing the oxygen concentration from 0.06 to 0.047 % [17—22].

After oxidation of the impurities, slag removal, and further oxidation of the melt (from the 6th minute onward), the oxidation of copper follows an almost linear course, with the oxygen concentration in the melt increasing at an average rate of Δ[O] = 0.07 %/min. This is due to the fact that, at the given temperature, all oxygen dissolves in copper, forming Cu_2O and acting as a reactive impurity that promotes overoxidation of the melt.

To assess the degree of oxygen solubility and to evaluate its effect on the electrical properties of anode copper, three samples with an average chemical composition were used (Table 2). The kinetic oxidation curves of ano-

Table 1. **Average chemical composition of blister copper samples**

Таблица 1. Средневзвешенный состав образцов черновой меди

Sample No.	Content, %								
	Pb	Sn	As	Sb	Zn	Fe	Ni	O	S
1	0.03	0.001	0.048	0.076	0.0027	0.0017	0.115	0.28	0.083
2	0.041	0.001	0.045	0.077	0.0055	0.037	0.015	0.02	0.23
3	0.13	0.004	0.156	0.24	0.0039	0.0059	0.4	0.047	0.019

de copper of different chemical compositions at 1170 °C are shown in Fig. 3. Analysis of these data shows a linear increase in the oxygen concentration in the melt, with an average rate of Δ[O] = 0.05 %/min. This trend can be attributed to the fact that molten anode copper contains almost no impurities, allowing its atomic structure to undergo continuous short-range ordering and disordering. This dynamic process creates fluctuating free volume (up to 6 %) and alters interatomic distances by 1—2 %. Because the atomic radius of oxygen (r_O = = $48 \cdot 10^{-12}$ m) is smaller than that of copper (r_{Cu} = = $145 \cdot 10^{-12}$ m), oxygen atoms are generally accommodated uniformly in interstitial positions, saturating the copper with oxygen up to its solubility limit.

The influence of oxygen on the electrical properties of copper in the solid state (binary Cu—O system) has been extensively studied in the literature. Experimental data show that the dependence of copper resistivity on oxygen concentration is nonlinear [23]. To obtain a quantitative description of this dependence, the published data were digitized with WebPlotDigitizer. The results are shown in Fig. 4. The graph indicates that low oxygen concentrations, up to 0.06 %, enhance the electrical conductivity of copper [23]. This effect is explained by the fact that oxygen in copper may exist not only as copper (I) oxide, but also in solid solution, where it interacts with detrimental metallic impurities (e.g., nickel), oxidizing them into less harmful forms [24—26].

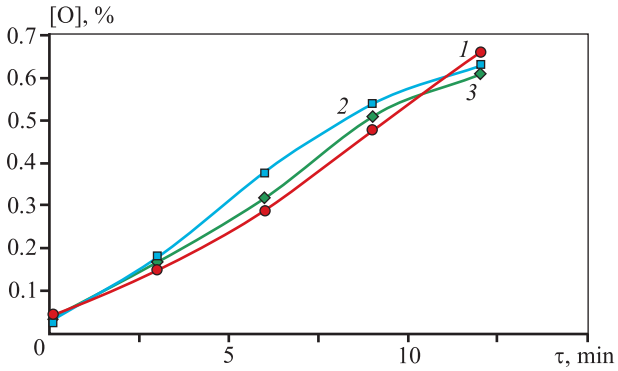

Fig. 3. Empirical dependence of oxygen concentration in copper melt on oxidation time

1–3 – anode copper samples of different chemical compositions (see Table 2)

Рис. 3. Эмпирическая зависимость концентрации кислорода в расплаве меди от продолжительности окисления

1–3 – образцы анодной меди различного химического состава (см. табл. 2)

In the oxygen concentration range above 0.06 %, copper resistivity increases linearly (Fig. 4), with oxygen acting as a detrimental impurity that reduces electrical conductivity.

By contrast, the effect of oxygen on the electrical conductivity of liquid copper of different chemical compositions has been studied only to a limited extent, and the available information is fragmentary. To evaluate the influence of oxidation kinetics of liquid copper on its electrical conductivity, resistivity of anode copper melts was measured simultaneously with oxygen sampling.

The empirical relationships between melt resistivity and oxygen dissolution in anode copper samples of different chemical compositions (Fig. 5) are comparable with the dependence of resistivity on oxygen content in solid copper in the region above 0.06 % (Fig. 4). Analysis of curves *1* and *3* (Fig. 5) shows a similar increase in melt resistivity with oxygen concentration, which can be approximated by an exponential function. This suggests that these anode copper samples have similar chemical compositions and contain only minor impurity levels. Curve *2* in Fig. 5 shows no increase in melt resistivity during oxygen saturation in the initial range of 0.066—0.3 %. This indicates that this anode copper sample has elevated impurity levels. In this case, the dissolved oxygen was consumed by further oxidation of impurities (Pb, Zn, Fe, S) that were not removed during anode smelting, which was manifested in slag formation during melt oxidation. After slag removal and continued oxygen dissolution, an increase in melt resistivity was recorded.

In conclusion, these results demonstrate the kinetic regularities of oxidation of solid and liquid cop-

Table 2. **Average chemical composition of anode copper samples**

Таблица 2. Средневзвешенный состав образцов анодной меди

Sample No.	Content, %								
	Pb	Sn	As	Sb	Zn	Fe	Ni	O	S
1	0.081	0.0056	0.0055	0.099	0.0028	0.0016	0.09	0.018	0.0071
2	0.08	0.0056	0.0054	0.099	0.0049	0.0032	0.092	0.023	0.0086
3	0.081	0.0054	0.0054	0.099	0.0023	0.0015	0.088	0.024	0.0055

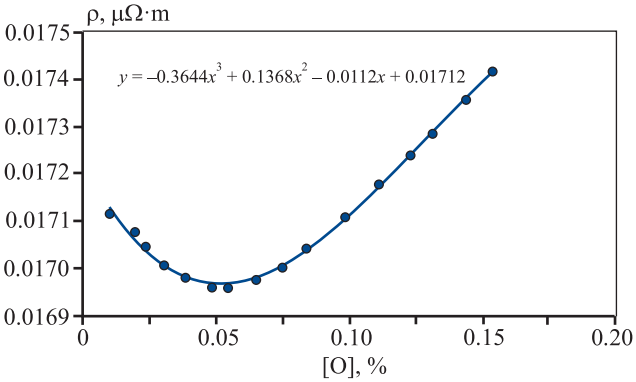

Fig. 4. Dependence of copper resistivity on oxygen concentration [23]

Рис. 4. Зависимость удельного сопротивления меди от содержания кислорода [23]

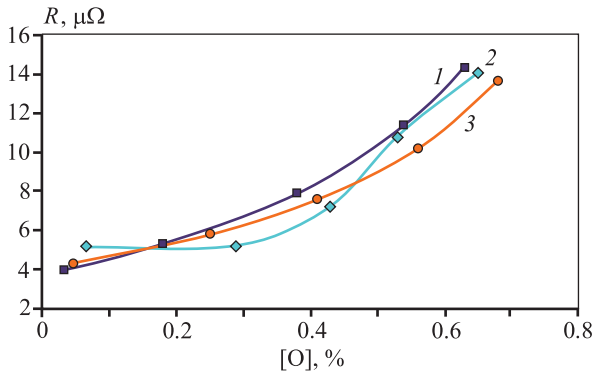

Fig. 5. Dependence of the resistance of copper (***1–3***) melt samples of different chemical (see table 2) composition on the oxygen content

Рис. 5. Зависимость электросопротивления образцов (***1–3***) расплава меди различного химического состава (см. табл. 2) от содержания кислорода

per of different chemical compositions and the effect of oxygen solubility on the electrical properties of the melt.

According to the Cu—Cu_2O phase diagram, the main condition for fire refining is to maintain the oxygen concentration in copper above the equilibrium level required for impurity oxidation (0.4—0.8 % at temperatures up to 1170 °C). Therefore, it is important to analyze the kinetics of oxygen dissolution in liquid copper during the oxidation stage to evaluate impurity transfer into slag and to avoid overoxidation. The influence of oxygen dissolution kinetics on the electrical conductivity of liquid copper should be assessed only after maximum impurity removal. This approach makes it possible to calculate and control the residual oxygen concentration in the copper melt by measuring melt resistivity [3].

Conclusion

The macroscopic oxidation kinetics of pure and blister copper samples of different chemical compositions were investigated using TG—DSC and surface oxidation by air blowing. The results show that all samples oxidize at almost the same rate and that the presence of impurities does not significantly influence copper oxidation.

All oxygen available for copper (I) oxide formation dissolves in copper up to the thermodynamic limit of 12 % Cu_2O. The effect of oxygen solubility in copper melts on their electrical properties was demonstrated. It was established that oxygen concentrations in the melt exceeding 0.08 % deteriorate the electrical properties of copper.

References

1. Belousov V.V., Klimashin A.A, High-temperature oxidation of copper. *Uspekhi khimii.* 2013;3:3—6. (In Russ.).
Белоусов В.В., Климашин А.А. Высокотемпературное окисление меди. *Успехи химии*. 2013;3:3—6.
2. Belousov A.A., Pastukhov E.A., Aleshina S.N. Effect of temperature, partial pressure of oxygen on the kinetics of oxidation of liquid copper. *Rasplavy.* 2003;2:3—6. (In Russ.).
Белоусов А.А., Пастухов Е.А., Алешина С.Н. Влияние температуры, парциального давления кислорода на кинетику окисления жидкой меди. *Расплавы.* 2003;2:3—6.
3. Lisienko V.G., Kholod S.I. Chesnokov Yu.N., Rogachev V.V., Kiselev V.V. Device for the production of anode copper. Patent 2779418 (RF). 2022. (In Russ.).
Лисиенко В.Г., Холод С.И. Чесноков Ю.Н., Рогачев В.В., Киселев В.В. Устройство для производства анодной меди: Патент 2779418 (РФ). 2022.
4. Zhukov V.P., Kholod S.I., Demin A.I., Menshikov V.A. Study of copper oxidation kinetics by differential thermographic analysis. In: Modern trends in the field of theory and practice of extraction and processing of mineral and technogenic raw materials: (November 6–7, 2024), Yekaterinburg: JSC Uralmekhanobr, 2024. P. 284–287. (In Russ.).
Жуков В.П., Холод С.И., Демин А.И., Меньшиков В.А. Исследование кинетики окисления меди методом дифференциально-термографического анализа. В сб.: *Современные тенденции в области теории и практики добычи и переработки минерального и техногенного сырья* (06—07 ноября 2024) г. Екатеринбург: АО «Уралмеханобр», 2024. С. 284—287.

5. Ferapontov Yu.A., Putin S.B., Ferapontova L.L., Putin P.Yu. Study of kinetics of topochemical processes in non-isothermal mode by derivatographic method. *Vestnik of TSTU*. 2009;15(14):826—834. (In Russ.).
Ферапонтов Ю.А., Путин С.Б., Ферапонтова Л.Л., Путин П.Ю. Исследование кинетики топохимических процессов неизотермическом режиме дериватографическим методом. *Вестник ТГТУ*. 2009;15(14):826—834.
6. Ivanic L., Kochovski B. Study of oxygen transfer kinetics in copper. *Tsvetnye metally*. 1997;9:24—25. (In Russ.).
Иванич Л., Кочовски Б. Исследование кинетики переноса кислорода в меди. *Цветные металлы*. 1997;9:24—25.
7. Safarov D.D. Kinetics of oxidation of copper-based alloys by a gas phase of variable composition: Diss. Cand. Sci. (Chem.). Sverdlovsk: IMET UrO RAS, 1983.
Сафаров Д. Д. Кинетика окисления сплавов на основе меди газовой фазой переменного состава: Дис. канд. хим. наук. Свердловск: ИМЕТ УрО РАН, 1983.
8. Martin T., Utigard T. The kinetigs and mechanism of molten copper oxidation by top blowing of oxygen. *Journal of Metals*. 2005;2:58—62.
9. Barton R.G., Brimacombe J.K.. Influence of surface tensioп-driven flow of the kinetics of oxygen absorption in molten copper. *Metallurgical Transactions* A. 1977;8 B:417—427.
10. Lyamkin S.A., Tanutrov I.N., Sviridova M.N. Kinetics of oxidation of molten copper by gas phase oxygen. *Rasplavy*. 2013;2:83—89. (In Russ.).
Лямкин С.А., Танутров И.Н., Свиридова М.Н. Кинетика окисления расплавленной меди кислородом газовой фазы. *Расплавы*. 2013; 2: 83 — 89.
11. Gerlach J., Schneider N., Wuth W. Oxygen absorption during blowing of molten Cu. *Journal of Metals*. 1972;25(11):1246—1251.
12. Avetissyan A.A., Chatilyan A.A., Kharatyan S.L. Kinetic features of the initial stages of high-temperature oxidation of copper. *Khimicheskii zhurnal Armenii*. 2013;3: 407—415. (In Russ.).
Аветесян А.А., Чатилян А.А., Харатян С.Л. Кинетические особенности начальных стадий высокотемпературного окисления меди. *Химический журнал Армении*. 2013;3:407—415.
13. Lovshenko G. F., Khina B. B. Macrokinetic mathematical model of internal oxidation of copper-based alloys during annealing of mechanically alloyed compositions of the Cu—Al—CuO system. *Vestnik Belorussko-Rossiiskogo universiteta*. 2006;4(13):119—127.
Ловшенко Г. Ф., Хина Б. Б. Макрокинетическая математическая модель внутреннего окисления сплавов на основе меди при отжиге механически легированных композиций системы Cu—Al—CuO. *Вестник Белорусско-Российского университета*. 2006;4(13): 119—127.
14. Warrczok A., Thorstein A. Reaction rate between carbon dioxide and graphite. *Steel Research International*. 2000;71(8):277—280.
15. Fromm E., Gebhardt E. Gases and carbon in metals. Moscow: Metallurgiya, 1980. 712 p. (In Russ.).
Фромм Е., Гебхардт Е. Газы и углерод в металлах. М.: Металлургия, 1980. 712 с.
16. Bryukvin V.A., Zadiranov A.N., Leontyev V.G., Tsybin O.I. Interaction of metallic copper melts with steam-air gas mixtures as applied to the tasks of their refining technology from impurities. *Tsvetnye metally*. 2003;5: 34—36. (In Russ.).
Брюквин В.А., Задиранов А.Н., Леонтьев В.Г., Цыбин О.И. Взаимодействие расплавов металлической меди с паровоздушными газовыми смесями применительно к задачам технологии их рафинирования от примесей. *Цветные металлы*. 2003;5:34—36.
17. Davenport W.G., King M., Schlesinger M., Biswas A.K. Extractive metallurgy of copper. Oxford: Elsever Sciense Ltd., 2002;452.
18. Biswas A.K., Davenport W.G. Extractive metallurgy of copper. Oxford: Pergamon, 1996. 441 p.
19. Gerlach J., Herfort P. The rate of oxyden uptake by molten copper. *Journal of Metals*. 1968;22(11):1068—1090.
20. Gerlach J., Schneider N., Wuth W. Oxyden absorption during blowing of molten Cu. *Journal of Metals*. 1972;25(11):1246—1251.
21. Frohne O., Rottmann G. Wuth W. Processing speeds in the pyrometallurgical refining of Cu by the top-blowing process. *Journal of Metals*. 1973;27(11):1112—1117
22. Volkhin A.I., Eliseev E.I., Zhukov V.P., Smirnov B.N. Anode and cathode copper. Chelyabinsk: South-Ural book publishing house, 2001. 431 p. (In Russ.).
Вольхин А.И., Елисеев Е.И., Жуков В.П., Смирнов Б.Н. Анодная и катодная медь. Челябинск: Юж.-Ур. кн. изд-во, 2001. 431 с.
23. Aglitsky V.A. Copper refining. Moscow: Metallurgiya, 1971. 184 p. (In Russ.).
Аглицкий В.А. Рафинирование меди. М.: Металлургия, 1971. 184 с.
24. Coursol P., Valencia C.N., Mackey V.P., BellS., Davis B. Minimizationof copper losses in copper smelting slag during electric furnace treatment. *Journal of Metals*. 2012;64(11):1305—1313.
https://doi.org/10.1007/s11837-012-0454-6
25. Namil Um, Seon-Oh Park, Cheol-Woo Yoon, Tae-Wan Jeon. A pretreatment method for effective utilization of copper product manufacturing waste. *Environmental Chemical Engineering*. 2021;9(4):105—109.

26. Zadiranov A.N., Meshcheryakov A.V., MalkovaM.Yu., Nurmagomedov T.N., Degtyarev S.V., Grigorievskaya I.I., Grusheva T.G., Eroshenko V.O. Ensuring the efficiency of refining copper scrap melt with a steam-air mixture based on mathematical modeling and experimental studies. *Metallurgist.* 2023;3:101—107. https://doi.org/10.52351/00260827_2023_03_101

Задиранов А.Н., Мещеряков А.В., Малькова М.Ю., Нурмагомедов Т.Н., Дегтярев С.В., Григорьевская И.И., Грушева Т.Г., Ерошенко В.О. Обеспечение эффективности рафинирования расплава медных ломов паровоздушной смесью на основе математического моделирования и экспериментальных исследований. *Металлург.* 2023;3:101—107.

Information about the authors

Sergey I. Kholod – Leading Engineer, Department of foundry and hardening technologies, Ural Federal University n.a. the First President of Russia B.N. Eltsin (UrFU); Deputy Head of the Department of metallurgy, Technical University of UMMC.
E-mail: hsi503@yandex.ru

Vladimir P. Zhukov – Dr. Sci. (Eng.), Professor, Leading Researcher, JSC "Uralmekhanobr"
E-mail: zhukov_vp@umbr.ru

Sergey V. Mamyachenkov – Dr. Sci. (Eng.), Professor, Head of the Department of non-ferrous metallurgy, UrFU.
https://orcid.org/0000-0002-4458-3792
E-mail: s.v.mamiachenkov@urfu.ru

Vladimir V. Rogachev – Cand. Sci. (Eng.), Associate Professor, Department of metallurgy of iron and alloys, UrFU.
E-mail: v.v.rogachev@urfu.ru

Информация об авторах

Сергей Иванович Холод – вед. инженер кафедры литейного производства и упрочняющих технологий, Уральский федеральный университет имени первого Президента России Б.Н. Ельцина (УрФУ); зам. заведующего кафедрой металлургии, Технический университет УГМК.
E-mail: hsi503@yandex.ru

Владимир Петрович Жуков – д.т.н., профессор, вед. науч. сотрудник, АО «Уралмеханобр».
E-mail: zhukov_vp@umbr.ru

Сергей Владимирович Мамяченков – д.т.н., профессор, зав. кафедрой металлургии цветных металлов, УрФУ.
https://orcid.org/0000-0002-4458-3792
E-mail: s.v.mamiachenkov@urfu.ru

Владимир Васильевич Рогачев – к.т.н., доцент кафедры металлургии железа и сплавов, УрФУ.
E-mail: v.v.rogachev@urfu.ru

Contribution of the authors

S.I. Kholod – conducted investigations, wrote the manuscript, participated in the discussion of results.

V.P. Zhukov – defined the research objectives, conducted investigations, participated in the discussion of results.

S.V. Mamyachenkov – wrote the manuscript, participated in the discussion of results.

V.V. Rogachev – conducted investigations, participated in the discussion of results.

Вклад авторов

С.И. Холод – проведение исследований, написание статьи, участие в обсуждении результатов.

В.П. Жуков – определение цели работы, проведение исследований, участие в обсуждении результатов.

С.В. Мамяченков – написание статьи, участие в обсуждении результатов.

В.В. Рогачев – проведение исследований, участие в обсуждении результатов.

The article was submitted 05.05.2025, revised 19.05.2025, accepted for publication 23.05.2025

Статья поступила в редакцию 05.05.2025, доработана 19.05.2025, подписана в печать 23.05.2025

METALLURGY OF NON-FERROUS METALS / МЕТАЛЛУРГИЯ ЦВЕТНЫХ МЕТАЛЛОВ

UDC 66.083.3
https://doi.org/10.17073/0021-3438-2025-3-16-27

Research article
Научная статья

Optimization of low-temperature sulfuric acid leaching of chalcopyrite and pyrite

M.A. Tretiak, K.A. Karimov, U.R. Sharipova, A.V. Kritskiy, D.A. Rogozhnikov

Ural Federal University n.a. the First President of Russia B.N. Yeltsin
19 Mira Str., Ekaterinburg 620002, Russia

✉ Maksim A. Tretiak (m.a.tretiak@urfu.ru)

Abstract: This study presents the results of oxidative leaching of chalcopyrite ($CuFeS_2$) and pyrite (FeS_2) in a sulfuric acid medium at low temperature in the presence of copper (Cu^{2+}) and iron (Fe^{3+}) ions. Using orthogonal experimental design, the optimal conditions were identified to maximize sulfide matrix decomposition and valuable metal recovery. Experiments were conducted at a constant temperature of 100 °C. The parameters investigated included partial oxygen pressure (0.2–0.75 MPa), concentrations of sulfuric acid (10–50 g/dm^3), Fe^{3+} ions (2–10 g/dm^3), Cu^{2+} ions (1–3 g/dm^3), and leaching time (60–240 min). The composition of the feed minerals and leach products was analyzed by *X*-ray fluorescence (XRF) analysis, *X*-ray diffraction (XRD) analysis, and atomic absorption spectrometry (AAS). Maximum copper recovery from chalcopyrite (55 %) was achieved under the following conditions: O_2 partial pressure of 0.25 MPa, initial concentrations of H_2SO_4 – 50 g/dm^3, Cu^{2+} – 1 g/dm^3, Fe^{3+} – 2.5 g/dm^3, and leaching time – 240 min. The maximum degree of pyrite oxidation (56 %) was obtained at an O_2 partial pressure of 0.75 MPa, initial concentrations of H_2SO_4 – 50 g/dm^3, Cu^{2+} – 2 g/dm^3, and Fe^{3+} – 10 g/dm^3. The results showed that leaching time and oxygen pressure have the greatest effect on chalcopyrite and pyrite decomposition ($p < 0.05$). The interaction between Fe^{3+} and Cu^{2+} ions was also established: excess Fe^{3+} (>10 g/dm^3) leads to hydrolysis and decreases chalcopyrite leaching efficiency, whereas Cu^{2+} promotes partial formation of secondary copper sulfides. Regression equations ($R^2 = 0.98$ for chalcopyrite and $R^2 = 0.96$ for pyrite) were derived, providing an adequate description of the process.

Keywords: chalcopyrite, pyrite, copper, iron, autoclave, autoclave leaching, sulfuric acid, oxygen.

Acknowledgments: The research was supported by the Russian Science Foundation (Project No. 25-29-00838, https://rscf.ru/project/25-29-00838/).

For citation: Tretiak M.A., Karimov K.A., Sharipova U.R., Kritskiy A.V., Rogozhnikov D.A. Optimization of low-temperature sulfuric acid leaching of chalcopyrite and pyrite. *Izvestiya. Non-Ferrous Metallurgy*. 2025;31(3):16–27.
https://doi.org/10.17073/0021-3438-2025-3-16-27

Оптимизация процессов низкотемпературного серно-кислотного выщелачивания халькопирита и пирита

М.А. Третьяк, К.А. Каримов, У.Р. Шарипова, А.В. Крицкий, Д.А. Рогожников

Уральский федеральный университет имени первого Президента России Б.Н. Ельцина
Россия, 620002, г. Екатеринбург, ул. Мира, 19

✉ Максим Алексеевич Третьяк (m.a.tretiak@urfu.ru)

Аннотация: В работе представлены результаты исследования процессов окислительного выщелачивания халькопирита ($CuFeS_2$) и пирита (FeS_2) в серно-кислой среде при низких температурах с добавлением ионов меди (Cu^{2+}) и железа (Fe^{3+}). Методом ортогонального планирования эксперимента установлены оптимальные условия процесса, обеспечивающие максимальную степень

деструкции сульфидной матрицы и извлечение ценных металлов. Эксперименты проводились при постоянной температуре 100 °С. Исследовались следующие параметры: парциальное давление кислорода (0,2–0,75 МПа), концентрации серной кислоты (10–50 г/дм^3), ионов Fe^{3+} (2–10 г/дм^3) и Cu^{2+} (1–3 г/дм^3), а также продолжительность процесса (60–240 мин). Состав исходных минералов и продуктов выщелачивания анализировали методами рентгеноспектрального флуоресцентного анализа, рентгенофазового анализа и атомно-абсорбционной спектрометрии. Установлено, что максимальное извлечение меди из халькопирита (55 %) достигается при следующих условиях: парциальном давлении O_2 – 0,25 МПа, исходных концентрациях H_2SO_4 – 50 г/дм^3, Cu^{2+} – 1 г/дм^3, Fe^{3+} – 2,5 г/дм^3, продолжительности процесса – 240 мин. Максимальная степень окисления пирита составила 56 % при парциальном давлении кислорода 0,75 МПа, исходных концентрациях H_2SO_4 – 50 г/дм^3, Cu^{2+} – 2 г/дм^3 и Fe^{3+} – 10 г/дм^3. Установлено, что продолжительность и давление кислорода оказывают наиболее значимое влияние на степень разложения халькопирита и пирита ($p < 0,05$). Выявлены особенности взаимодействия ионов Fe^{3+} и Cu^{2+}: избыток Fe^{3+} (>10 г/дм^3) приводит к гидролизу и снижению эффективности выщелачивания халькопирита, тогда как Cu^{2+} способствует частичному образованию вторичных сульфидов меди. Выведены уравнения регрессии ($R^2 = 0,98$ для халькопирита и $R^2 = 0,96$ для пирита), адекватно описывающие процесс.

Ключевые слова: халькопирит, пирит, медь, железо, автоклав, выщелачивание, серная кислота, кислород.

Благодарности: Исследование выполнено за счет гранта Российского научного фонда № 25-29-00838, https://rscf.ru/project/25-29-00838/

Для цитирования: Третьяк М.А., Каримов К.А., Шарипова У.Р., Крицкий А.В., Рогожников Д.А. Оптимизация процессов низкотемпературного серно-кислотного выщелачивания халькопирита и пирита. *Известия вузов. Цветная металлургия.* 2025;31(3):16–27. https://doi.org/10.17073/0021-3438-2025-3-16-27

Introduction

Sulfide minerals, particularly chalcopyrite ($CuFeS_2$) and pyrite (FeS_2), are of significant interest in modern hydrometallurgy as the main sources of non-ferrous and noble metals. However, their processing presents substantial technological challenges due to the high chemical stability of the sulfide matrix. Conventional pyrometallurgical methods are characterized by high energy consumption and the release of toxic gaseous emissions, which highlights the need for the development of more environmentally friendly and economically efficient hydrometallurgical technologies [1—3].

Recent trends in the hydrometallurgy of non-ferrous metals demonstrate growing interest in the creation of energy-efficient methods for processing sulfide raw materials [4—10].

In recent years, autoclave hydrometallurgy has seen a shift toward the development and implementation of low-temperature mineral processing techniques [11—14]. This direction is of particular scientific and practical interest, as it makes it possible to significantly optimize both technological and economic performance indicators. Conducting leaching processes at low temperatures (60—110 °C) under either atmospheric or autoclave conditions can reduce energy consumption, simplify process equipment, and enable the oxidation of sulfur predominantly to its elemental form compared to conventional high-temperature autoclave processes [15]. However, during oxidative leaching of sulfide minerals, the formation of elemental sulfur leads to the development of passivating layers on particle surfaces, which substantially slows down the reaction.

Modern approaches to addressing this issue involve a range of technological solutions that combine different process intensification methods. The most common techniques include preliminary mechanochemical activation in mills, which generates a defect-rich crystal structure, as well as the use of surfactants and catalytic additives (Ag^+, Cu^{2+}, Fe^{3+} ions) that destabilize sulfur films by modifying their morphology and increasing the porosity of the passivating layer [16—18]. Studies [19—21] have demonstrated that the addition of silver during chalcopyrite leaching with ferric sulfate solutions significantly enhances the leaching process, resulting in shorter leaching times and higher copper recovery into solution. The low rate of chalcopyrite oxidation by Fe^{3+} is attributed to the formation of a passivating elemental sulfur layer, which acts as a barrier to reagent access at the mineral surface. This interpretation is supported by studies [22; 23], which reported oxidation of sulfide concentrates containing chalcopyrite, sphalerite, and arsenopyrite in ferric-containing solutions in the presence of pyrite. The authors analyzed the kinetics and proposed a mechanism for the interaction of sulfide minerals with ferric ions and pyrite.

Experimental studies of the kinetics and mechanisms of chalcopyrite- and pyrite-containing material

oxidation under hydrothermal conditions, conducted since the 1950s, reveal considerable variation in reported results. These discrepancies arise from differences in the mineralogical and chemical composition of the feed, process conditions (temperature, oxygen pressure, pH, etc.), and methodological approaches to interpreting experimental data. Therefore, the study of sulfide raw material processing remains an important research objective, especially in view of advances in analytical methods and the evolving mineral composition of ores being processed.

In autoclave sulfuric acid leaching, the oxidation of $CuFeS_2$ and FeS_2 is described by the following principal reactions:

$$2CuFeS_2 + 2H_2SO_4 + 7O_2 = 2CuSO_4 + Fe_2(SO_4)_3 + S^0 + 2H_2O, \quad (1)$$

$$CuFeS_2 + H_2SO_4 + 2.5O_2 = CuSO_4 + FeSO_4 + S^0 + H_2O, \quad (2)$$

$$CuFeS_2 + 2Fe_2(SO_4)_3 = CuSO_4 + 5FeSO_4 + 2S^0, \quad (3)$$

$$CuFeS_2 + 4O_2 = CuSO_4 + FeSO_4, \quad (4)$$

$$5FeS_2 + 4H_2SO_4 + 4O_2 = 5FeSO_4 + 9S^0 + 4H_2O, \quad (5)$$

$$FeS_2 + 3.5O_2 + H_2O = FeSO_4 + H_2SO_4, \quad (6)$$

$$7FeS_2 + 4Fe_2(SO_4)_3 + 4H_2SO_4 = 14FeSO_4 + 14S^0 + 4H_2O, \quad (7)$$

$$4FeS_2 + 9O_2(g) + 4H_2SO_4 = 4\,Fe_2(SO_4)_3 + 8S^0 + 4H_2O, \quad (8)$$

$$4FeSO_4 + O_2(g) + 2H_2SO_4 = 2Fe_2(SO_4)_3 + 2H_2O. \quad (9)$$

These reactions show that sulfide sulfur in chalcopyrite may be oxidized by oxygen to elemental sulfur and sulfate ions (reactions (1)—(3)). Ferric ions can also act as oxidants, in which case sulfide sulfur is oxidized to the elemental state (reaction (4)), while ferrous ions react with oxygen to regenerate ferric ions.

Given the significance of this issue, the present study focuses on low-temperature oxidative autoclave leaching of chalcopyrite and pyrite in a sulfuric acid medium with copper (Cu^{2+}) and iron (Fe^{3+}) ions as catalytic additives. The main objective is to determine the optimal process parameters (temperature, partial oxygen pressure, sulfuric acid concentration, and catalytic additives) that ensure maximum recovery of non-ferrous metals.

Materials and methods

Chalcopyrite and pyrite from the Vorontsovskoye and Berezovskoye deposits (Sverdlovsk region, Russia), respectively, were used as the objects of study in low-temperature oxidative autoclave leaching. The chemical composition of the minerals (Table 1) was determined by *X*-ray fluorescence (XRF) analysis using an ED-XRF spectrometer (EDX-7000, Shimadzu, Japan).

Particle size distribution of the minerals was determined by laser diffraction using a Bettersize ST analyzer (Bettersize, China) (Fig. 1). The characteristic chalcopyrite particle sizes d_{10}, d_{50}, and d_{90} are 3.8, 28.8, and 79.9 μm, respectively. Analysis of the particle size distribution indicates that the predominant fraction of the sample lies within 30—90 μm. The wide gap between d_{10} and d_{90} (>76 μm) confirms a high degree of particle size heterogeneity.

For pyrite, the d_{10}, d_{50}, and d_{90} are 3.41, 14.81, and 53.77 μm, respectively. Differential distribution analysis shows that the main fraction was within 10—45 μm, accounting for more than 50 % of the sample.

The minerals were ground and sieved on laboratory screens, after which the working fraction was selected with 80 % passing ≤40 μm.

X-ray diffraction (XRD) analysis was performed using an XRD-7000 Maxima diffractometer (Shimadzu, Japan). Diffraction data were processed using Match!3 software with the PDF-2 database and the WWW-MINCRYST database of minerals and structural analogs. The results are shown in Fig. 2.

XRD analysis of the CuFeS2 and FeS2 samples showed minor peaks of silicon dioxide, with concentrations not exceeding 0.5 % in chalcopyrite and 5.1 % in pyrite.

To achieve the required initial concentrations of sulfuric acid, Cu^{2+}, and Fe^{3+} ions, analytical-grade rea-

Chemical composition of sulfide minerals

Химический состав сульфидных минералов

Mineral	Content, wt. %			
	Cu	Fe	S	Other
$CuFeS_2$	33.4	32.0	34.1	0.5
FeS_2	–	44.1	50.8	5.1

gents H_2SO_4, $CuSO_4 \cdot 5H_2O$, and $Fe_2(SO_4)_3 \cdot 9H_2O$ were used, dissolved in double-distilled water.

Statistical processing of results was carried out using Statgraphics 19 software with Microsoft Excel visualization tools. Chemical analysis of the leach products was performed by flame atomic absorption spectrometry (FAAS) on a NovAA 300 spectrometer (Analytik Jena, Germany). Classical titrimetric methods [24] were used to determine Fe^{2+} and residual H_2SO_4 concentrations in the solutions.

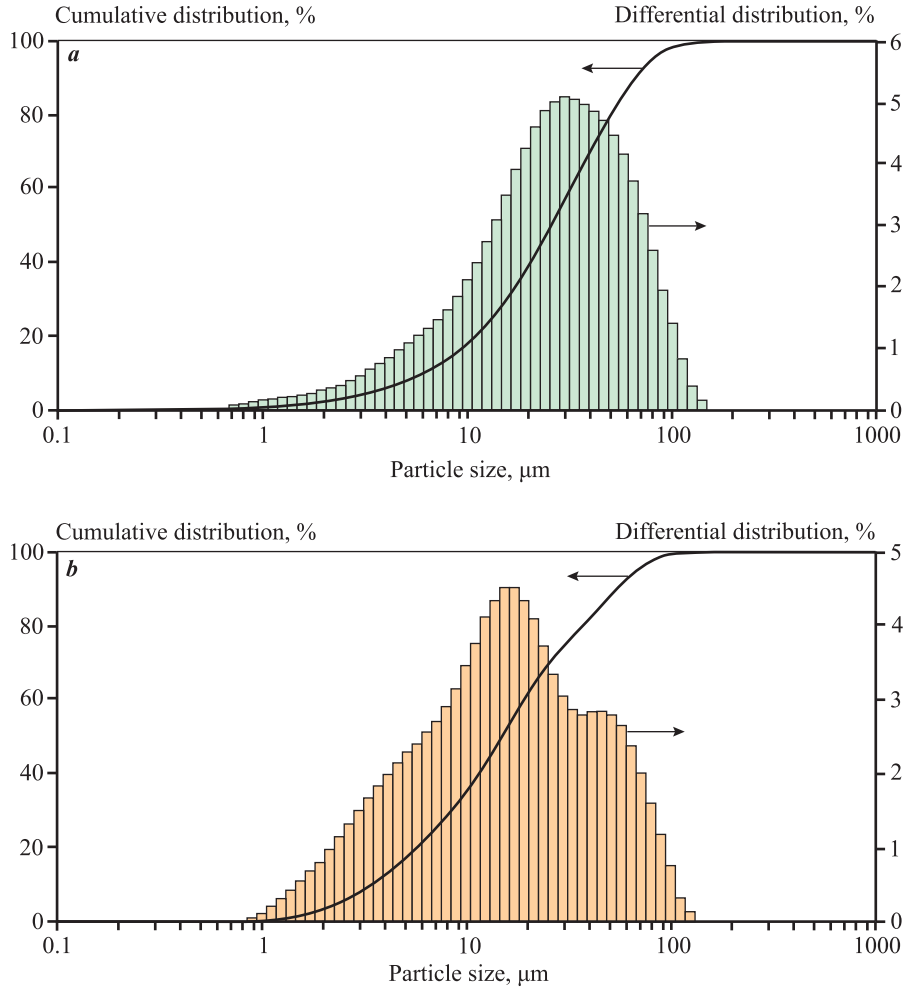

Fig. 1. Particle size distribution of chalcopyrite (***a***) and pyrite (***b***)

Рис. 1. Результаты гранулометрического анализа халькопирита (***a***) и пирита (***b***)

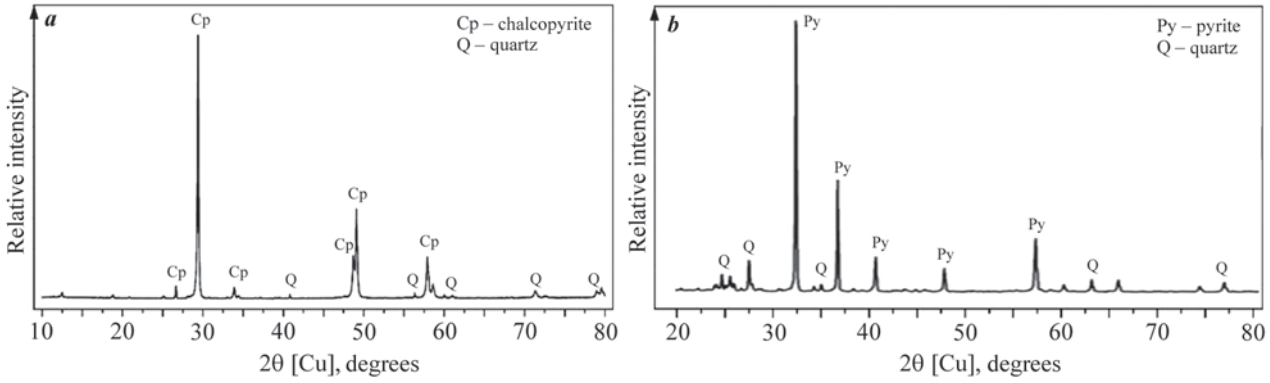

Fig. 2. XRD patterns of chalcopyrite (***a***) and pyrite (***b***)

Рис. 2. Дифрактограммы проб халькопирита (***a***) и пирита (***b***)

Leaching experiments were conducted in a sealed laboratory autoclave reactor system made of titanium alloy (Parr Instrument Company, USA), with a nominal volume of 1.0 dm^3 and a filling ratio of 0.6. The autoclave was equipped with a multifunctional monitoring system (temperature sensor, pressure sensor, and stirrer rotation speed sensor), a mixing mechanism (electromagnetic drive with variable speed control), and an oxygen flowmeter. A distinctive feature of the reactor was its ability to introduce reagents during operation without depressurization. Temperature control was provided by a two-section electric heating system connected to a digital PID controller, which maintained the set temperature within ±1 °C.

Before the experiment, a 20 g sulfide mineral sample was weighed on an analytical balance, and a 600 cm^3 solution containing the required concentrations of H_2SO_4, Fe^{3+}, and Cu^{2+} was prepared. After loading the slurry, the autoclave was sealed, stirring was started, and the pulp was heated to 100 °C. The stirring speed was maintained at 800 rpm. Once the target temperature was reached, oxygen was supplied and the experiment start time was recorded. At the end of the test, oxygen flow was stopped and the autoclave was cooled to 70 °C. The slurry was filtered, the residue washed, and dried to constant weight. Solid and liquid samples were then prepared for analysis.

Experimental studies were performed according to a second-order orthogonal design, including five variable factors at a fixed process temperature of 100 ± 1 °C, which prevents elemental sulfur melting. This temperature regime was selected as a constant parameter for all tests.

The independent variables were partial oxygen pressure (0.2—0.75 MPa), initial concentrations of sulfuric acid (10—50 g/dm^3), Fe^{3+} ions (2—10 g/dm^3), Cu^{2+} ions (1—3 g/dm^3), and leaching time (60—240 min). The dependent variables were copper and iron recoveries from chalcopyrite and pyrite, respectively.

Results and discussion

To assess the effect of copper and iron ions on chalcopyrite oxidation in a sulfuric acid medium, the degree of $CuFeS_2$ decomposition was plotted as a function of time (Fig. 3). In an earlier study [25], the kinetics of copper mineral dissolution, including $CuFeS_2$, were examined at low temperature and an oxygen pressure of 0.15—0.95 MPa, with a particle size of −0.44 μm (100 %).

As shown in Fig. 3, in the absence of sulfuric acid and ferric ions, chalcopyrite oxidation does not exceed 8 % after 240 min of leaching. In a weakly acidic medium ($[H_2SO_4]_0$ = 5 g/dm^3) [25], Fe^{2+} ions and covellite are formed according to

$$5CuFeS_2 + 3O_2 + 6H_2SO_4 = \\ = CuSO_4 + FeSO_4 + 4CuS + 6S^0 + 6H_2O, \quad (10)$$

which raises the degree of $CuFeS_2$ oxidation to 27 %.

When $[H_2SO_4]_0$ = 0 и $[Fe^{3+}]_0$ = 20 g/dm^3, the presence of Fe^{3+}, in accordance with the stoichiometric reaction (3), leads to the formation of ferrous sulfate and elemental sulfur. The low concentrations of H_2SO_4 (4.3 g/dm^3) and Fe^{2+} (3.5 g/dm^3) detected in the final solution indicate partial oxidation of sulfide sulfur to sulfate through

$$CuFeS_2 + Fe_2(SO_4)_3 + 3.5O_2 + H_2O = \\ = CuSO_4 + 3FeSO_4 + H_2SO_4, \quad (11)$$

thereby creating a weakly acidic medium that facilitates chalcopyrite oxidation via reactions (1) and (2), and Fe^{2+} oxidation to Fe^{3+} via reaction (9).

With an excess sulfuric acid concentration ($[H_2SO_4]_0$ = 50 g/dm^3) and the presence of Fe^{3+} ions, the degree of chalcopyrite dissolution increases to 35 %.

The addition of Cu_{2+} promotes the formation of secondary copper sulfides (CuS, Cu_2S) and makes it possible to reduce the initial $[Fe^{3+}]_0$ to <10 g/dm^3 due to the

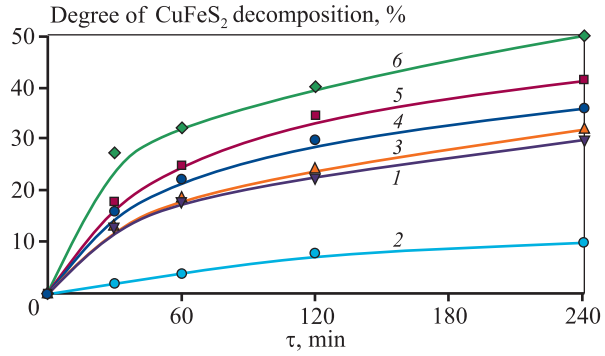

Fig. 3. Degree of $CuFeS_2$ decomposition vs. leaching time (P_{O_2} = 0.475 MPa)

Concentrations, g/dm^3: ***1*** – $[H_2SO_4]_0$ = 5, *t* = 110 °C, [25]; ***2*** – $[H_2SO_4]_0$ = 0, $[Fe^{3+}]_0$ = 0; ***3*** – $[H_2SO_4]_0$ = 50, $[Fe^{3+}]_0$ = 0; ***4*** – $[H_2SO_4]_0$ = 0, $[Fe^{3+}]_0$ = 20; ***5*** – $[H_2SO_4]_0$ = 50, $[Fe^{3+}]_0$ = 20; ***6*** – $[H_2SO_4]0$ = 50, $[Fe^{3+}]_0$ = 3,$[Cu^{2+}]_0$ = 2

Рис. 3. Степень разложения $CuFeS_2$ в зависимости от продолжительности эксперимента (P_{O_2} = 0,475 МПа)

Концентрации, г/$дм^3$: ***1*** – $[H_2SO_4]_0$ = 5, *t* = 110 °C, [25]; ***2*** – $[H_2SO_4]_0$ = 0, $[Fe^{3+}]_0$ = 0; ***3*** – $[H_2SO_4]_0$ = 50, $[Fe^{3+}]_0$ = 0; ***4*** – $[H_2SO_4]_0$ = 0, $[Fe^{3+}]_0$ = 20; ***5*** – $[H_2SO_4]_0$ = 50, $[Fe^{3+}]_0$ = 20; ***6*** – $[H_2SO_4]0$ = 50, $[Fe^{3+}]_0$ = 3,$[Cu^{2+}]_0$ = 2

formation and subsequent oxidation of $FeSO_4$ according to reactions (9), (12), and (13):

$$CuFeS_2 + CuSO_4 \rightarrow 2CuS + FeSO_4, \quad (12)$$

$$5CuFeS_2 + 11CuSO_4 + 8H_2O \rightarrow$$
$$\rightarrow 8Cu_2S + 5FeSO_4 + 8H_2SO_4. \quad (13)$$

Under these conditions, the degree of chalcopyrite decomposition reaches approximately 50 % within 240 min.

To determine the statistically significant parameters and evaluate their effect on chalcopyrite dissolution, a Pareto chart was constructed (Fig. 4).

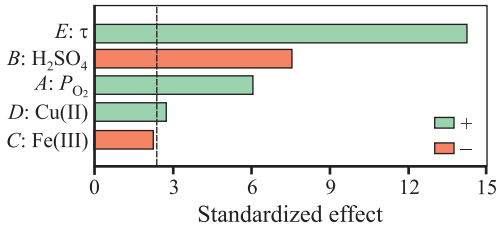

Fig. 4. Pareto chart for chalcopyrite oxidation

Рис. 4. Диаграмма Парето для окисления халькопирита

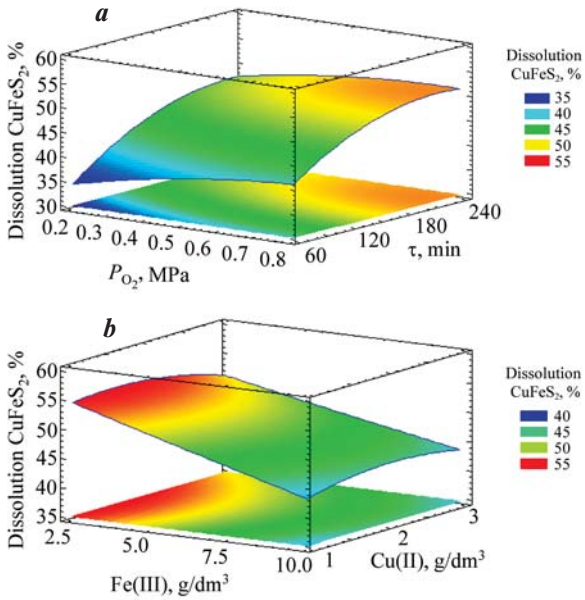

Fig. 5. Dependence of chalcopyrite dissolution on partial oxygen pressure and leaching time (***a***), and the initial concentrations of Cu^{2+} and Fe^{3+} ions (***b***)

Рис. 5. Зависимость растворения халькопирита от парциального давления кислорода и продолжительности опыта (***a***), а также от исходных концентраций ионов Cu^{2+} и Fe^{3+} (***b***)

Leaching time, initial sulfuric acid concentration, partial oxygen pressure, and Cu^{2+} concentration exert the strongest effects on chalcopyrite dissolution under low-temperature oxidative autoclave conditions.

Based on the experimental results, a three-dimensional response surface was generated to describe chalcopyrite dissolution as a function of partial oxygen pressure and leaching time at $[H_2SO_4]_0$ = = 31 g/dm^3, $[Cu^{2+}]_0$ = 2 g/dm^3, $[Fe^{3+}]_0$ = 6,25 g/dm^3 (Fig. 5, *a*).

As shown earlier, leaching time has the strongest positive effect on chalcopyrite dissolution. At P_{O_2} = = 0.6÷0.8 MPa and τ = 180 min, copper recovery reaches 50—55 %. Reducing the leaching time to 60 min results in a sharp decrease in copper recovery to 35—40 %.

Fig. 5, *b* illustrates the effects of Cu^{2+} and Fe^{3+} concentrations on chalcopyrite dissolution under constant conditions: $[H_2SO_4]_0$ = 50 g/dm^3, P_{O_2} = 0.475 MPa, τ = 240 min.

It was observed that increasing $[Fe^{3+}]_0$ from 2.5 to 10 g/dm^3 decreases copper recovery from 55 % to 44 %. This effect may be attributed to the accumulation of Fe^{3+} in solution, which promotes oxidation of $CuFeS_2$ to elemental sulfur via reaction (3), followed by sulfur passivation of the mineral particles [26; 27].

When the oxygen pressure is reduced to 0.2—0.4 MPa and the initial Fe^{3+} concentration to 2.5 g/dm^3 (Fig. 6), the contribution of reaction (9) — the generation and excess accumulation of Fe^{3+} — is limited, thereby reducing the likelihood of iron hydrolysis. Under these conditions, sulfuric-acid decomposition of chalcopyrite via reactions (1)—(4) proceeds with less restriction on reagent access to the mineral surface and remains at ~55 % after 240 min of leaching.

From the experimental data, the following regression equation was derived:

$$CuFeS_2 = 11.6514 + 2.55712P_{O_2} -$$
$$- 0.205448C_{H_2SO_4} + 0.319954C_{Fe(III)} +$$
$$+ 7.55577C_{Cu(II)} + 0.272454\tau - 0.130897P_{O_2} +$$
$$+ 0.00604642C_{H_2SO_4} + 0.00724245C^2_{Fe(III)} -$$
$$- 1.61708C^2_{Cu(II)} - 0.000451762\tau^2, \quad (14)$$

where P_{O_2} is the partial oxygen pressure, MPa; $C_{H_2SO_4}$, $C_{Fe(III)}$, $C_{Cu(II)}$ — are the initial concentrations of sulfuric acid, Fe^{3+}, and Cu^{2+} ions (g/dm^3), respectively; and τ is the leaching time (min).

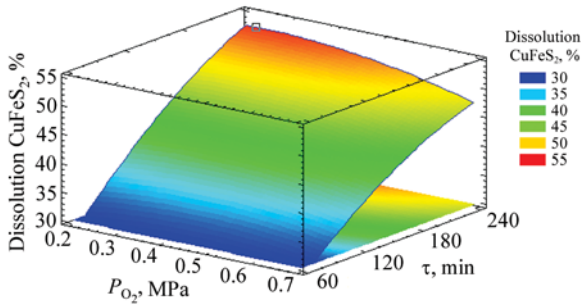

Fig. 6. Dependence of chalcopyrite dissolution on partial oxygen pressure and leaching time
$[H_2SO_4]_0$ – 50 g/dm^3, $[Cu^{2+}]_0$ – 1 g/dm^3, $[Fe^{3+}]_0$ – 2,5 g/dm^3

Рис. 6. Зависимость растворения халькопирита от парциального давления кислорода и продолжительности опыта
$[H_2SO_4]_0$ – 50 г/дм^3, $[Cu^{2+}]_0$ – 1 г/дм^3, $[Fe^{3+}]_0$ – 2,5 г/дм^3

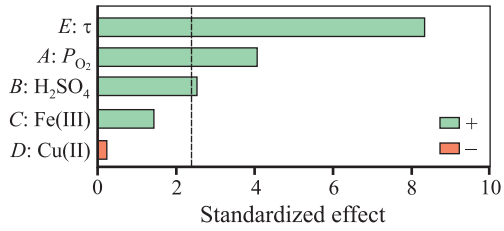

Fig. 7. Pareto chart for pyrite oxidation

Рис. 7. Диаграмма Парето для окисления пирита

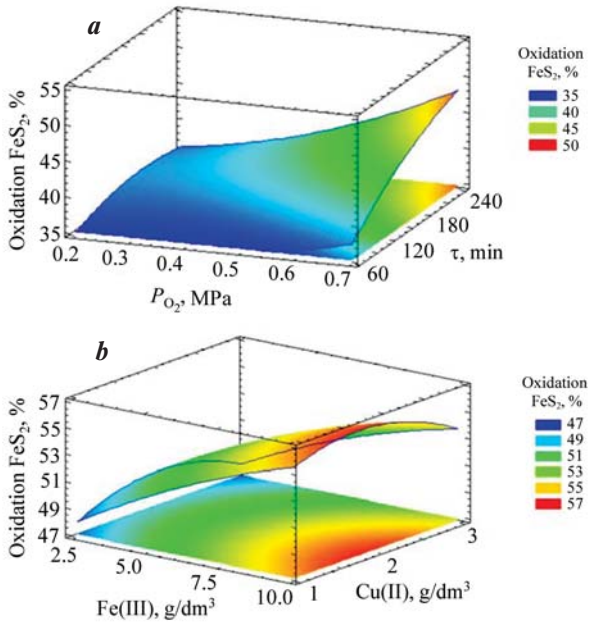

Fig. 8. Dependence of pyrite dissolution on partial oxygen pressure and leaching time (***a***), and initial concentrations of Cu^{2+} and Fe^{3+} ions (***b***)
a: $[H_2SO_4]_0$ – 31 g/dm^3, $[Cu^{2+}]_0$ – 2 g/dm^3, $[Fe^{3+}]_0$ – 6,25 g/dm^3
b: $[H_2SO_4]_0$ – 50 g/dm^3, P_{O_2} – 0,475 MPa, τ – 240 min

Рис. 8. Зависимость растворения пирита от парциального давления кислорода и продолжительности опыта (***a***), а также от исходных концентраций ионов Cu^{2+} и Fe^{3+} (***b***)
a: $[H_2SO_4]_0$ – 31 г/дм^3, $[Cu^{2+}]_0$ – 2 г/дм^3, $[Fe^{3+}]_0$ – 6,25 г/дм^3
b: $[H_2SO_4]_0$ – 50 г/дм^3, P_{O_2} – 0,475 МПа, τ – 240 мин

The coefficients of determination was $R^2 = 0.98$, confirming the adequacy of the model.

To identify statistically significant parameters and evaluate their effect on pyrite oxidation, a Pareto chart was constructed (Fig. 7).

The most influential factors are leaching time, oxygen pressure, and solution acidity. The addition of Cu^{2+} and Fe^{3+} ions has only a limited effect on oxidation efficiency, as indicated by the small change in the degree of oxidation when their concentrations are varied within the studied range.

These findings are consistent with [15], where a direct correlation was established between leaching time, oxygen pressure, and pyrite decomposition. At the same time, pyrite oxidation is accompanied by the formation of ferrous sulfate via reactions (6) and (7).

The dependence of iron leaching from pyrite on oxygen pressure and leaching time is presented in Fig. 8. At oxygen pressures below 0.5 MPa and leaching times of 60—120 min, pyrite oxidation does not exceed 35—40 %. A marked increase to 50 % is observed at $P_{O_2} = 0.75$ and $\tau = 240$ min. A nonlinear relationship between oxidation efficiency and acidity was also identified: increasing the sulfuric acid concentration from 10 to 35 g/dm^3 promoted pyrite decomposition.

Fig. 8, *b* shows the dependence of pyrite oxidation on the initial Cu^{2+} and Fe^{3+} concentrations. Introducing Fe^{3+} in the range 2.5—10.0 g/dm^3 markedly enhances pyrite oxidation, increasing the oxidation degree by ~10 % after 240 min. Pyrite is oxidized by Fe^{3+} ions, while the resulting Fe^{2+} is regenerated via reaction (10). According to the literature [28], Cu^{2+} ions exert a catalytic effect on the oxidation of Fe^{2+} to Fe^{3+}, which explains the synergistic effect observed when both ions are present. Adding Cu^{2+} at concentrations up to 2 g/dm^3 significantly accelerates Fe^{2+} oxidation to Fe^{3+}, thereby promoting further pyrite decomposition.

Optimal parameters were obtained at $P_{O_2} = 0.75$ MPa, $[H_2SO_4]_0 = 50$ g/dm^3, $[Cu^{2+}]_0 = 1.5 \div 2.0$ g/dm^3, and $[Fe^{3+}]_0 = 8 \div 10$ g/dm^3. Under these conditions, the maximum degree of pyrite oxidation reached 56 %.

From the experimental data, the following regression equation was derived:

$$Fe_2S = 38.4072 - 4.76472P_{O_2} + 0.513402C_{H_2SO_4} - 0.52213C_{Fe(III)} + 6.56917C_{Cu(II)} - 0.0712372\tau + 0.271903\,P^2_{O_2} - 0.0117899C^2_{H_2SO_4} - 0.0466268C^2_{Fe(III)} - 1.69325C^2_{Cu(II)} + 0.0000383004\tau^2. \quad (15)$$

with a coefficient of determination of $R^2 = 0.96$, confirming the adequacy of the model.

SEM images and EDS mapping of residues from low-temperature oxidation of chalcopyrite and pyrite are presented in Figs. 9 and 10. The residues were obtained at t = 100 °C, P_{O_2} = 0.75 MPa, $[H_2SO_4]_0$ = = 50 g/dm^3, $[Cu^{2+}]_0$ = 3 g/dm^3, $[Fe^{3+}]_0$ = 10 g/dm^3, τ = 240 min.

As seen in Fig. 9, chalcopyrite leach residue particles exhibit a heterogeneous surface, combining smooth areas with porous zones. EDS mapping showed the following distribution of the main components: sulfur (red), iron (green), and copper (yellow). Particles containing these zones correspond to chalcopyrite. Bright red surface deposits indicate local accumulation of elemental sulfur on chalcopyrite.

Similar studies of pyrite residues (Fig. 10) revealed a comparable but not identical pattern of surface transformations. A clear correlation was observed between particle size and composition: fine fractions consisted almost entirely of elemental sulfur, whereas larger particles corresponded to pyrite. Sulfur deposits were also detected at surface defect sites. Irregularly shaped conglomerates were especially evident on particles with developed surface morphology.

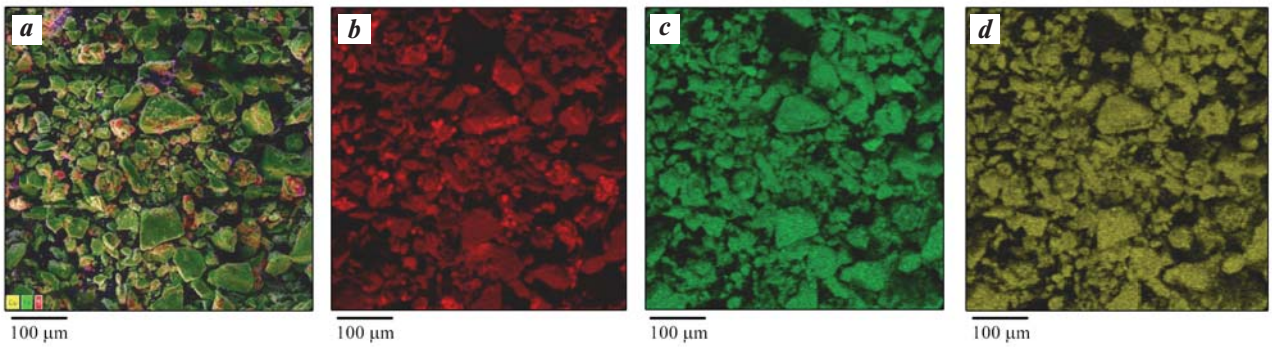

Fig. 9. SEM images of chalcopyrite oxidation residue and EDS mapping
a – general view, ***b*** – sulfur, ***c*** – iron, ***d*** – copper

Рис. 9. СЭМ-изображения частиц кека окисления халькопирита и результаты ЭДС-картирования
a – общий вид, ***b*** – сера, ***c*** – железо, ***d*** – медь

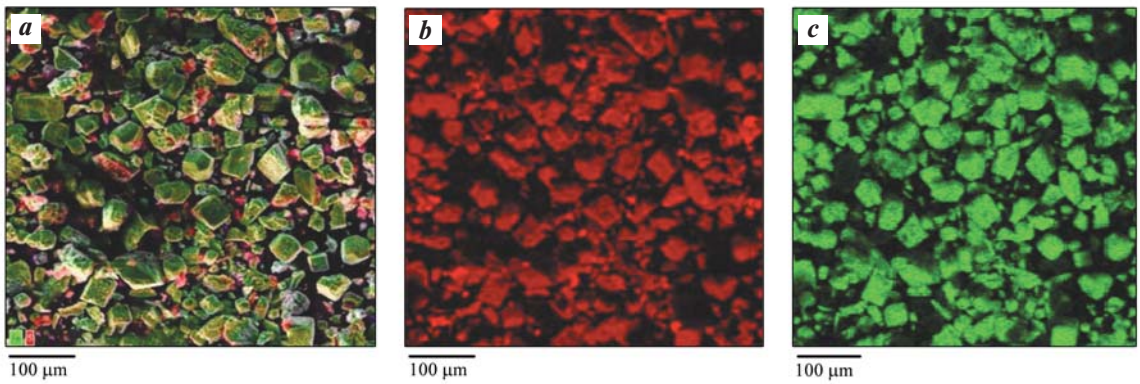

Fig. 10. SEM images of pyrite oxidation residue and EDS mapping
a – general view, ***b*** – sulphur, ***c*** – iron

Рис. 10. СЭМ-изображения частиц кека окисления пирита и результаты ЭДС-картирования
a – общий вид, ***b*** – сера, ***c*** – железо

Conclusion

This study investigated the low-temperature autoclave oxidation of the sulfide minerals, namely chalcopyrite and pyrite. Mathematical models were developed to describe the effects of oxygen pressure, sulfuric acid concentration, copper and iron ion concentrations, and leaching time, with coefficients of determination of $R^2 = 0.98$ for chalcopyrite and $R^2 = 0.96$ for pyrite, confirming the adequacy of the models. Optimal technological parameters were identified for effective decomposition of chalcopyrite, yielding 55 % copper recovery (P_{O_2} = 0.25 MPa; initial concentrations: $[H_2SO_4]_0$ = = 50 g/dm^3, $[Cu^{2+}]_0$ = 1 g/dm^3, $[Fe^{3+}]_0$ = 2.5 g/dm^3; τ = 240 min), and for pyrite, yielding 56 % iron recovery (P_{O_2} = 0.75 MPa; $[H_2SO_4]_0$ = 50 g/dm^3, $[Cu^{2+}]_0$ = = 2 g/dm^3, $[Fe^{3+}]_0$ = 10 g/dm^3; τ = 240 min).

The role of catalytic additives was also examined. Variation of the initial concentrations of $[Cu^{2+}]_0$ (1—3 g/dm^3) and $[Fe^{3+}]_0$ (2.5—10.0 g/dm^3) increased the degree of chalcopyrite oxidation by 8—11 % and pyrite oxidation by 10—13 %. SEM analysis of residues revealed local accumulation of elemental sulfur on the particle surfaces.

References

1. Shaibakova L. F. Global and Russian trends in the innovative development of copper production. *Regional'naya ekonomika i upravlenie: Elektronnyi nauchnyi zhurnal*. 2018;3(55):5. (In Russ.).
Шайбакова Л.Ф. Мировые и российские тенденции инновационного развития производства меди. *Региональная экономика и управление: Электронный научный журнал*. 2018;3(55):5.
2. Kondratiev V.B. Base metals: prospects in 2021. *Gornaya promishlennost'*. 2021;1:14—22. (In Russ.).
https://doi.org/10.30686/1609-9192-2021-1-14-22
Кондратьев В.Б. Базовые металлы: Перспективы в 2021 г. *Горная промышленность*. 2021;1:14—22.
https://doi.org/10.30686/1609-9192-2021-1-14-22
3. Vira D.Yu. Prospects for the development of Russian copper industry markets under new conditions. *Vestnik Altayskoy akademii ekonomiki i prava*. 2024;3(3):344—354. (In Russ.). https://doi.org/10.17513/vaael.3354
Вира Д.Ю. Перспективы развития рынков медной промышленности России в новых условиях. *Вестник Алтайской академии экономики и права*. 2024;3(3):344—354.
https://doi.org/10.17513/vaael.3354
4. Khopunov E.A. Modern directions of mineral raw materials processing. *Natsional'naya Assotsiatsiya Uchenykh (NAU)*. 2015;4-7(9):89—92. (In Russ.).
Хопунов Э.А. Современные направления переработки минерального сырья. *Национальная Ассоциация Ученых (НАУ)*. 2015;4-7(9):89—92.
5. Chanturia V.A., Shadrunova I.V., Gorlova O.E., Kolodezhnaya E.V. Development of technological innovations for deep and complex processing of man-made raw materials in the context of new economic challenges. *Izvestiya Tulskogo gosudarstvennogo universiteta. Nauki o zemle*. 2020;1:159—171. (In Russ.).
https://doi.org/10.46689/2218-5194-2020-1-1-159-171
Чантурия В.А., Шадрунова И.В., Горлова О.Е., Колодежная Е.В. Развитие технологических инноваций глубокой и комплексной переработки техногенного сырья в условиях новых экономических вызовов. *Известия Тульского государственного университета. Науки о земле*. 2020;1:159—171.
https://doi.org/10.46689/2218-5194-2020-1-1-159-171
6. Shumskaya E.N., Poperechnikova O.Yu., Tikhonov N.O. Development of technology for processing refractory pyrite polymetallic ore of Korbakhinskoye deposit. *Gornyy zhurnal*. 2014;(11):78—83. (In Russ.).
Шумская Е.Н., Поперечникова О.Ю., Тихонов Н.О. Разработка технологии обогащения труднообогатимой колчеданной полиметаллической руды Корбалихинского месторождения. *Горный журнал*. 2014;(11):78—83.
7. Shneerson Ya.M., Naboychenko S.S. Trends in the development of autoclave hydrometallurgy of nonferrous metals. *Tsvetnye metally*. 2011;(3):15—20. (In Russ.).
Шнеерсон Я.М., Набойченко С.С. Тенденции развития автоклавной гидрометаллургии цветных металлов. *Цветные металлы*. 2011;(3):15—20.
8. Lapshin D.A., Shneerson Ya.M. Autoclave processes in platinum metals hydrometallurgy. *Tsvetnye metally*. 2014;(5):39—43. (In Russ.).
Лапшин Д.А., Шнеерсон Я.М. Автоклавные процессы в гидрометаллургии платиновых металлов. *Цветные металлы*. 2014;(5):39—43.
9. Lapin A.Yu. History of development and implementation of autoclave-hydrometallurgical technology for processing nickel-pyrrhotite concentrates. *Tsvetnye metally*. 2020;(9):57—64. (In Russ.).
Лапин А.Ю. История создания и освоения автоклавно-гидрометаллургической технологии по пе-

переработке никель-пирротиновых концентратов. *Цветные металлы*. 2020;(9):57—64.

10. Padilla R., Vega D., Ruiz M.C. Pressure leaching of sulfidized chalcopyrite in sulfuric acid-oxygen media. *Hydrometallurgy*. 2007;86(1-2):80—88. https://doi.org/10.1016/j.hydromet.2006.10.006
11. McDonald R.G., Muir D.M. Pressure oxidation leaching of chalcopyrite. Part I. Comparison of high and low temperature reaction kinetics and products. *Hydrometallurgy*. 2007;86(3-4):191—205. https://doi.org/10.1016/j.hydromet.2006.11.015
12. Rusanen L., Aromaa J., Forsen O. Pressure oxidation of pyrite-arsenopyrite refractory gold concentrate. *Physicochemical Problems of Mineral Processing*. 2013;49:101—109. https://doi.org/10.5277/ppmp130110
13. Shoppert A., Valeev D., Loginova I., Pankratov D. Low-temperature treatment of boehmitic bauxite using the Bayer reductive method with the formation of high-iron magnetite concentrate. *Materials*. 2023;16(13):4678. https://doi.org/10.3390/ma16134678
14. Vasilyeva A.A., Boduen A.Ya., Vasilyev R.E. Analysis of the possibility of using hydrometallurgical methods to improve copper concentrate processing. *Vestnik IrGTU*. 2022;26(2):320—335. (In Russ.).
Васильева А.А., Бодуэн А.Я., Васильев Р.Е. Анализ возможности применения гидрометаллургических методов с целью улучшения переработки медных концентратов. *Вестник ИрГТУ*. 2022;26(2):320—335.
15. Epiforov A.V., Nabiulin R.N., Balikov S.V. Low-temperature autoclave oxidation of refractory sulfide gold-copper flotation concentrates followed by sulfite leaching of precious metals from oxidized cakes. *Izvestiya vuzov. Prikladnaya khimiya i biotekhnologiya*. 2014;3(8):31—38. (In Russ.).
Епифоров А.В., Набиулин Р.Н., Баликов С.В. Низкотемпературное автоклавное окисление упорных сульфидных золото-медных флотоконцентратов с последующим сульфитным выщелачиванием драгоценных металлов из окисленных кеков. *Известия вузов. Прикладная химия и биотехнология*. 2014;3(8):31—38.
16. Rogozhnikov D.A., Zakharian S.V., Dizer O.A., Karimov K.A. Nitric acid leaching of the copper-bearing arsenic sulphide concentrate of Akzhal. *Tsvetnye Metally*. 2020;8:11—16. https://doi.org/10.17580/tsm.2020.08.02
17. Gordeev D.V., Petrov G.V., Nikitina T.Yu. Application of two-stage sulfuric and chloride leaching for processing sulfide polymetallic concentrates. *Vestnik Magnitogorskogo gosudarstvennogo universiteta imeni G.I. Nosova*. 2022;20(3):13—25. (In Russ.).
Гордеев Д.В., Петров Г.В., Никитина Т.Ю. Применение двухстадийного сернокислого и хлоридного выщелачивания для переработки сульфидных полиметаллических концентратов. *Вестник Магнитогорского государственного университета им. Г.И. Носова*. 2022;20(3):13—25.
18. Rasskazova A.V., Sekisov A.G., Rasskazov M.I. Nitric-nitrite oxidation of copper-porphyry ores followed by activation chloride-sulfuric acid leaching of copper and noble metals. *GIAB*. 2023;9:130—140. (In Russ.).
Рассказова А.В., Секисов А.Г., Рассказов М.И. Азотнокислотно-нитритное окисление медно-порфировых руд с последующим активационным хлоридносернокислотным выщелачиванием меди и благородных металлов. *ГИАБ*. 2023;9:130—140.
19. Córdoba E.M., Muñoz J.A., Blázquez M.L., González F., Ballester A. Leaching of chalcopyrite with ferric ion. Part I: General aspects. *Hydrometallurgy*. 2008;93(3-4):81-87. https://doi.org/10.1016/j.hydromet.2008.04.015
20. Nourmohamadi H., Esrafili M.D., Aghazadeh V., Rezai B. The influence of Ag^{+} cation on elemental sulfur passive layer and adsorption behavior of chalcopyrite toward Fe^{3+} and Fe^{2+} ions: Insights from DFT calculations and molecular dynamics simulations. *Physica B: Condensed Matter*. 2022;627:413611. https://doi.org/10.1016/j.physb.2021.413611
21. Fomchenko N.V., Muravyov M.I. Effect of sulfide mineral content in copper-zinc concentrates on the rate of leaching of non-ferrous metals by biogenic ferric iron. *Hydrometallurgy*. 2019;185:82—87. https://doi.org/10.1016/j.hydromet.2019.02.002
22. Dizer O., Rogozhnikov D., Karimov K., Kuzas E., Suntsov A. Nitric acid dissolution of tennantite, chalcopyrite and sphalerite in the presence of Fe(III) ions and FeS_2. *Materials*. 2022;15(4):1545. https://doi.org/10.3390/ma15041545
23. Rogozhnikov D., Karimov K., Shoppert A., Dizer O., Naboichenko S. Kinetics and mechanism of arsenopyrite leaching in nitric acid solutions in the presence of pyrite and Fe(III) ions. *Hydrometallurgy*. 2021;199:105525. https://doi.org/10.1016/j.hydromet.2020.105525
24. Vasilyev V.I. Titrimetric and gravimetric methods of analysis: Textbook for university students. Moscow: Drofa, 2005. 366 p. (In Russ.).
Васильев В.И. Титриметрические и гравиметриче-

ские методы анализа: Учебник для студентов вузов. М.: Дрофа, 2005. 366 с.

25. Shneerson Ya.M., Frumina L.M., Ivanovsky V.V., Kasatkin S.V. Kinetics of oxidative pressure leaching of copper sulfide minerals. Sbornik nauchnih trudov instituta Gipronickel, Leningrad: Gipronickel, 1981. P. 53–61. (In Russ.).
Шнеерсон Я.М., Фрумина Л.М., Ивановский В.В., Касаткин С.В. Кинетика окислительного автоклавного выщелачивания медных сульфидных минералов. *Сборник научных трудов института Гипроникель*. Л.: Гипроникель, 1981. С. 53—61.
26. Córdoba E.M., Muñoz J.A., Blázquez M.L., González F., Ballester A. Leaching of chalcopyrite with ferric ion. Part IV: The role of redox potential in the presence of mesophilic and thermophilic bacteria. *Hydrometallurgy*. 2008;93(3-4):106—115. https://doi.org/10.1016/j.hydromet.2007.11.005
27. Li Y., Kawashima N., Li J., Chandra A.P., Gerson A.R. A review of the structure, and fundamental mechanisms and kinetics of the leaching of chalcopyrite. *Advances in Colloid and Interface Science*. 2013;(197-198):1—32. https://doi.org/10.1016/j.cis.2013.03.004
28. Michael J. Nicol. A comparative study of the kinetics of the oxidation of iron (II) by oxygen in acidic media — mechanistic and practical implications. *Hydrometallurgy*. 2020;192:105246. https://doi.org/10.1016/j.hydromet.2020.105246

Information about the authors

Maksim A. Tretiak – Cand. Sci. (Eng.), Junior Researcher, Scientific laboratory of advanced technologies for complex processing of mineral and man-made raw materials of non-ferrous and ferrous metals, Ural Federal University n.a. the First President of Russia B.N. Yeltsin (UrFU).
https://orcid.org/0000-0001-8405-8100
E-mail: m.a.tretiak@urfu.ru

Kirill A. Karimov – Cand. Sci. (Eng.), Senior Researcher, Scientific laboratory of advanced technologies for complex processing of mineral and man-made raw materials of non-ferrous and ferrous metals, UrFU.
https://orcid.org/0000-0003-1415-4484
E-mail: k.a.karimov@urfu.ru

Ulyana R. Sharipova – Master's Student, Research Engineer, Scientific laboratory of advanced technologies for complex processing of mineral and man-made raw materials of non-ferrous and ferrous metals, UrFU.
https://orcid.org/0000-0003-2598-8046
E-mail: ursharipova@urfu.ru

Aleksey V. Kritsky – Cand. Sci. (Eng.) Researcher, Scientific laboratory of advanced technologies for complex processing of mineral and man-made raw materials of non-ferrous and ferrous metals, UrFU.
https://orcid.org/0000-0002-8575-5925
E-mail: a.v.kritsky@urfu.ru

Denis A. Rogozhnikov – Dr. Sci. (Eng.), Head of the Scientific laboratory of perspective technologies for complex processing of mineral and man-made raw materials of non-ferrous and ferrous metals, UrFU.
https://orcid.org/0000-0002-5940-040X
E-mail: darogozhnikov@urfu.ru

Информация об авторах

Максим Алексеевич Третьяк – к.т.н., мл. науч. сотрудник научной лаборатории перспективных технологий комплексной переработки минерального и техногенного сырья цветных и черных металлов, Уральский федеральный университет имени первого Президента России Б.Н. Ельцина (УрФУ).
https://orcid.org/0000-0001-8405-8100
E-mail: m.a.tretiak@urfu.ru

Кирилл Ахтямович Каримов – к.т.н., ст. науч. сотрудник научной лаборатории перспективных технологий комплексной переработки минерального и техногенного сырья цветных и черных металлов, УрФУ.
https://orcid.org/0000-0003-1415-4484
E-mail: k.a.karimov@urfu.ru

Ульяна Рамильевна Шарипова – магистрант УрФУ, инженер-исследователь научной лаборатории перспективных технологий комплексной переработки минерального и техногенного сырья цветных и черных металлов, УрФУ.
https://orcid.org/0000-0003-2598-8046
E-mail: ursharipova@urfu.ru

Алексей Владимирович Крицкий – к.т.н., науч. сотрудник научной лаборатории перспективных технологий комплексной переработки минерального и техногенного сырья цветных и черных металлов, УрФУ.
https://orcid.org/0000-0002-8575-5925
E-mail: a.v.kritsky@urfu.ru

Денис Александрович Рогожников – д.т.н., зав. лабораторией перспективных технологий комплексной переработки минерального и техногенного сырья цветных и черных металлов, УрФУ.
https://orcid.org/0000-0002-5940-040X
E-mail: darogozhnikov@urfu.ru

Contribution of the authors

M.A. Tretiak – defined the research objectives and plan, conducted the first-stage experiments, processed the results, and prepared the article materials.

K.A. Karimov – supervised and monitored the progress of the work, participated in the discussion of the results, and contributed to the preparation of the article materials.

U.R. Sharipova – processed the results, prepared the article materials and documentation.

A.V. Kritskiy – conducted the second-stage experiments and participated in the discussion of the results.

D.A. Rogozhnikov – supervised and monitored the progress of the work and participated in the discussion of the results.

Вклад авторов

М.А. Третьяк – определение цели и плана работы, проведение экспериментов первого этапа, обработка результатов, подготовка материалов статьи.

К.А. Каримов – курирование и контроль хода работы, участие в обсуждении результатов, подготовка материалов статьи.

У.Р. Шарипова – обработка результатов, подготовка материалов статьи и документации.

А.В. Крицкий – проведение экспериментов второго этапа, участие в обсуждении результатов.

Д.А. Рогожников – курирование и контроль хода работы, участие в обсуждении результатов.

The article was submitted 05.05.2025, revised 19.05.2025, accepted for publication 23.05.2025

Статья поступила в редакцию 05.05.2025, доработана 19.05.2025, подписана в печать 23.05.2025

UDC 543.54 : 544.72
https://doi.org/10.17073/0021-3438-2025-3-28-36

Research article
Научная статья

Oxidative degradation of lignosulfonates during pressure leaching of zinc concentrates

T.N. Lugovitskaya, O.S. Anisimova, D.A. Rogozhnikov

Ural Federal University n.a. the First President of Russia B.N. Yeltsin
19 Mira Str., Ekaterinburg 620002, Russia

✉ Tatyana N. Lugovitskaya (t.n.lugovitskaia@urfu.ru)

Abstract: This study investigates the effect of preliminary autoclave oxidation with molecular oxygen (T = 423 K, P_{O_2} = 0.6 MPa, τ = 2 h) on lignosulfonates differing in chemical composition and molecular weight distribution. Oxidation resulted in a reduction of hydroxyl groups and an increase in carbonyl groups, along with marked changes in solution properties such as redox potential, pH, specific conductivity, and surface tension at the liquid–gas interface. The functional activity of the initial and oxidized lignosulfonates was compared in terms of their ability to remove elemental sulfur films from the sphalerite surface under high-temperature oxidative pressure leaching conditions. The findings show that oxidative treatment decreases the effectiveness of lignosulfonates by diminishing their surface activity.

Keywords: high-temperature pressure leaching, sphalerite, surfactant, lignosulfonates, oxidative degradation, recovery, leaching.

Acknowledgments: The study was financially supported by the State Assignment of the Russian Federation (grant No. 075-03-2024-009/1, FEUZ-2024-0010).

For citation: Lugovitskaya T.N., Anisimova O.S., Rogozhnikov D.A. Oxidative degradation of lignosulfonates during pressure leaching of zinc concentrates. *Izvestiya. Non-Ferrous Metallurgy.* 2025;31(3):28–36. https://doi.org/10.17073/0021-3438-2025-3-28-36

Деструктивные превращения лигносульфонатов при автоклавном выщелачивании цинковых концентратов

Т.Н. Луговицкая, О.С. Анисимова, Д.А. Рогожников

Уральский федеральный университет имени первого Президента России Б.Н. Ельцина
Россия, 620002, г. Екатеринбург, ул. Мира, 19

✉ Татьяна Николаевна Луговицкая (t.n.lugovitskaia@urfu.ru)

Аннотация: Представлены результаты влияния предварительной окислительной обработки молекулярным кислородом в автоклавных условиях (T = 423 K, P_{O_2} = 0,6 МПа, τ = 2 ч) образцов лигносульфонатов, отличающихся химическим составом и молекулярно-массовым распределением. Показано, что их окисление сопровождается уменьшением гидроксогрупп и увеличением в продуктах окисления карбонильных групп, а также изменением физико-химических свойств растворов – окислительно-восстановительного потенциала, pH, удельной электропроводности, поверхностного натяжения на границе жидкость/газ. Приведена сравнительная оценка функциональной активности исходных и окисленных образцов лигносульфонатов в части удаления

с поверхности сфалерита пленок элементной серы непосредственно в условиях высокотемпературного окислительного выщелачивания. Установлено, что окислительная автоклавная обработка лигносульфонатов ухудшает их функциональный эффект (поверхностную активность).

Ключевые слова: высокотемпературное автоклавное выщелачивание, сфалерит, поверхностно-активные вещества, лигносульфонаты, деструкция, извлечение, выщелачивание.

Благодарности: Исследование выполнено при финансовой поддержке Госзадания РФ по гранту № 075-03-2024-009/1 (FEUZ-2024-0010).

Для цитирования: Луговицкая Т.Н., Анисимова О.С., Рогожников Д.А. Деструктивные превращения лигносульфонатов при автоклавном выщелачивании цинковых концентратов. *Известия вузов. Цветная металлургия*. 2025;31(3):28–36.
https://doi.org/10.17073/0021-3438-2025-3-28-36

Introduction

High-temperature pressure leaching of sulfide concentrates containing zinc, lead, copper, and nickel is now widely practiced worldwide [1; 2]. Compared with the conventional roasting — leaching route, pressure leaching provides [3; 4]:

— clear environmental benefits, as it avoids SO_2 emissions by converting sulfur in the concentrate into elemental sulfur (S0), which can be safely stored and transported;

— greater processing flexibility, making it possible to treat low-grade sulfide ores and those with a high iron content;

— more efficient resource utilization, with the potential to recover not only the principal metals but also valuable by-products such as gallium, germanium, indium, silver, and cadmium.

Pressure leaching of sulfide concentrates is carried out at temperatures above 373 K and is accompanied by the formation of molten elemental sulfur films on the mineral surface, resulting in sulfur passivation and consequent inhibition or complete cessation of oxidative dissolution [5—7]. Certain surfactants can counteract this shielding effect of sulfur, opening up the possibility of applying higher-temperature conditions and further intensifying autoclave processes [8; 9].

In hydrometallurgical practice, particularly in the processing of zinc, lead—zinc, and nickel—pyrrhotite concentrates, the most common surfactants are technical lignosulfonates (LS) — by-products of wood pulping [10—12]. Transitioning from low- to high-temperature leaching (410—425 K) boosts process throughput by a factor of at least 2.5. At the same time, more complete exposure of sphalerite inclusions in associated minerals such as pyrite and chalcopyrite provides an additional 2—5 % zinc recovery into solution.

Chemically, lignosulfonates are branched aromatic polymers with a wide molecular weight distribution (5000—80 000 Da), high functional diversity (hydroxyl, methoxy, carboxyl, carbonyl, and sulfonic groups), and pronounced polydispersity [13—15]. Fig. 1 shows a representative fragment of the lignosulfonate macromolecule.

The amphiphilic structure of lignosulfonates accounts for their surface activity: along with ionogenic

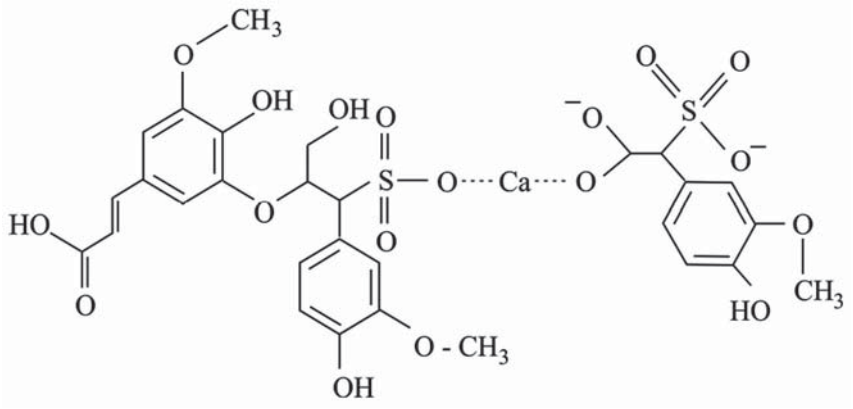

Fig. 1. Fragment of a lignosulfonate macromolecule [16]

Рис. 1. Фрагмент макромолекулы лигносульфонатов [16]

functional groups, they contain cross-linked aliphatic and aromatic carbon chains [17—19].

Surface activity and other physicochemical properties of lignosulfonates depend on both the type of wood used (softwood or hardwood) and the pulping conditions. Because lignosulfonates are by-products, their quality is not standardized.

Their use in hydrometallurgy is further complicated by the instability of their properties over time; efficiency also decreases as the duration of pressure leaching increases. This decline is likely due to chemical degradation of lignosulfonates under the harsh thermo-oxidative conditions applied to ores and concentrates [11].

To investigate this effect, in this work, lignosulfonate samples differing in chemical composition and molecular weight distribution were deliberately subjected to autoclave oxidation with molecular oxygen (T = 423 K, P_{O_2} = 0.6 MPa, τ = 2 h). Their functional performance was then evaluated directly under high-temperature oxidative pressure leaching of a zinc concentrate. This allowed us to assess how oxidative treatment influences the structure and efficiency (i.e., surface properties) of lignosulfonates during pressure leaching.

Materials and methods

The study employed the following samples and reagents:

1. Lignosulfonates (LS). Samples were obtained from the Solikamsk Pulp and Paper Mill (JSC "Solikamskbumprom", Russia, TU 2455-028-00279580-2014) (LSNo.1) and from LignoTech (Norway) (LSNo.2). Their elemental and functional compositions are given in Table 1. The samples were oxidized in an autoclave with molecular oxygen at T = 423 K and P_{O_2} = = 0.6 MPa for 2 h. The oxidation products of LSNo.1 and LSNo.2 — hereafter LSONo.1 and LSONo.2 — were subsequently characterized by physicochemical methods.

2. Zinc concentrate. A standard zinc concentrate from the Belousovsky Mining and Processing Plant was used. At least 90 % of the material was finer than 74 μm, with the following composition (wt. %): Zn — 48.9, Cu — 0.9, Fe — 8.7, S — 32.5. The principal minerals were sphalerite, present as liberated grains 1—100 μm in size (≥70 %), and pyrite containing fine inclusions of sphalerite and chalcopyrite (1—25 μm) amounting to 20—25 %.

3. Gangue minerals. Represented mainly by oxides of Si (0.3 %), Al (0.2 %), and Ca (0.3 %).

Table 1. **Elemental and functional composition of lignosulfonates**

Таблица 1. Элементный и функциональный состав лигносульфонатов

Element/group	LS samples	
	No. 1	No. 2
C	29.0	41.7
O	54.5	38.2
S	5.5	5.4
Na	6.6	0.8
K	0.04	–
Ca	–	4.0
SO_3H	12.11	12.3
OCH_3	9.6	9.2
OH_{phen}	2.1	2.0

4. Sulfuric acid. Solution with a concentration of 140 g/dm^3.

5. Oxygen. Technical-grade oxygen supplied from cylinders.

Elemental composition of lignosulfonates was determined with an Elementar Vario MICRO cube analyzer (Germany) with an accuracy of ±0.5 wt. %. IR spectra of the initial and oxidized LS samples were recorded on a Bio-Rad FTS-175 FT-IR spectrometer in the range 400—5000 cm^{-1}, with a resolution of 0.5 cm^{-1} and an absolute error of ±0.1 cm^{-1}. Gravimetric measurements were performed on Ohaus Discovery analytical balances (USA) with an accuracy of ±0.0001 g. pH values were measured on a Mettler Toledo FiveEasy FE20 pH meter (Singapore), calibrated with NIST-traceable buffers (pH 4.01, 7.00, and 10.01). Surface tension of LS solutions at the liquid—gas interface ($\sigma_{liq\text{-}g}$, J/m^2) was measured with a Rehbinder tensiometer. The surface morphology of the leach residue (particles, grains, and granules) was examined by scanning electron microscopy (SEM) using a dual-beam Carl Zeiss Auriga CrossBeam dual-beam FIB-SEM (Germany) equipped with an Oxford Instruments INCA 350 EDS system and an X-Max 80 detector (UK). Imaging was performed in backscattered electron mode with compositional contrast at an accelerating voltage of 20 kV and a probe current of 1.2 nA.

Pressure leaching experiments were performed in a Vishnevsky-type autoclave (titanium, 1 dm^3 capacity) equipped with stirring, temperature control, sampling,

and instrumentation. The reactor filling ratio was maintained at 0.60.

Experiments were conducted at a fixed temperature of 415 K, oxygen partial pressure of 0.4—0.5 MPa, and stoichiometric consumption of sulfuric acid relative to sphalerite (molar ratio H_2SO_4 : ZnS = 1.0). The LS concentration in the slurry was varied from 0.05 to 1.50 g/dm^3.

After loading the concentrate, initial or oxidized LS samples (sealed in glass ampoules), and sulfuric acid solution, the reactor was sealed and the slurry heated to the target temperature. Once the set temperature was reached, oxygen was introduced via a regulator to establish the required partial pressure, and stirring was initiated. The hydrodynamic conditions in the leaching slurry were kept constant at Re = 10^4 (Reynolds number). The start of agitation and the breaking of ampoules with LS were taken as time zero for the leaching process.

Samples were collected at regular intervals (5, 15, 30, 60, and 120 min) for chemical analysis. The solutions were analyzed for Zn, Fe(II), Fe(III), and H_2SO_4 concentrations. After each run, the reactor was cooled, the slurry filtered, the solid phase washed with distilled water, dried, and analyzed for Zn, Pb, total sulfur (S_{total}), and elemental sulfur (S^0). The progress of oxidation in the presence of LS was monitored by zinc recovery (ε_{Zn}, %), iron recovery (ε_{Fe}, %), degree of acid neutralization (ε_{acid}, %), and conversion of sulfide sulfur to elemental sulfur (ε_S, %). The leach residues were further characterized for particle size distribution and the fraction of sulfur—sulfide aggregates.

Results and discussion

Before comparing the functional activity of the initial and oxidized lignosulfonates (LS) under high-temperature oxidative pressure leaching, it is useful to examine their composition and physicochemical properties.

As reported earlier [20], he weight-average molecular masses of LSNo.1 and LSNo.2 were 9250 and 46300 Da, respectively. Elemental analysis (Table 1) showed that LSNo.2 contained 13 % more carbon and 16 % less oxygen compared with LSNo.1. The cationic composition of LS in sulfite liquors also differed: LSNo.1 contained sodium ions (6.6 %), whereas LSNo.2 contained calcium ions (4 %).

The IR spectra of the initial samples (Fig. 2) exhibited broad absorption bands at ν = 3420 cm^{-1} and 1510—1610 cm^{-1}, attributable to hydroxyl groups and aromatic ring vibrations. Methoxy groups (—OCH_3) were confirmed by absorptions in the range ν = = 1039÷1042 cm^{-1} [21—23]. A broad band at ν = = 1210÷1190 cm^{-1}, along with medium and weak absorptions at 655 cm^{-1} and 540—520 cm^{-1}, indicated the presence of sulfonate groups. Peaks in the region ν = 1675÷1640 cm^{-1} corresponded to carboxyl groups conjugated with the benzene ring. In LSNo.1, a weak band at ν = 1720÷1715 cm^{-1} was assigned to non-conjugated carbonyl groups (C=O), which were absent in LSNo.2. These findings confirm that the two samples differ in chemical composition and molecular weight distribution.

The LS samples were then subjected to oxidative treatment (T = 423 K, P_{O_2} = 0.6 MPa, τ = 2 h), and the structural features of the oxidation products and the physicochemical properties of their aqueous LSO solutions were determined.

Comparative analysis of the IR spectra of the initial LS and their oxidation products (LSO) (Fig. 2) revealed new absorption bands at ν = 1720 and 1640 cm^{-1}, corresponding to stretching vibrations of non-conjugated and conjugated carbonyl groups (C=O). At the same time, the intensity of the hydroxyl band at ν = 3420 cm^{-1} decreased.

Under more severe oxidation conditions (higher temperature, longer duration, or elevated oxygen pressure), the band at ν = 1510 cm^{-1}, characteristic of skeletal vibrations of the aromatic ring, disappeared.

This indicates that oxidation of LS leads to the formation of carboxyl, carbonyl, and orthoquinone groups and, under harsher conditions, to chemical degradation of aromatic rings with the formation of lower carboxylic derivatives.

Oxidation also significantly altered the physicochemical properties of LS solutions. Measurements of specific conductivity (κ), redox potential (Eh), pH, and surface tension (σ_{liq-g}) as a function of LSO concentration (Table 2) showed the following trends:

— as LSO concentration increased from 0.01 to 0.64 g/dm^3, pH decreased from 4.3—5.4 to 3.4—3.5, while Eh rose from 185 to 385 mV and conductivity increased from (12÷20)·10^{-5} to (370÷440)·10^{-5} μS/m;

— compared with the initial LS, the oxidized samples exhibited greater surface activity: the minimum surface tension (σ_{liq-g} ≈ 0.068 J/m^2) for LSONo.1 was observed at 0.16—0.32 g/dm^3, whereas for LSONo.2 it was reached only at higher concentrations (>0.16 g/dm^3).

Thus, the observed changes in the structure and physicochemical properties of LS indicate that their

Table 2. **Physicochemical characteristics of solutions of the initial and oxidized LS**

Таблица 2. Физико-химические характеристики растворов исходных и окисленных ЛС

Sample	LS concentration, g/dm^3	$\kappa \cdot 10^5$, μS/m		pH		$\sigma_{liq\text{-}g} \cdot 10^3$, J/m^2		Eh, mV	
		LS	LSO	LS	LSO	LS	LSO	LS	LSO
LSNo.1	0.01	7	12	4.4	5.4	80.0	78.1	280	185
	0.02	10	19	5.5	5.2	76.7	79.6	275	195
	0.04	14	34	6.0	5.1	75.2	72.6	240	215
	0.08	22	55	5.7	4.6	75.9	70.6	240	235
	0.16	39	104	5.6	4.2	75.2	68.2	220	245
	0.32	82	200	5.7	4.0	78.1	68.6	200	325
	0.64	130	379	5.8	3.5	75.2	69.1	200	385
LSNo.2	0.01	28	20	5.8	4.3	80.0	79.6	349	310
	0.02	37	26	6.6	4.3	82.3	81.0	280	300
	0.04	40	36	6.7	4.1	86.8	79.5	284	315
	0.08	44	65	6.8	3.9	88.2	79.6	264	320
	0.16	55	116	7.0	3.8	79.6	79.6	280	345
	0.32	70	320	7.3	3.7	79.6	72.3	279	345
	0.64	85	400	7.3	3.5	78.2	75.2	285	340

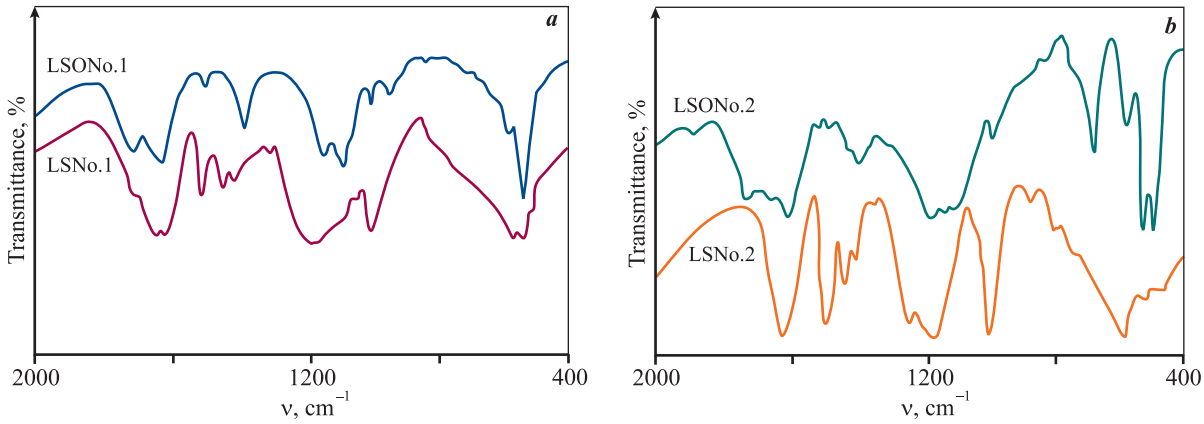

Fig. 2. IR spectra of the initial and oxidized samples of lignosulfonates: LSNo.1 (***a***) and LSNo.2 (***b***)

Рис. 2. ИК-спектры исходных и окисленных образцов лигносульфонатов ЛС№1 (***a***) и ЛС№2 (***b***)

efficiency may differ under high-temperature pressure leaching conditions.

Subsequently, the effect of the initial and oxidized LS samples on the performance of zinc concentrate pressure leaching was investigated.

Preliminary tests were carried out without lignosulfonates in the leaching slurry (baseline case). A sharp decrease in the oxidation rate indicated onset of sulfur passivation by molten elemental sulfur films within the first 15—20 min of oxidative treatment, at a mineral conversion of 35—40 %. The insoluble residues were dominated by spheroidal aggregates larger than 0.25 mm, consisting of unreacted sphalerite cores encased in poorly crystallized polygonal elemental sulfur.

Overall, zinc recovery into solution did not exceed 50 % after 2.0—2.5 h of leaching without LS.

Similar results were obtained in the presence of LSNo.1. Within the studied concentration range, the kinetic curves leveled off at 55—65 % conversion, reflecting sulfur passivation of the sphalerite surface. As in the baseline case, the residues contained sulfur—sulfide granules larger than 0.25 mm. Elemental sulfur films on sphalerite were also observed at low LSNo.2 additions (<0.15 g/dm^3). Oxidation of sphalerite accelerated after 30—40 min of leaching and was significantly more intense in the presence of LSNo.2.

By the time sphalerite had been leached for about 100—140 min, most of the added LS were expected to have undergone oxidation, so that oxidized forms would predominate in solution. This made it relevant to evaluate their functional activity directly under these conditions. After 3 h of leaching, zinc recovery with LSONo.1 was 9—10 percentage points lower than with unoxidized LS (at comparable concentrations of 1.0 g/dm^3), amounting to only 62—63 %.

The most favorable results were obtained with the high-molecular-weight LSNo.2. At concentrations of 0.25—0.50 g/dm^3, zinc recovery reached 90—91 % within 2 h. Beyond this point, the leaching rate slowed, reflecting zinc release from sphalerite inclusions enclosed in pyrite grains. At insufficient LSNo.2 concentrations (<0.15 g/dm^3), sulfur passivation limited sphalerite oxidation to 72—75 %. This was confirmed by residue morphology: fine gangue particles, spherical particles 15—25 μm in size consisting of unleached sulfides coated with elemental sulfur (Fig. 3, *a*), and sulfur—sulfide granules larger than 0.5 mm.

Concurrent oxidation of LS during leaching impaired their functional efficiency, as confirmed by experiments with pre-oxidized samples. After 2 h of leaching, zinc recovery in the presence of LSONo.2 was 18—19 percentage points lower than with unoxidized LSNo.2. The reduced interfacial activity of oxidized samples was accompanied by the formation of sulfur—sulfide aggregates 0.10—0.15 mm in size in the residues. Similar degradation of LS and lower metal recovery have also been reported in the literature [11; 12].

Balance tests were conducted under conditions optimized for the composition and concentration of LS (Table 3). As expected, LSNo.2 provided the most effective performance: after 2 h of leaching, 90.5 % Zn and 38.1 % Fe were extracted into solution, while acid neutralization reached 85.9 %. The residue yield was 39—41 % with an elemental sulfur content of 45—46 %, and no sulfur—sulfide granules were detected (Fig. 3, *b*).

Thus, testing of different LS samples under pressure leaching conditions was consistent with the predictive assessments obtained earlier from physicochemical studies of lignosulfonates and confirmed the high functional efficiency of the high-molecular-weight sample (LSNo.2). The unsatisfactory performance of low-molecular-weight LS, as well as their oxidation products, is attributed to an insufficient interfacial wedge effect at the sphalerite—sulfur boundary.

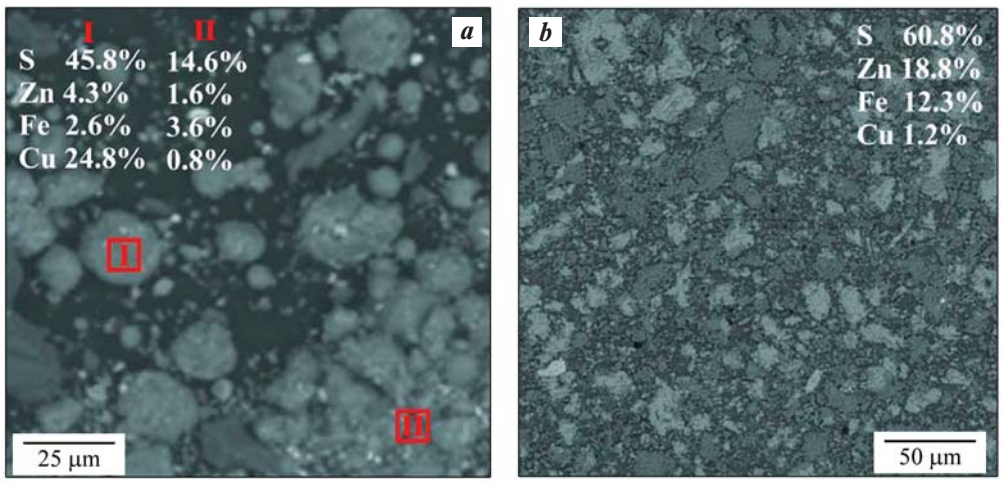

Fig. 3. SEM images and elemental analysis of leach residues obtained with LSNo.2 (***a***) and LSONo.2 (***b***)

Рис. 3. СЭМ-изображения и результаты элементного анализа кека, полученного при выщелачивании в присутствии образцов ЛСN°2 (***a***) и ЛСО№2 (***b***)

Table 3. **Parameters of zinc concentrate pressure leaching in the presence of various LS samples**

Таблица 3. Показатели автоклавного выщелачивания цинкового концентрата в присутствии различных образцов ЛС

LS samples	Test conditions*		Content in solution, g/dm^3				Recovery, %			Granule formation
	LS concentration, g/dm^3	τ, min	Zn	Fe(II)	$Fe_{общ}$	H_2SO_4	Zn	Fe**	H_2SO_4	
–	0.00	180	51.0	2.3	2.7	70.9	54.0	16.0	50.2	Yes
LSNo.1	0.25	180	61.5	2.9	3.2	58.5	65.1	18.9	58.9	Yes
LSNo.1	1.00	180	67.8	3.3	3.5	54.7	71.8	20.8	61.6	Yes
LSONo.1	1.00	180	58.6	3.1	3.5	62.9	62.1	20.8	55.8	Yes
LSNo.2	0.10	120	68.5	3.3	4.0	45.3	72.5	23.8	68.2	Yes
LSNo.1	0.25	120	85.5	5.4	6.4	20.1	90.5	38.1	85.9	No
LSONo.2	0.25	120	68.5	4.3	4.8	4.6	72.5	28.8	69.4	Yes

* Conditions: $T = 413$ K, $P_{O_2} = 0{,}5$ MPa, $[H_2SO_4] = 140$ g/dm^3.
** From pyrite (according to phase analysis of residues).

Conclusion

The investigation of the physicochemical properties of LS used to remove elemental sulfur films from the sphalerite surface during pressure leaching of zinc-bearing sulfide feed is not only of theoretical interest but also provides a foundation for optimizing oxidation processes and subsequent operations for the processing of solutions and leach residues.

The effect of LS of different composition, including samples pre-oxidized with molecular oxygen, was evaluated during sulfuric acid pressure leaching of zinc concentrate from the Belousovsky Mining and Processing Plant under the following conditions: $T = 415$ K, $P_{O_2} = 0.5$ MPa, $[H_2SO_4]_0 = 140$ g/dm^3, Re = 10^4, H_2SO_4 : ZnS = 1.0.

High-molecular-weight LS (46300 Da) proved to be the most effective both in removing elemental sulfur films from the sphalerite surface and in ensuring intensive and near-quantitative zinc dissolution. At LSNo.2 concentrations above 0.15 g/dm^3, stable leaching proceeded without the formation of sulfur—sulfide aggregates. Within 120 min of leaching, 90.5 % Zn and up to 38 % Fe were recovered into solution. The leach residues, which accounted for 39—41 % of the mass, contained no less than 45 % elemental sulfur.

The results demonstrated that LS efficiency depends not only on their molecular-weight distribution but also on the chemical transformations they undergo under pressure leaching conditions. Compared with unoxidized LS, the oxidation products were less effective in removing elemental sulfur films from the sphalerite surface: zinc recovery decreased by 10—12 percentage points and did not exceed 72—75 %.

References

1. Jorjani E., Ghahreman A. Challenges with elemental sulfur removal during the leaching of copper and zinc sulfides, and from the residues: A review. *Hydrometallurgy*. 2017;(171):333—343. https://doi.org/10.1016/j.hydromet.2017.06.011
2. Kolmachikhina E.B., Lugovitskaya T.N., Tretiak M.A., Rogozhnikov D.A. Surfactants and their mixtures under conditions of autoclave sulfuric acid leaching of zinc concentrate: Surfactant selection and laboratory tests. *Transactions of Nonferrous Metals Society of China*. 2023;33(11):3529—3543. https://doi.org/10.1016/S1003-6326(23)66352-6
3. Wang Y., Wang H., Li X., Zheng C. Study on the improvement of the zinc pressure leaching process. *Hydrometallurgy*. 2020;(195):105400. https://doi.org/10.1016/j.hydromet.2020.105400
4. Qiang L., Cun-xiong L., Zhi-hui G., Chang-wen L., Qi-liang W. Study on pre-oxidation of silver concentrate and leaching behaviour of Zn, Cu and In during oxygen-pressure leaching. *Hydrometallurgy*. 2024;(228):106358. https://doi.org/10.1016/j.hydromet.2024.106358
5. Collins M. J. Autoclave leaching. *Treatise on Process Metallurgy*. 2025;(2B): 373—388. https://doi.org/10.1016/B978-0-443-40294-4.00030-X

6. Tong L., Dreisinger D. Interfacial properties of liquid sulfur in the pressure leaching of nickel concentrate. *Minerals Engineering*. 2009;22(5):456—461. https://doi.org/10.1016/j.mineng.2008.12.003
7. Dizer O., Rogozhnikov D., Karimov K., Kuzas E., Suntsov A. Nitric acid dissolution of tennantite, chalcopyrite and sphalerite in the presence of Fe (III) ions and FeS_2. *Materials*. 2022;15(4):1545. https://doi.org/10.3390/ma15041545
8. Xi J., Liao Y., Ji G., Liu Q., Wu Y. Mineralogical characteristics and oxygen pressure acid leaching of low-grade polymetallic complex chalcopyrite. *Journal of Sustainable Metallurgy*. 2022;8(4):1628—1638. https://doi.org/10.1007/s40831-022-00594-w
9. Ai C., Wang S., Liu C., Li T. Experimental study on the influence of surfactants on ore surface wettability. *ACS Omega*. 2023;9(1):1056—1068. https://doi.org/10.1021/acsomega.3c07218
10. Lugovitskaya T., Rogozhnikov D. Surface phenomena with the participation of sulfite lignin under pressure leaching of sulfide materials. *Langmuir*. 2023;39(16):5738—5751. https://doi.org/10.1021/acs.langmuir.2c03481
11. Jiang T., Jiao G., Wang P., Zhu D., Liu Z., Liu Z. Lignosulphonates in zinc pressure leaching: Decomposition behaviour and effect of lignosulphonates' characteristics on leaching performance. *Journal of Cleaner Production*. 2024;(435):140355. https://doi.org/10.1016/j.jclepro.2023.140355
12. Yang S., Li Y., Yang Y., Liu R., Zhao Y. Behavior of calcium lignosulfonate under oxygen pressure acid leaching condition. *Hydrometallurgy*. 2024;(227):106317. https://doi.org/10.1016/j.hydromet.2024.106317
13. Lugovitskaya T.N., Rogozhnikov D.A. Construction of lignosulphonate-containing polymersomes and prospects for their use for elemental sulfur encapsulation. *Journal of Molecular Liquids*. 2024;(400):124612. https://doi.org/10.1016/j.molliq.2024.124612
14. Yang D., Qiu X., Pang Y., Zhou M. Physicochemical properties of calcium lignosulfonate with different molecular weights as dispersant in aqueous suspension. *Journal of Dispersion Science and Technology*. 2008;(29(9)): 1296—1303. https://doi.org/10.1080/01932690701866534
15. Fink F., Emmerling F., Falkenhagen J. Identification and classification of technical lignins by means of principle component analysis and k-Nearest neighbor algorithm. *Chemistry-Methods*. 2021;(1(8)):354—361. https://doi.org/10.1002/cmtd.202100028
16. Shen W., Zhu H., Cheng X., Li X. Synthesis of mesoporous niobium phosphosilicate with high catalytic activity in the conversion of glucose to 5-hydroxymethylfurfural in water solvent. *Biofuels, Bioproducts and Biorefining*. 2024;(18(6)):1994—2004. http://dx.doi.org/10.1002/bbb.2677
17. Ge Y., Li D., Li Z. Effects of lignosulfonate structure on the surface activity and wettability to a hydrophobic powder. *BioResources*. 2014;(9(4)):7119—7127.
18. Rana D., Neale G., Hornof V. Surface tension of mixed surfactant systems: lignosulfonate and sodium dodecyl sulfate. *Colloid and Polymer Science*. 2002;(280):775—778. https://doi.org/10.1007/s00396-002-0687-y
19. Chong A.S., Manan M.A., Idris A.K. Readiness of lignosulfonate adsorption onto montmorillonite. *Colloids and Surfaces A: Physicochemical and Engineering Aspects*. 2021;(628):127318. https://doi.org/10.1016/j.colsurfa.2021.127318
20. Bolatbaev K.N., Lugovitskaya T.N., Kolosov A.V., Naboichenko S.S. Fundamental aspects of the behavior of various lignosulfonates in solutions. *Russian Journal of Applied Chemistry*. 2010;83(9);1553—1557. https://doi.org/10.1134/S1070427210090090
Болатбаев К.Н., Луговицкая Т.Н., Колосов А.В., Набойченко С.С. Закономерности поведения различных лигносульфонатов в растворах. *Журнал прикладной химии*. 2010;83(9):1453—1457.
21. Shi Z., Xu G., Deng J., Dong M., Murugadoss V., Liu C., Guo Z. Structural characterization of lignin from D. sinicus by FTIR and NMR techniques. *Green Chemistry Letters and Reviews*. 2019;(12(3)):235—243. https://doi.org/10.1080/17518253.2019.1627428
22. Karpukhina E.A., Volkov D.S., Proskurnin M.A. Quantification of lignosulfonates and humic components in mixtures by ATR FTIR spectroscopy. *Agronomy*. 2023; 13(4):1141. https://doi.org/10.3390/agronomy13041141
23. Xu F., Yu J., Tesso T., Dowell F., Wang D. Qualitative and quantitative analysis of lignocellulosic biomass using infrared techniques: a mini-review. *Applid Energy*. 2013; (104):801—809. https://doi.org/10.1016/j.apenergy.2012.12.019

Information about the authors

Tatyana N. Lugovitskaya – Cand. Sci. (Eng.), Associate Professor-Researcher, Department of the metallurgy of non-ferrous metals (NFM), Ural Federal University n.a. the First President of Russia B.N. Yeltsin (UrFU).
https://orcid.org/0000-0002-8286-0711
E-mail: t.n.lugovitskaia@urfu.ru

Olga S. Anisimova – Cand. Sci. (Eng.), Associate Professor of the Department of NFM, UrFU.
https://orcid.org/0000-0002-5090-437X
E-mail: o.s.anisimova@urfu.ru

Denis A. Rogozhnikov – Dr. Sci. (Eng.), Head of the Scientific, Laboratory of advanced technologies for complex processing of mineral and man-made raw materials of non-ferrous and ferrous metals, UrFU.
https://orcid.org/0000-0002-5940-040X
E-mail: darogozhnikov@urfu.ru

Информация об авторах

Татьяна Николаевна Луговицкая – к.т.н., доцент-исследователь кафедры металлургии цветных металлов (МЦМ), Уральский федеральный университет имени первого Президента России Б.Н. Ельцина (УрФУ).
https://orcid.org/0000-0002-8286-0711
E-mail: t.n.lugovitskaia@urfu.ru

Ольга Сергеевна Анисимова – к.т.н., доцент кафедры МЦМ, УрФУ.
https://orcid.org/0000-0002-5090-437X
E-mail: o.s.anisimova@urfu.ru

Денис Александрович Рогожников – д.т.н., зав. лабораторией перспективных технологий комплексной переработки минерального и техногенного сырья цветных и черных металлов, УрФУ.
https://orcid.org/0000-0002-5940-040X
E-mail: darogozhnikov@urfu.ru

Contribution of the authors

T.N. Lugovitskaya – conducted the experiments; took part in the discussion of the results; manuscript preparation.

O.S. Anisimova – defined the study objective; took part in the discussion of the results; writing of the manuscript.

D.A. Rogozhnikov – literature and patent search; contribution to manuscript writing.

Вклад авторов

Т.Н. Луговицкая – проведение экспериментов, участие в обсуждении результатов, оформление статьи.

О.С. Анисимова – определение цели работы, участие в обсуждении результатов, написание статьи.

Д.А. Рогожников – литературно-патентный поиск по теме, участие в написании статьи.

The article was submitted 12.05.2025, revised 28.05.2025, accepted for publication 02.06.2025

Статья поступила в редакцию 12.05.2025, доработана 28.05.2025, подписана в печать 02.06.2025

UDC 546.74:66.081
https://doi.org/10.17073/0021-3438-2025-3-37-43

Research article
Научная статья

Assessment of the prospects for processing oxidized nickel ores using microwave energy

S.E. Polygalov, V.G. Lobanov, D.S. Sedelnikova, O.B. Kolmachikhina, O.Yu. Makovskaya

Ural Federal University n.a. the First President of Russia B.N. Yeltsin
19 Mira Str., Ekaterinburg 620002, Russia

✉ Sergei E. Polygalov (sergey.polygalov@urfu.ru)

Abstract: The Ural region holds an estimated 1.5 million tons of nickel reserves, located in the industrially developed Chelyabinsk, Sverdlovsk, and Orenburg regions. At present, however, these deposits are not being exploited, and metallic nickel is not produced in the Urals, as metallurgical facilities have been completely shut down. The reserves are represented by oxidized nickel ores (ONO) – a complex raw material with low nickel and cobalt contents, whose processing by existing technologies is economically unfeasible. The challenge is compounded by the absence of a beneficiation method for ONO that yields a concentrate; therefore, all current technologies require processing the entire ore mass, which results in high reagent consumption and substantial energy costs. Research is ongoing to develop new technological approaches, including alternative methods for extracting nickel and cobalt from ONO in the Ural deposits. One promising option is the use of microwave (MW) energy to unlock nickel-bearing minerals and accelerate the dissolution of nickel and cobalt. This study evaluates the effect of microwave energy on nickel recovery from oxidized nickel ores of the Ural region. Comparative data are presented for conventional sulfuric acid leaching and for the process with microwave energy applied. A series of test studies was carried out to assess the feasibility of using microwave energy for ONO processing. The comparison of technological parameters demonstrated the advantage of atmospheric sulfuric acid leaching with microwave energy, which achieved nickel recovery of up to 95 % in a relatively short time. These results identify this approach as the most promising for practical implementation.

Keywords: microwave energy, oxidized nickel ores, leaching, sulfuric acid, nickel.

For citation: Polygalov S.E., Lobanov V.G., Sedelnikova D.S., Kolmachikhina O.B., Makovskaya O.Yu. Assessment of the prospects for processing oxidized nickel ores using microwave energy. *Izvestiya. Non-Ferrous Metallurgy.* 2025;31(3):37–43.
https://doi.org/10.17073/0021-3438-2025-3-37-43

Оценка перспективности переработки окисленных никелевых руд с использованием СВЧ-энергии

С.Э. Полыгалов, В.Г. Лобанов, Д.С. Седельникова, О.Б. Колмачихина, О.Ю. Маковская

Уральский федеральный университет имени первого Президента России Б.Н. Ельцина
Россия, 620002, г. Екатеринбург, ул. Мира, 19

✉ Сергей Эдуардович Полыгалов (sergey.polygalov@urfu.ru)

Аннотация: Урал обладает запасами никеля на уровне 1,5 млн т. Месторождения находятся в промышленно развитом регионе – на территории Челябинской, Свердловской и Оренбургской областей. Однако в настоящее время их не разрабатывают, и метал-

лический никель на Урале не производят, так как металлургические предприятия полностью остановлены. Причиной является то, что запасы никеля представлены окисленными никелевыми рудами (ОНР), которые являются сложным сырьем с низким содержанием никеля и кобальта, переработка которого по существующим технологиям нерентабельна. Осложняет задачу и то, что на сегодняшний день не существует метода обогащения ОНР с получением концентрата, поэтому все технологии предусматривают переработку всей массы руды, что ведет к значительным расходам на реагенты и энергетическим затратам. В то же время не прекращается поиск новых технологических подходов, ориентированных на применение альтернативных вариантов извлечения никеля и кобальта из ОНР уральских месторождений. Одним из подобных методов является применение СВЧ-энергии для вскрытия никелевых минералов и интенсификации перевода в раствор никеля и кобальта. В настоящей работе оценено влияние воздействия СВЧ-энергии на извлечение никеля из окисленных никелевых руд Уральского региона. Приводятся данные по сравнению показателей классического серно-кислотного выщелачивания и процесса с наложением СВЧ-энергии. Выполнен комплекс тестовых исследований, цель которых – оценить перспективность применения СВЧ-энергии для переработки ОНР. Сравнение технологических параметров обоих подходов выявило преимущество атмосферного серно-кислотного выщелачивания ОНР с наложением СВЧ-энергии, в ходе которого было достигнуто извлечение никеля в раствор до 95 % за небольшой промежуток времени. На основании полученных результатов данное направление выбрано как наиболее перспективное для практической реализации.

Ключевые слова: СВЧ-энергия, окисленные никелевые руды, выщелачивание, серная кислота, никель.

Для цитирования: Полыгалов С.Э., Лобанов В.Г., Седельникова Д.С., Колмачихина О.Б., Маковская О.Ю. Оценка перспективности переработки окисленных никелевых руд с использованием СВЧ-энергии. *Известия вузов. Цветная металлургия*. 2025;31(3):37–43. https://doi.org/10.17073/0021-3438-2025-3-37-43

Introduction

In both global and domestic practice, nickel is extracted from sulfide and oxidized ores. Sulfide ores are subjected to flotation beneficiation, and the resulting flotation concentrate is processed by pyrometallurgical methods [1]. Oxidized (lateritic) ores account for 60—70 % of the world's nickel reserves. These ores cannot be beneficiated by conventional methods, and nickel extraction directly from raw ore is associated with high specific costs. Therefore, the search for efficient technologies for processing oxidized nickel ores (ONO) remains highly relevant [2—4]. Abroad, laterite ore processing is generally carried out by hydrometallurgical or combined methods [5—8].

Hydrometallurgical technologies implemented in practice for ONO processing are based on direct leaching of nickel and cobalt with sulfuric acid in two main variants:

— heap leaching of raw ore with sulfuric acid solutions [9—12];

— high-pressure acid leaching under autoclave conditions (HPAL) [13;14].

In some cases, heap leaching is combined with autoclave leaching to reduce specific costs: raw ore is subjected to pressure leaching, while the residue from the autoclave stage is processed by heap leaching.

The main challenges in applying hydrometallurgical technologies to ONO from the Ural region stem from the low contents of valuable components (nickel and cobalt). The specific mineralogical features of these ores result in high reagent consumption, low recovery of target metals, and the formation of large volumes of solid waste requiring disposal. These factors render traditional hydrometallurgical technologies economically unfeasible and hinder the adaptation of foreign processing schemes to domestic ores.

It is known that in ONO, most nickel occurs as an isomorphic substitute for iron in poorly soluble silicate minerals [14]. To intensify solid—liquid reactions, elevated temperatures, pressure, and vigorous mixing are used.

The greatest potential for accelerating hydrometallurgical interactions under optimal reagent conditions in liquid—solid systems lies in enhancing mass transfer. Various approaches have been proposed to accelerate heterogeneous solid—liquid processes, including the application of oscillations of different frequencies — acoustic and ultrasonic waves, industrial-frequency current, as well as high and ultra-high frequencies.

Microwave (MW) energy is widely applied across diverse industries such as petrochemistry, agriculture, food processing, wood drying, medicine, and others. In these applications, it is generally used solely for accelerated heating of materials. Only in petrochemistry and catalytic chemistry has microwave energy been applied to intensify mass transfer processes.

The aim of the present work is to evaluate the potential for intensifying acid leaching of nickel from oxidized ore by applying microwave energy to the reaction mass

and to compare the results with those of conventional nickel leaching methods..

Research methods and results

The object of study was an increment of oxidized nickel ore from the Ural region. The increments were composited, and a laboratory sample was prepared and ground to a particle size below 0.074 mm. Phase analysis revealed that the main minerals in the ore were goethite ($Fe(OH)_2 \cdot nH_2O$), silica (SiO_2), and nickel silicate ($NiO_2 \cdot SiO_2$). In addition, alumina (Al_2O_3), manganese hydroxides, calcium compounds, and other phases were present. Alumina and silica constituted the basis of the clay-forming minerals. According to chemical analysis, the ore contained (wt. %): Ni — 0.92, Co — 0.064, and Fe — 39.32.

To investigate the effect of microwave irradiation on ONO, a laboratory unit was assembled based on a commercially available inverter-type microwave oven, which maintains constant output power during operation. This allowed more accurate evaluation of specific energy consumption and minimized pulp overheating.

The pulp (ore mixed with acidic solution) was placed in a heat-resistant laboratory beaker and set inside the microwave oven directly over the waveguide outlet. To achieve this configuration, the oven was oriented vertically. To evaluate the effect of microwave irradiation, it was necessary to ensure that the entire microwave energy generated by the magnetron was focused on the reaction mass. For this purpose, the beaker was wrapped in an aluminum foil shield. These methodological arrangements allowed reliable determination of specific energy consumption, optimal pulp layer thickness (i.e., effective penetration depth of microwave energy), and the overall efficiency of the method.

A schematic of the laboratory setup is presented in Fig. 1.

Concentrated sulfuric acid solutions (≥80 g/dm^3) were used in the experiments, heated directly by microwave irradiation. To protect the magnetron from thermal and chemical effects of the reaction mass, the waveguide outlet was additionally covered with a screen made of mica and asbestos, both transparent to microwaves.

At the first stage, the effect of microwave energy on the kinetics of nickel leaching was examined by conducting comparative tests under identical conditions: liquid-to-solid ratio (L/S) = 5 : 1, stirring intensity 400 rpm, temperature ≤75 °C, and H_2SO_4 concentration 200 g/dm^3. Parallel ore charges of equal mass were leached in a beaker on a conventional heating plate and in the microwave-assisted setup. Microwave activation was performed at an output power of 180 W for 20 min in both cases.

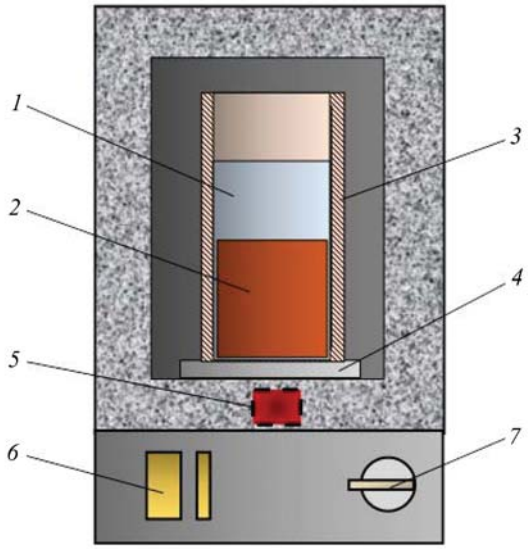

Fig. 1. Schematic of the laboratory setup

1 – reaction beaker, ***2*** – pulp, ***3*** – aluminum foil shield, ***4*** – support for the reaction beaker made of microwave-transparent material, ***5*** – magnetron, ***6*** – timer, ***7*** – power controller

Рис. 1. Схема лабораторной установки

1 – реакционный стакан, ***2*** – пульпа, ***3*** – экранирующий кожух, ***4*** – подставка под реакционный стакан из СВЧ-прозрачного материала, ***5*** – магнетрон, ***6*** – датчик времени, ***7*** – регулятор управления

At specified time intervals, aliquots of the pregnant solution were withdrawn and analyzed for nickel content by atomic absorption spectroscopy (Analytik Jena, Germany). Nickel recovery into solution was then calculated (Fig. 2).

As expected, microwave irradiation significantly accelerated nickel dissolution compared with conventional thermal leaching, increasing the leaching rate by approximately fourfold. Although the maximum achievable nickel recovery was not determined in this series, the observed trend suggests that microwave activation substantially shortens the time required to achieve high extraction.

For practical implementation of the proposed method and reactor design, it was important to estimate the penetration depth of microwave energy into the solid—liquid system (a pulp consisting of sulfuric acid solution and ground ore at a liquid-to-solid ratio of 1 : 1). To vary the pulp layer thickness, different volumes of pulp were loaded into the reaction vessel. A separate beaker containing a fixed volume of distilled

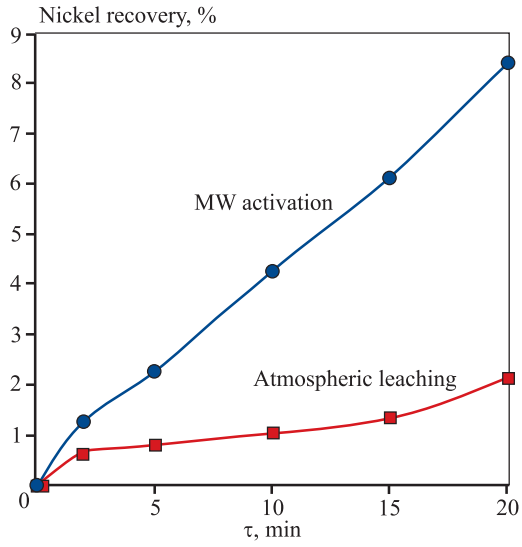

Fig. 2. Nickel recovery as a function of time under microwave-assisted and atmospheric leaching of ONO

Рис. 2. Сравнение динамики выщелачивания никеля из ОНР

water was placed above the reaction vessel. When the microwave oven was switched on, the extent of heating of the water indicated the fraction of microwave energy that had not been absorbed by the pulp. Thus, by comparing the temperature rise in the water at different pulp heights, the penetration depth of the microwave energy flux through the reaction mass was assessed. The chosen pulp density (L/S = 1 : 1) minimized particle settling during the test, ensuring reliable evaluation of microwave penetration depth.

The absorbed energy was calculated from the temperature difference before and after irradiation according to the equation:

$$E = \frac{mC\Delta t}{\tau},$$

where E is the absorbed energy, W/s; m is the mass of water, g; C = 4.18 J/g·°C is the specific heat capacity of water; Δt is the temperature difference, °C; and τ is time, s.

The amount of microwave energy absorbed by the reaction mass at different layer thicknesses is presented in the table.

The results show that in dense pulp, the microwave flux is fully absorbed within a 4—6 cm layer. Naturally, this parameter depends on microwave power, pulp density, and mixing conditions. The penetration depth of microwave energy — where heating occurs and reactions are intensified — is referred to as the effective microwave depth. Within this zone, heating, the skin effect, and accelerated dissolution of target metals can be expected.

In the next stage, the effect of specific sulfuric acid consumption on nickel leaching was evaluated. Since an additional aim was to estimate the maximum achievable recovery, experiments were performed at maximum magnetron power (900 W) with deliberately excess acid addition.

The leaching solution was prepared by dissolving the required mass of acid in water and diluting to a fixed volume. Ore charges weighed 30 g, and the solution volume was 60 ml. At this power, the reaction mass rapidly evaporated, forming a dense sinter that fundamentally altered the process. To avoid this, the experiment duration was limited to 4 minutes. Monitoring the temperature of the reaction mass during microwave activation was not feasible; post-experiment measurements showed that under steady-state conditions the temperature rapidly reached 95—100 °C.

Given the expected high reaction rate between nickel-bearing minerals and sulfuric acid, the acid concentration was the critical factor in the leaching process. To enable proper comparison of experimental results at equal slurry volumes (effective layer thickness of 4 cm) and different acid concentrations, the specific acid consumption was varied from 0.4 to 2.0 g H_2SO_4 per gram of ore.

The ore charges were mixed with sulfuric acid solution and subjected to microwave irradiation for a set leaching time (e.g., 1 min). The pulp was then removed, diluted with water, filtered, and the filtrate analyzed for nickel concentration and residual acid. Leaching was repeated at the same acid consumption but with different leaching times. Thus, each point on the curves in Figs. 3 and 4 corresponds to a separate test. For comparison, additional experiments at 2 g H_2SO_4 per g ore were performed by heating the pulp to 95 °C without microwave activation. Based on these results, nickel recovery into solution and the fraction of sulfuric acid consumed in the target reaction were calculated.

Microwave energy absorbed by the reaction mass at different pulp layer heights

Количество СВЧ-энергии, поглощенной реакционной массой при разной высоте слоя пульпы

Pulp height , mm	Absorbed energy, J	Energy loss, %
10	253.6	71.8
20	612.3	32.0
40	891.4	1.0
60	895.1	0.5

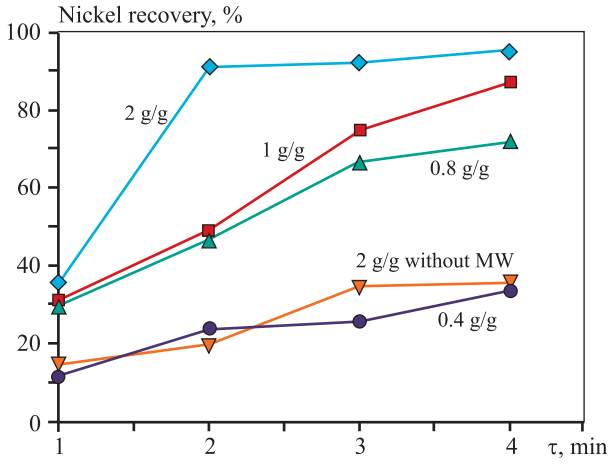

Fig. 3. Dependence of nickel recovery on sulfuric acid consumption under microwave-assisted leaching of ONO (g/g ore)

Рис. 3. Зависимость извлечения Ni в раствор при выщелачивании с наложением СВЧ-энергии при различном расходе серной кислоты (г/г руды)

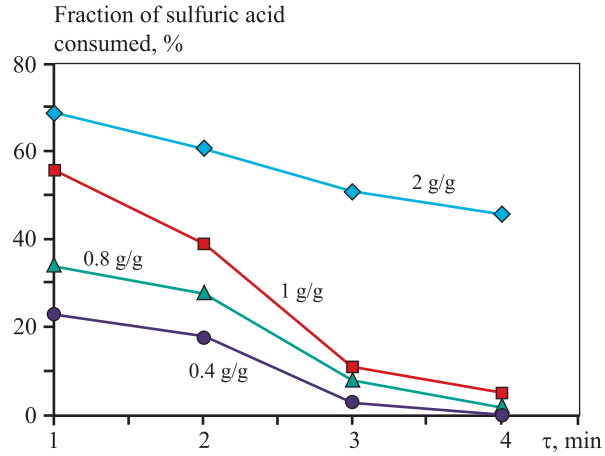

Fig. 4. Dependence of sulfuric acid consumption on time under microwave-assisted leaching of ONO (g/g ore)

Рис. 4. Зависимость расхода серной кислоты при СВЧ-выщелачивания ОНР (г/г руды)

The results show that under excess (i.e., high concentration of) sulfuric acid, the nickel leaching rate under microwave activation increased severalfold compared with conventional methods.

The experiments were not aimed at determining reagent consumption coefficients or performing an economic assessment of this approach, but the results demonstrate that under certain conditions, near 100 % nickel recovery can be achieved in a very short time. With countercurrent leaching — widely used in hydrometallurgy — this method could achieve the required metal recovery at high rates. Overall, the findings confirm the potential of microwave energy for enhancing the efficiency of metallurgical ore processing.

Further studies will focus on the features of microwave-assisted leaching of oxidized nickel ore under countercurrent liquid—solid conditions.

Conclusions

1. An original methodology was proposed for studying metal leaching from mineral raw materials using microwave energy.

2. It was established that the effective penetration depth of microwave energy through a dense solid—liquid system (“ground ore — leaching solution”) at a liquid-to-solid ratio of 1 : 1 does not exceed 40 mm.

3. Atmospheric sulfuric acid leaching of ONO with microwave activation was shown to accelerate the process severalfold, achieving up to 95 % nickel recovery into solution.

References

1. Peiyu Zhang, Qiang Guo, Guangye Wei, Long Meng, Linxin Han, Jingkui Qu, Tao Qi. Extraction of metals from saprolitic laterite ore through pressure hydrochloric-acid selective leaching. *Hydrometallurgy.* 2015; (157):149—158. https://doi.org/10.1016/j.hydromet.2015.08.007
2. Fatahi Mohammadreza, Noaparast Mohammad, Shafaei Seyyed Ziaeddin. Nickel extraction from low grade laterite by agitation leaching at atmospheric pressure. *International Journal of Mining Science and Technology.* 2014;4:543—548. https://doi.org/10.1016/j.ijmst.2014.05.019
3. Jian-ming Gao, Mei Zhang, Min Guo. Innovative methodology for comprehensive utilization of saprolite laterite ore: Recovery of metal-doped nickel ferrite and magnesium hydroxide. *Hydrometallurgy.* 2015;(158):27—34. https://doi.org/10.1016/j.hydromet.2015.09.027
4. Pickles C.A. Microwave heating behavior of nickeliferous limonitic laterite ores. *Minerals Engineering.* 2004;6: 775—784. https://doi.org/10.1016/j.mineng.2004.01.007
5. Reid J., Barnett S. Nickel laterite hydrometallurgical processing update. In: *Nickel-Cobalt-8. Technical Sessions Proceedings «Alta Metallurgical Services».* Perth, W. Australia, 2002. 27 p.
6. Berezowsky R.M. Laterite: new life of limonite. *Minerals Industry International.* 1997;1034:46—55.
7. Urbain D., Duterque J. P., Palanque Ph., Rey P. Economic comparison between the sulphuric acid leach process

and other processes for oxidized nickel ores. In: *Proceedings-nickel metallurgy. Vol. I: Extraction and refining of nickel*. 1986. P. 578—596.

8. Motteram G., Ryan M., Berezowsky R.M., Raudsepp R., Murrin M. Nickel-Cobalt Project: Project Development Overview. In: *Proc. of Nickel-Cobalt Pressure Leaching and Hydrometallurgy Forum* (May 13-14, 1996), Perth, Australia: Alta Metallurgical Services, 1996.
9. Alenichev V.M., Umansky A.B., Klyushnikov A.M. Physicochemical features of the process of heap leaching of oxidized nickel ores of the Urals using sulfuric acid solutions. *Vestnik Voronezhskogo universiteta*. 2013;(2):9—14.
   Аленичев В.М., Уманский А.Б., Клюшников А.М. Физико-химические особенности процесса кучного выщелачивания окисленных никелевых руд Урала с использованием растворов серной кислоты. *Вестник Воронежского университета*. 2013;(2):9—14.
10. Umansky A.B., Klyushnikov A.M. Hydrometallurgical technology of processing serpentinite dumps with the release of nickel concentrate. In: *Proceedings of the International Congress "Fundamentals of technologies for processing and utilization of technogenic waste"* (June 14—16 2012). Yekaterinburg: Уральский издательский полиграфический центр, P. 419—422.
    Уманский А.Б., Клюшников А.М. Гидрометаллургическая технология переработки отвалов серпентинита с выделением никелевого концентрата. В сб.: *Труды международного конгресса «Фундаментальные основы технологий переработки и утилизации техногенных отходов»*. 2012.
11. McDonald R.G., Whittington B.I. Atmospheric acid leaching of nickel laterites review. Part I. Sulphuric acid technologies. *Hydrometallurgy*. 2008;(1-4):35—55. https://doi.org/10.1016/j.hydromet.2007.11.009
12. Alenichev V.M., Umansky A.B., Klyushnikov A.M. Development of heap leaching technology for oxidized nickel ores of the Ural deposits. *Izvestiya Tomskogo politekhnicheskogo universiteta*. 2013;(3):124—128.
    Аленичев В.М., Уманский А.Б., Клюшников А.М. Разработка технологии кучного выщелачивания окисленных никелевых руд Уральских месторождений. *Известия Томского политехнического университета*. 2013;(3):124—128.
13. Naboychenko S.S., Ni L.P., Shneerson Ya.M., Chugaev L.V. Autoclave hydrometallurgy of non-ferrous metals. Yekaterinburg: Ural State Technical University–UPI, 2002. 940 p. (In Russ.).
    Набойченко С.С., Ни Л.П., Шнеерсон Я.М., Чугаев Л.В. Автоклавная гидрометаллургия цветных металлов. Екатеринбург: УГТУ—УПИ, 2002. 940 с.
14. Kolmachikhina O.B. Combined technology for processing oxidized nickel ores (using the Serovskoye deposit as an example): Diss. Cand Sci. (Eng.). Yekaterinburg: UrFU, 2018. (In Russ.).
    Колмачихина О.Б. Комбинированная технология переработки окисленных никелевых руд (на примере Серовского месторождения): Дис. на соискание ученой степени канд. техн. наук. Екатеринбург: УрФУ, 2018.

Information about the authors

Sergei E. Polygalov – Senior Lecturer at the Department of non-ferrous metallurgy (NFM), Ural Federal University n.a. the First President of Russia B.N. Yeltsin (UrFU).
E-mail: sergey.polygalov@urfu.ru

Vladimir G. Lobanov – Cand. Sci. (Eng.), Associate Professor of the Department of NFM, UrFU.
https://orcid.org/0000-0001-6450-8434
E-mail: lobanov-vl@yandex.ru

Dar'ya S. Sedelnikova – Student of the Department of NFM, UrFU.
E-mail: Daria.Sedelnikova@urfu.me

Ol'ga B. Kolmachikhina – Cand. Sci. (Eng.), Associate Professor of the Department of NFM, UrFU.
https://orcid.org/0000-0002-7879-8791
E-mail: o.b.kolmachikhina@urfu.ru

Ol'ga Yu. Makovskaya – Cand. Sci. (Eng.), Associate Professor of the Department of NFM, UrFU.
E-mail: o.i.makovskaia@urfu.ru

Информация об авторах

Сергей Эдуардович Полыгалов – ст. преподаватель кафедры металлургии цветных металлов (МЦМ), Уральский федеральный университет имени первого Президента России Б.Н. Ельцина (УрФУ).
E-mail: sergey.polygalov@urfu.ru

Владимир Геннадьевич Лобанов – к.т.н., доцент кафедры МЦМ, УрФУ.
https://orcid.org/0000-0001-6450-8434
E-mail: lobanov-vl@yandex.ru

Дарья Сергеевна Седельникова – студент кафедры МЦМ, УрФУ.
E-mail: lev.sokolov@urfu.ru

Ольга Борисовна Колмачихина – к.т.н., доцент кафедры МЦМ, УрФУ.
https://orcid.org/0000-0002-7879-8791
E-mail: o.b.kolmachikhina@urfu.ru

Ольга Юрьевна Маковская – к.т.н., доцент кафедры МЦМ, УрФУ.
E-mail: o.i.makovskaia@urfu.ru

Contribution of the authors

S.E. Polygalov – development of the main concept, definition of research objectives and tasks, preparation of the manuscript, formulation of conclusions.

V.G. Lobanov – scientific supervision, revision of the manuscript and conclusions.

D.S. Sedelnikova – experiment preparation and experimental work.

O.B. Kolmachikhina – calculations and preparation of the manuscript.

O.Yu. Makovskaya – calculations and analysis of research results.

Вклад авторов

С.Э. Полыгалов – формирование основной концепции, постановка цели и задачи исследования, подготовка текста, формулировка выводов.

В.Г. Лобанов – научное руководство, корректировка текста и выводов.

Д.С. Седельникова – подготовка и проведение экспериментов.

О.Б. Колмачихина – осуществление расчетов, подготовка текста статьи.

О.Ю. Маковская – проведение расчетов, анализ результатов исследований.

The article was submitted 12.05.2025, revised 23.05.2025, accepted for publication 29.05.2025

Статья поступила в редакцию 12.05.2025, доработана 23.05.2025, подписана в печать 29.05.2025

UDC 669.2/.8
https://doi.org/10.17073/0021-3438-2025-3-44-53

Research article
Научная статья

Investigation of nitric acid dissolution of stibnite in the presence of tartaric acid

O.A. Dizer, D.I. Golovkin, Yu.E. Shklyaev, D.A. Rogozhnikov

Ural Federal University n.a. the First President of Russia B.N. Yeltsin
19 Mira Str., Ekaterinburg 620002, Russia

✉ Oleg A. Dizer (oleg.dizer@yandex.ru)

Abstract: This study explores the nitric acid leaching of stibnite in the presence of tartaric acid, which acts as a complexing agent. The proposed approach is of considerable interest, as antimony is widely used across industries, from electronics to alloying applications. Thermodynamic analysis showed that nitric acid dissolution of stibnite inevitably leads to the formation of antimony oxides, which markedly reduces the extraction of the target metal into solution. To counteract these losses and enhance process efficiency, tartaric acid was introduced as an additive. The results demonstrated that tartaric acid promotes the formation of stable complexes with antimony ions, thereby retaining the metal in solution and minimizing the risk of oxide precipitation. Experimental design analysis revealed that the mass ratio of tartaric acid to antimony and the nitric acid concentration exert a stronger influence on leaching efficiency than temperature and leaching duration. Optimal conditions were established, achieving an antimony extraction of 87 %: temperature 35 °C, nitric acid concentration 5 mol/dm^3, leaching time 45 min, and a tartaric acid-to-antimony mass ratio of 4.5 : 1.0.

Keywords: stibnite, antimony, leaching, nitric acid, tartaric acid, optimal parameters.

Acknowledgments: The study was supported by the Russian Science Foundation and the Government of the Sverdlovsk Region, Joint Grant No. 24-29-20158.

For citation: Dizer O.A., Golovkin D.I., Shklyaev Yu.E., Rogozhnikov D.A. Investigation of nitric acid dissolution of stibnite in the presence of tartaric acid. *Izvestiya. Non-Ferrous Metallurgy.* 2025;31(3):44–53. https://doi.org/10.17073/0021-3438-2025-3-44-53

Исследование азотно-кислотного растворения стибнита с добавлением винной кислоты

О.А. Дизер, Д.И. Головкин, Ю.Е. Шкляев, Д.А. Рогожников

Уральский федеральный университет имени первого Президента России Б.Н. Ельцина
Россия, 620002, г. Екатеринбург, ул. Мира, 19

✉ Олег Анатольевич Дизер (oleg.dizer@yandex.ru)

Аннотация: Работа посвящена изучению процесса азотно-кислотного выщелачивания стибнита с добавлением винной кислоты, выполняющей функцию комплексообразующего агента. Предлагаемый способ переработки стибнита обладает высокой актуальностью, поскольку сурьма широко используется в промышленности – от электроники до применения в качестве легирующих добавок. В ходе термодинамического анализа выявлено, что в процессе азотно-кислотного растворения стибнита неизбежно образуются оксиды сурьмы, что приводит к существенному снижению извлечения целевого металла в раствор. Для того чтобы снизить эти потери и повысить эффективность процесса, в качестве добавки предложено использовать винную кислоту. Исследования показали, что она способствует образованию стабильных комплексов с ионами сурьмы, что позволяет сохранить

металл в растворе и минимизировать риск осаждения оксидов. С использованием математического планирования эксперимента установлено, что массовое соотношение винной кислоты к сурьме, а также концентрация азотной кислоты оказывают большее влияние на эффективность процесса выщелачивания, чем температура и продолжительность процесса. Определены оптимальные условия для достижения максимального значения извлечения сурьмы в раствор – 87 %: температура 35 °С, концентрация азотной кислоты 5 моль/дм^3, время выщелачивания 45 мин и массовое соотношение винной кислоты к сурьме 4,5 : 1,0.

Ключевые слова: стибнит, сурьма, выщелачивание, азотная кислота, винная кислота, оптимальные параметры.

Благодарности: Исследование выполнено при поддержке Российского научного фонда и Правительства Свердловской области, совместный грант № 24-29-20158.

Для цитирования: Дизер О.А., Головкин Д.И., Шкляев Ю.Е., Рогожников Д.А. Исследование азотно-кислотного растворения стибнита с добавлением винной кислоты. *Известия вузов. Цветная металлургия*. 2025;31(3):44–53.
https://doi.org/10.17073/0021-3438-2025-3-44-53

Introduction

Antimony, a critical element in various industrial applications, remains in high demand due to its unique physicochemical properties [1; 2]. It is used in the production of flame-retardant materials, lead—acid batteries, semiconductor devices, and as an alloying element in metallurgy. The primary source of antimony is the mineral stibnite (Sb2S3). However, efficient recovery of antimony from stibnite is complicated by a number of technological and environmental challenges [3—8], which has driven the search for innovative processing methods [9—14].

One promising approach to antimony extraction is nitric acid leaching [15—20]. Despite its advantages, this method has drawbacks such as slow reaction kinetics and the formation of sparingly soluble compounds. A potential strategy to improve acid leaching is the addition of organic complexing agents that stabilize metal ions in solution, thereby preventing their premature precipitation. In this regard, tartaric acid ($C_4H_6O_6$) is of particular interest [21; 22] Its molecules readily form stable complexes with metal cations, including antimony, which may enhance extraction efficiency and process selectivity.

Previous research has shown the successful application of organic acids in hydrometallurgical processes. For instance, citric and oxalic acids have been used to improve the leaching of oxide and sulfide ores of nickel, copper, and zinc [23—26]. However, in the case of antimony — particularly in combination with nitric acid — such studies remain limited. Most existing work has focused on single-agent systems or combinations of inorganic acids, whereas the synergistic effect of introducing tartaric acid into a HNO_3 medium has received little attention. This defines the relevance of the present study, which examines the effects of temperature, nitric acid concentration, leaching duration, and tartaric acid dosage on the efficiency of nitric acid dissolution of stibnite. The optimal conditions for maximum antimony recovery were also established.

The findings of this study may contribute to the development of more efficient and sustainable methods for processing antimony-bearing raw materials, thereby promoting more rational use of natural resources and reducing environmental impact.

Experimental procedure

Materials, equipment, and methods

The chemical composition of stibnite was determined by complete dissolution of a 0.2—0.3 g portion of the material in a PreeKem M3 microwave digestion system (PreeKem, China). The resulting solutions were analyzed using an EXPEC 6500 inductively coupled plasma optical emission spectrometer (ICP—OES) (Focused Photonics Inc., China), which was also used to determine the composition of the leach solutions.

The phase composition of the stibnite sample (Fig. 1) and the leach residue was analyzed with an XRD 7000 Maxima diffractometer (Shimadzu Corp., Tokyo, Japan).

A natural stibnite sample (Sb2S3) served as the starting material. The mineral was ground in a Pulverisette 6 planetary mill (FRITSCH GmbH, Germany) and sieved through laboratory screens to obtain a –56 μm working fraction. All other reagents were of analytical grade.

Nitric acid leaching experiments were carried out under laboratory conditions using a 500 mL Lenz Minni-60 reactor (Lenz Laborglas GmbH, Germany). The leaching solution was preheated to the de-

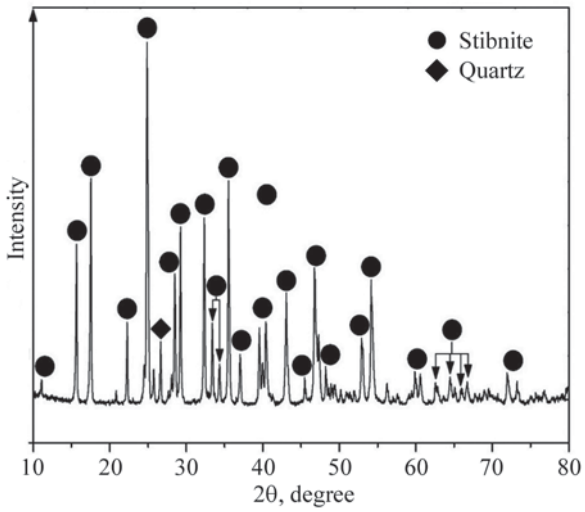

Fig. 1. Phase composition of stibnite

Рис. 1. Фазовый состав стибнита

sired temperature with a Huber Kiss K6 precision thermostat (Peter Huber Kältemaschinenbau, Germany). After thermostating, the weighed sample of stibnite was introduced into the reactor. Slurry homogenization was achieved using an IKA Eurostar 20 digital overhead stirrer (IKA-Werke GmbH, Germany).

After the reaction, the slurry was vacuum-filtered through a Büchner funnel. The filtrate was analyzed for antimony content by ICP—OES. The leach residue was sequentially washed with distilled water and then dried in a convection oven at 80 °C to constant weight.

Thermodynamic calculations were performed using HSC Chemistry Software v. 9.5 (Metso Outotec Finland Oy, Tampere, Finland).

Results and discussion

Thermodynamics of nitric acid leaching of stibnite

To establish the possibility of stibnite interacting with nitric acid solution, Gibbs free energy changes (ΔG) were calculated in the temperature range of 25—85 °C for the following reactions:

$$Sb_2S_3 + 6HNO_3 = Sb_2O_3 + 6NO_2 + 3S + 3H_2O, \quad (1)$$

$$Sb_2S_3 + 28HNO_3 = Sb_2O_5 + 3H_2SO_4 + 28NO_2 + 11H_2O, \quad (2)$$

$$Sb_2S_3 + 24HNO_3 = 2HSbO_2 + 3H_2SO_4 + 24NO_2 + 8H_2O, \quad (3)$$

$$2HSbO_2 + 4HNO_3 = Sb_2O_5 + 3H_2O + 4NO_2, \quad (4)$$

$$Sb_2O_3 + 4HNO_3 = Sb_2O_5 + 4NO_2 + 2H_2O. \quad (5)$$

As shown in Table 1, stibnite dissolution in nitric acid can proceed along several pathways, leading either to sparingly soluble antimony oxides (Sb_2O_3, Sb_2O_5) or to antimonous acid ($HSbO_2$) via reactions (1)—(3). Subsequently, both antimonous acid and antimony (III) oxide can be oxidized by nitric acid to antimony (V) oxide.

Pourbaix (Eh—pH) diagrams are a useful tool for predicting the thermodynamic stability of chemical species in aqueous media. To examine the behavior of antimony species at different pH and Eh values, an Eh—pH diagram was constructed for the S—Sb—H_2O system at 25 °C (Fig. 2, *a*). In addition, to more accurately predict the products of nitric acid leaching of stibnite, a distribution diagram was constructed (Fig. 2, *b*), showing the equilibrium concentrations of various antimony species as a function of nitric acid consumption.

The Pourbaix diagram (Fig. 2, *a*) indicates that in acidic media, dissolution of stibnite begins at a potential of about −0.4 V with the formation of antimonous acid ($HSbO_2$). A further increase in oxidation potential to approximately −0.61 V results in the conversion of $HSbO_2$ to Sb_2O_5, indicating more complete oxidation. These transformations are consistent with Gibbs free energy calculations for reactions (3) and (4).

The distribution diagram (Fig. 2, *b*), unlike the Pourbaix diagram, highlights the effect of nitric acid (HNO_3) consumption on the composition of stibnite dissolution products. At the initial stages, both $HSbO_2$ and Sb_2O_3 are formed. With nitric acid consumption exceeding 7 M,

Table 1. **Gibbs free energy change (ΔG) for reactions (1)–(5)**

Таблица 1. Результаты расчета изменения энергии Гиббса для реакций (1)–(5)

Reaction	ΔG, kJ/mol				
	25 °C	40 °C	55 °C	70 °C	85 °C
(1)	−344	−355	−367	−378	−389
(2)	−1630	−1683	−1735	−1787	−1839
(3)	−1411	−1455	−1498	−1541	−1583
(4)	−219	−228	−237	−246	−255
(5)	−168	−175	−182	−189	−196

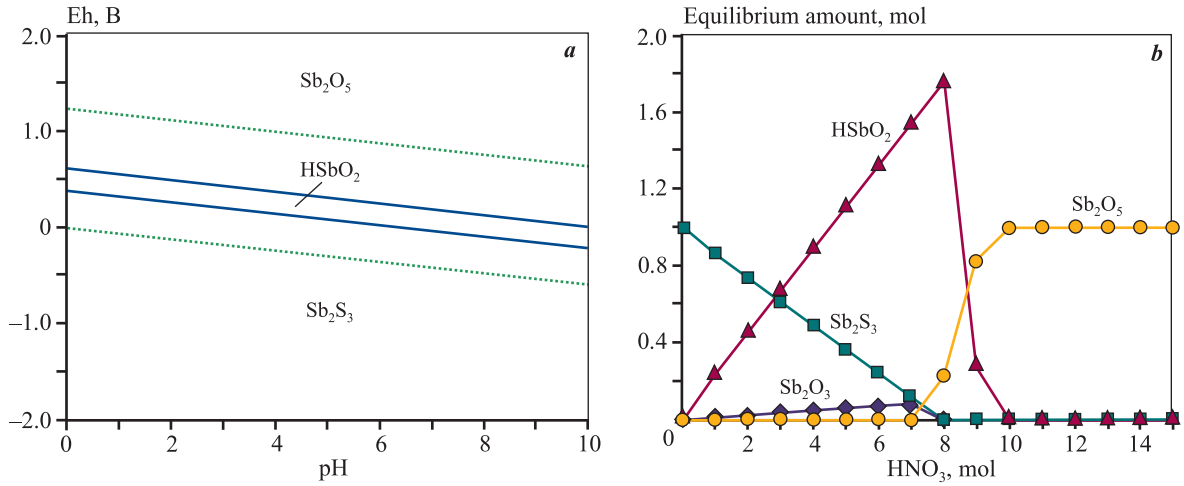

Fig. 2. Eh–pH diagram for the S–Sb–H_2O system (***a***), equilibrium distribution diagram of antimony species during nitric acid leaching of stibnite (***b***)

Рис. 2. Диаграмма Eh–pH для системы S–Sb–H_2O (***a***), диаграмма равновесного распределения соединений сурьмы при азотно-кислотном выщелачивании стибнита (***b***)

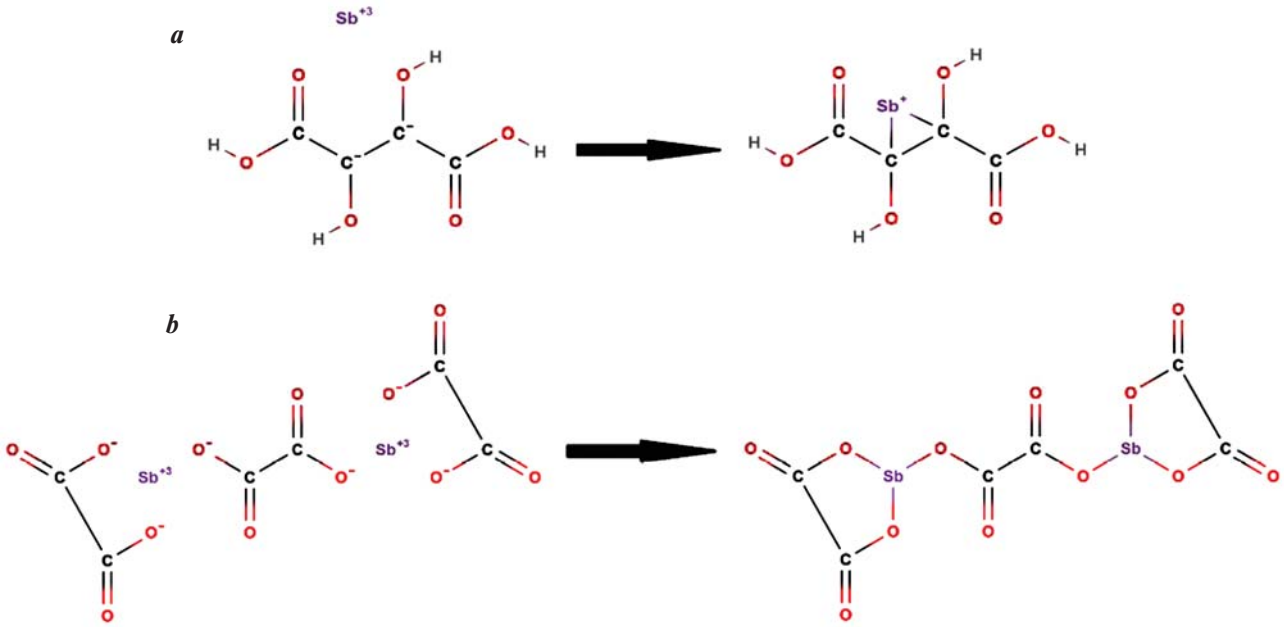

Fig. 3. Interaction schemes of antimony with tartaric acid (***a***) and oxalic acid (***b***)

Рис. 3. Схема взаимодействия сурьмы с винной (***a***) и щавелевой (***b***) кислотами

antimony is predominantly present as Sb_2O_5. This is attributed to the sharp increase in oxidation potential at high HNO_3 concentrations, which drives further oxidation of Sb(III) to Sb(V). At concentrations above 8 M, nearly complete oxidation of Sb_2O_3 and $HSbO_2$ to Sb_2O_5 is observed.

The thermodynamic analysis shows that nitric acid leaching of stibnite results primarily in the formation of antimony oxides, followed by their precipitation. To prevent antimony losses and improve leaching efficiency, it is therefore advisable to introduce additives that intensify the process and increase the degree of metal extraction. According to the literature [22], oxalic and tartaric acids are among the most effective complexing agents. They promote the formation of stable antimony complexes (Fig. 3), which helps retain the metal in solution and minimize oxide precipitation.

Investigation of nitric acid leaching and determination of optimal parameters

To evaluate the effect of tartaric acid on stibnite dissolution in nitric acid solution, experiments were conducted under the following conditions: nitric acid concentration — 6 mol/dm^3, liquid-to-solid ratio (L : S) = = 6 : 1, leaching duration — 60 min, temperature — 50 °C, and tartaric and oxalic acid concentrations — 50 g/dm^3 each.

As shown in Fig. 4, in the experiment without additives, antimony extraction into solution reached 44 % within the first 2 min, but subsequently decreased to 13 %. This effect is most likely associated with the transformation of antimony from antimonous acid ($HSbO_2$) into the insoluble oxide form (Sb_2O_5) according to reaction (4). The addition of tartaric and oxalic acids improved stibnite dissolution in nitric acid. Acting as complexing agents, they formed stable antimony complexes and prevented its conversion into insoluble oxide. However, tartaric acid achieved higher extraction (52 %) than oxalic acid (45 %), so further experiments were carried out with tartaric acid.

To determine the optimal parameters for nitric acid leaching of stibnite with tartaric acid, a statistical experimental design method was applied using the StatGraphics software package. A second-order orthogonal matrix was employed, comprising four variables: process temperature (35—85 °C), nitric acid concentration (1—9 mol/dm^3), leaching duration (10—70 min), and the tartaric acid-to-antimony mass ratio in stibnite (0.5÷4.5 : 1.0). The liquid-to-solid ratio (L : S) was maintained at 6 : 1 in all experiments.

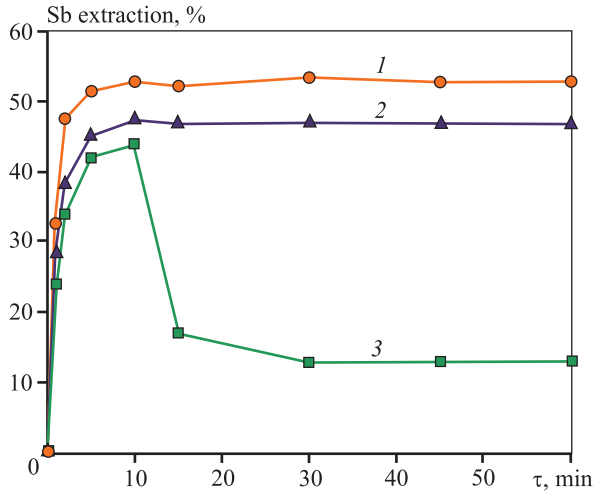

Fig. 4. Dependence of Sb extraction on time during nitric acid leaching with tartaric acid (***1***), oxalic acid (***2***), and without additives (***3***)

Рис. 4. Зависимость извлечения Sb от времени при азотно-кислотном выщелачивании с добавлением винной (***1***) и щавелевой (***2***) кислот, а также без добавок (***3***)

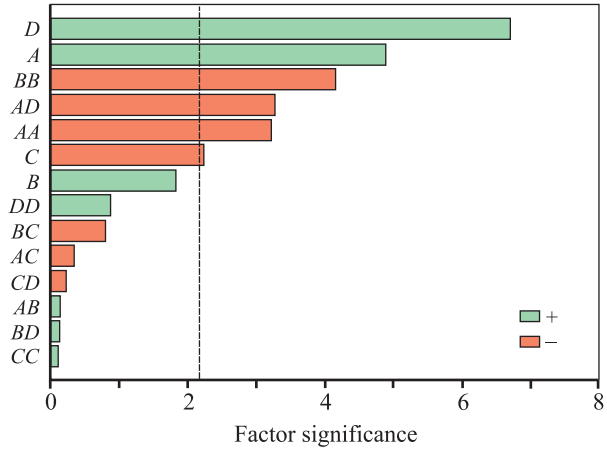

Fig. 5. Pareto chart for the parameters of nitric acid leaching of stibnite
D – tartaric acid-to-antimony ratio; *A* –nitric acid concentration; *C* – temperature; B – leaching duration

Рис. 5. Диаграмма Парето для изменяемых параметров азотно-кислотного выщелачивания стибнита
D – соотношение винной кислоты к сурьме; *A* – концентрация азотной кислоты; *C* – температура; *B* – продолжительность

Fig. 5 presents the Pareto chart for antimony leaching under the experimental conditions. The results indicate that the tartaric acid-to-antimony ratio and nitric acid concentration are the most statistically significant factors affecting antimony leaching, while leaching duration and temperature are less significant.

The dependence of antimony extraction on temperature, nitric acid concentration, leaching duration, and tartaric acid-to-antimony ratio is shown in Fig. 6.

As shown in Fig. 6, maximum antimony extraction from stibnite (>85 %) can be achieved under the following conditions: liquid-to-solid ratio — 6 : 1, temperature — 35 °C, nitric acid concentration — 5 mol/dm^3, leaching duration — 45 min, and tartaric acid-to-antimony mass ratio — 4.5 : 1.0. The regression equation for antimony leaching is

$$\begin{aligned}\mathrm{Sb} = {} & -36.4551 + 13.2264A + 1.4411B - 0.0825433C + \\ & + 0.609196D - 0.631207A^2 + 0.00311979AB - \\ & - 0.0101319AC - 0.0722656AD - 0.0144331B^2 - \\ & - 0.00313426BC + 0.000390972BD + \\ & + 0.000639506C^2 - 0.00089537CD + 0.00306981D^2, \quad (6)\end{aligned}$$

where A — nitric acid concentration, mol/dm^3; B — leaching duration, min; C — temperature, °C; D — tar-

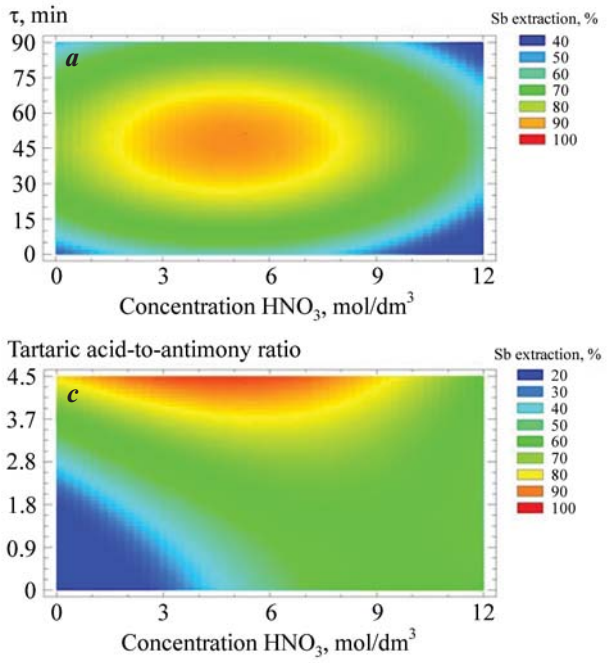

Fig. 6. Dependence of antimony extraction on nitric acid concentration (***a***–***c***), leaching duration (***a***), temperature (***b***), and tartaric acid-to-antimony ratio (***c***)

Рис. 6. Зависимость извлечения сурьмы от концентрации азотной кислоты (***a***–***c***), а также продолжительности (***a***), температуры (***b***) и соотношения винной кислоты к сурьме (***c***)

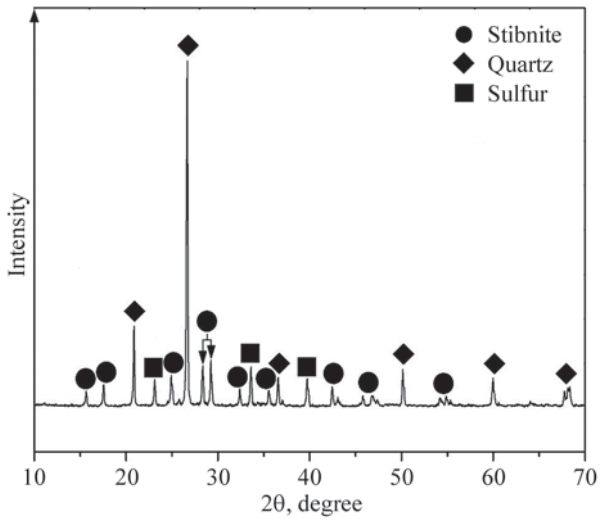

Fig. 7. XRD pattern of the leach residue after nitric acid leaching of stibnite with tartaric acid under optimal conditions

Рис. 7. Рентгенограмма нерастворенного остатка после азотно-кислотного выщелачивания стибнита с добавлением винной кислоты при оптимальных условиях

Table 2. **EDS analysis results of nitric acid leach residues of stibnite**

Таблица 2. Результаты исследования спектров кеков азотно-кислотного выщелачивания стибнита

Spectrum	Content, %			Identified phases
	O	Sb	S	
Without acid (see Fig. 8, *a*)				
1	15.1	56.6	28.3	$Sb_2O_5 + Sb_2S_3 + S^0$
2	17.5	55.3	27.2	$Sb_2O_5 + Sb_2S_3 + S^0$
3	16.4	57.2	26.4	$Sb_2O_5 + Sb_2S_3 + S^0$
With tartaric acid (see Fig. 8, *b*)				
1	–	48.6	51.4	$Sb_2S_3 + S^0$
2	–	44.8	55.2	$Sb_2S_3 + S^0$
3	–	54.3	45.7	$Sb_2S_3 + S^0$
4	–	67.1	32.9	$Sb_2S_3 + S^0$

taric acid-to-antimony mass ratio. The adequacy of the chosen model and regression equation is confirmed by a correlation coefficient of 0.92.

To validate the optimal parameters of nitric acid leaching of stibnite, an experiment was carried out under these conditions. The results showed antimony extraction of 87 % and sulfur extraction of 77 %. Of the total sulfur remaining in the leach residue, 61 % was present as sulfide and 39 % as elemental sulfur. The XRD pattern of the leach residue is shown in Fig. 7.

Fig. 8 presents SEM images and EDS analysis results at selected points (Table 2) of the leach residues after nitric acid leaching (L : S = 6 : 1, T = 35 °C,

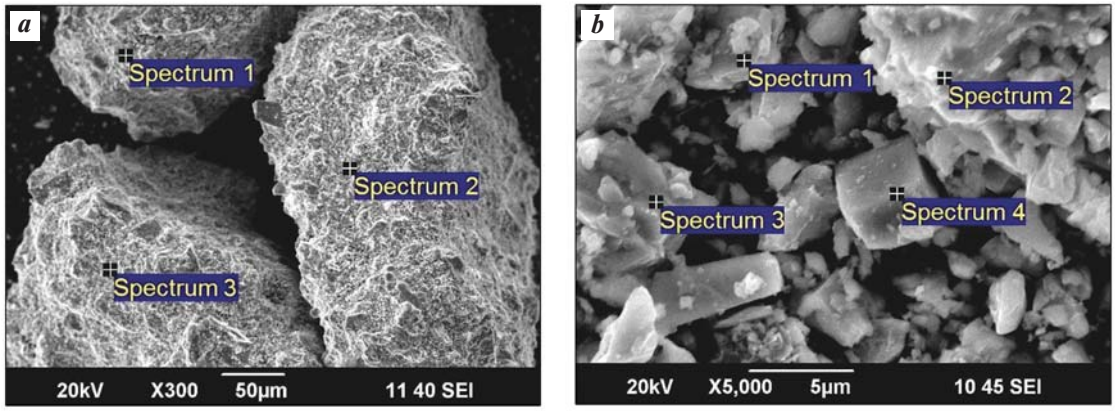

Fig. 8. SEM images of the leach residue from nitric acid leaching of stibnite without tartaric acid (***a***) and with tartaric acid (***b***)

Рис. 8. SEM-изображения кека азотно-кислотного выщелачивания стибнита без винной кислоты (***a***) и при ее наличии (***b***)

$[HNO_3]$ = 5 mol/dm^3, τ = 15 min) without and with tartaric acid (tartaric acid-to-antimony mass ratio 4.5 : 1.0).

The SEM images in Fig. 8 highlight differences in the composition of the leach residue depending on tartaric acid addition. In the sample without tartaric acid (Fig. 8, *a*), the residue contains antimony pentoxide (Sb_2O_5), stibnite (Sb_2S_3), and elemental sulfur (S^0). In contrast, in the presence of tartaric acid (Fig. 8, *b*), the residue consists mainly of unreacted stibnite and elemental sulfur, while antimony oxides are absent. This confirms that tartaric acid binds Sb ions in solution, preventing their hydrolysis and precipitation as oxides.

Conclusion

The present study on nitric acid leaching of stibnite with tartaric acid confirmed the effectiveness of this complexing agent in improving antimony extraction.

Thermodynamic analysis demonstrated that direct nitric acid leaching inevitably leads to the formation of antimony oxides, resulting in metal losses. The addition of tartaric acid promotes the formation of stable water-soluble complexes with antimony, which significantly reduces oxide precipitation.

Statistical experimental design showed that the tartaric acid-to-antimony mass ratio and nitric acid concentration are the most significant factors affecting leaching efficiency. Maximum antimony extraction of 87 % was achieved under the following conditions: temperature — 35 °C, $[HNO_3]$ = 5 mol/dm^3, leaching duration — 45 min, and tartaric acid-to-antimony mass ratio — 4.5 : 1.0.

SEM and XRD analyses of the leach residue further confirmed that tartaric acid addition minimizes antimony losses. In the absence of tartaric acid, the residue contains antimony pentoxide (Sb_2O_5), indicating oxidation and hydrolysis of Sb ions with their conversion to insoluble forms, leading to metal losses. In contrast, in the presence of tartaric acid, oxide phases were not detected; the residue consisted mainly of unreacted stibnite (Sb_2S_3) and elemental sulfur (S^0).

Thus, tartaric acid ensures that antimony remains in a recoverable form by preventing its conversion into stable oxides, thereby improving leaching efficiency. This approach is relevant for developing more effective processing technologies for antimony-bearing raw materials.

References

1. Moosavi-Khoonsari E., Mostaghel S., Siegmund A., Cloutier J-P. A review on pyrometallurgical extraction of antimony from primary resources: Current practices and evolving processes. *Processes*. 2022;10:1590. https://doi.org/10.3390/pr10081590
2. Multani R.S., Feldmann T., Demopoulos G.P. Antimony in the metallurgical industry: A review of its chemistry and environmental stabilization options. *Hydrometallurgy*. 2016;164:141—53. https://doi.org/10.1016/j.hydromet.2016.06.014
3. Dembele S., Akcil A., Panda S. Technological trends, emerging applications and metallurgical strategies in antimony recovery from stibnite. *Minerals Engineering*. 2022;175:107304. https://doi.org/10.1016/j.mineng.2021.107304

4. Ye L., Ouyang Z., Chen Y., Chen Y., Xiao L. Sulfur fixation and reduction roasting of stibnite for clean extraction of antimony by a combined metallurgy and beneficiation process. *Minerals Engineering*. 2019;144:106049. https://doi.org/10.1016/j.mineng.2019.106049
5. Zekavat M., Yoozbashizadeh H., Khodaei A. Leaching of antimony from stibnite ore in KOH solution for sodium pyroantimonate production: Systematic optimization and kinetic study. *Thermodynamic Optimization of Critical Metals Processing and Recovery*. 2021;73:903—912. https://doi.org/10.1007/s11837-020-04531-8
6. Aghazadeh S., Abdollahi H., Gharabaghi M., Mirmohammadi M. Selective leaching of antimony from tetrahedrite rich concentrate using alkaline sulfide solution with experimental design: Optimization and kinetic studies. *Journal of the Taiwan Institute of Chemical Engineers*. 2021;119:298—312. https://doi.org/10.1016/j.jtice.2021.01.021
7. Sudova M., Sisol M., Kanuchova M., Marcin M., Kurty J. Environmentally friendly leaching of antimony from mining residues using deep eutectic solvents: Optimization and sustainable extraction strategies. *Processes*. 2024;12(3):555. https://doi.org/10.3390/pr12030555
8. Wang X., Yang Y., Tao L., He M. Antimonite oxidation and adsorption onto two tunnel-structured manganese oxides: Implications for antimony mobility. *Chemical Geology*. 2021;579:120336. https://doi.org/10.1016/j.chemgeo.2021.120336
9. Ye L., Ouyang Z., Chen Y., Chen Y. Ferric chloride leaching of antimony from stibnite. *Hydrometallurgy*. 2019;186:210—217. https://doi.org/10.1016/j.hydromet.2019.04.021
10. Xiang L., Liu C., Liu D., Ma L., Qiu X., Wang H., Liu X. Antimony transformation and mobilization from stibnite by an antimonite oxidizing bacterium Bosea sp. AS-1. *Journal of Environmental Sciences*. 2022;111:273—281. https://doi.org/10.1016/j.jes.2021.03.042
11. Zhang F., Cui Y., He X., Lv C., Li L., Zhang J., Nan J. Selective alkaline leaching of antimony from Low-grade refractory gold ores and process optimization. *Minerals Engineering*. 2023;201:108198. https://doi.org/10.1016/j.mineng.2023.108198
12. Cornelis G., Gerven T., Vandecasteete C. Antimony leaching from MSWI bottom ash: Modelling of the effect of pH and carbonation. *Waste Management*. 2012;32(2):278—286. https://doi.org/10.1016/j.wasman.2011.09.018
13. Madkur L.H. Thermodynamic behaviour of complex antimonite ore for electrodeposition of metal value. *Journal de Chimie Physique*. 1997;94:620—634. https://doi.org/10.1051/jcp/1997940620
14. Smincakova E., Raschman P. Leaching of natural stibnite using Na_2S and NaOH solutions. *International Journal of Energy Engineering*. 2011;1(2):85—89. https://doi.org/ 10.5963/IJEE0102006
15. Rogozhnikov D., Dizer O., Karimov K., Zakhar'yan S. Nitric acid leaching of the copper-bearing arsenic sulphide concentrate of Akzhal. *Tsvetnye Metally*. 2020;8:11—17. https://doi.org/10.17580/tsm.2020.08.02
16. Kuzas E., Rogozhnikov D., Dizer O., Karimov K., Shoppert A., Suntsov A., Zhidkov I. Kinetic study on arsenopyrite dissolution in nitric acid media by the rotating disk method. *Minerals Engineering*. 2022;187:107770. https://doi.org/10.1016/j.mineng.2022.107770
17. Rusalev R., Rogozhnikov D., Dizer O., Golovkin D., Karimov K. Development of a two-stage hydrometallurgical process for gold—antimony concentrate treatment from the olimpiadinskoe deposit. *Materials*. 2023;16:4767. https://doi.org/10.3390/ma16134767
18. Dizer O., Rogozhnikov D., Karimov K., Kuzas E., Suntsov A. Nitric acid dissolution of tennantite, chalcopyrite and sphalerite in the presence of Fe (III) ions and FeS_2. *Materials*. 2022;15:1545. https://doi.org/10.3390/ma15041545
19. Madkour L.H., Salem I.A. Electrolytic recovery of antimony from natural stibnite ore. *Hydrometallurgy*. 1996;43:265—75. https://doi.org/10.1016/0304-386X(95)00113-U
20. Davidenko P.S., Troshkin A.M., Melnikov Yu.T. Kinetics of interaction of antimony sulfide with nitric acid solution. *Izvestiya. Non-Ferrous Metallurgy*. 2006;(1):24—27. (In Russ.).
Давиденко П.С., Трошкин А.М., Мельников Ю.Т. Кинетика взаимодействия сульфида сурьмы с раствором азотной кислоты. *Известия вузов. Цветная металлургия*. 2006;(1):24—27.
21. Besold J., Kumar N., Scheinost A., Pacheco J., Fendorf S., Planer-Friedrich B. Antimonite complexation with thiol and carboxyl/phenol groups of peat organic matter. *Environmental Science & Technology*. 2019;53(9):5005—5015. https://doi.org/10.1021/acs.est.9b00495
22. Shabdanova E.A. The use of organic oxyacids in the

processes of leaching and complexation of metals. *Izvestiya Vuzov (Kyrgyzstan).* 2015;2:95—102. (In Russ.).
Шабданова Э.А. Использование органических оксикислот в процессах выщелачивания и комплексообразования металлов. *Известия вузов (Кыргызстан).* 2015;2:95—102.

23. Larba R., Boukerche I., Alane N., Habbache N., Djerad S., Tifouti L. Citric acid as an alternative lixiviant for zinc oxide dissolution. *Hydrometallurgy.* 2013;134—135:117—23. https://doi.org/10.1016/j.hydromet.2013.02.002
24. Oke E.A., Potgieter H., Mondlane F., Skosana N.P., Teimouri S., Nyembwe J.K. Concurrent leaching of copper and cobalt from a copper—cobalt ore using sulfuric and organic acids. *Minerals Engineering.* 2024;216:108853. https://doi.org/10.1016/j.mineng.2024.108853
25. Borda J., Torres R. Effect of pretreatments to improve nickel leaching from laterites in carboxylic media: Mechanism and kinetic model. *South African Journal of Chemical Engineering.* 2023;46:12—21. https://doi.org/10.1016/j.sajce.2023.07.001
26. Tzeferis P.G., Agatzini-Leonardou S. Leaching of nickel and iron from Greek non-sulphide nickeliferous ores by organic acids. *Hydrometallurgy.* 1994;36:345—60. https://doi.org/10.1016/0304-386X(94)90031-0

Information about the authors

Oleg A. Dizer – Cand. Sci. (Eng.), Senior Researcher of the Laboratory of advanced technologies in non-ferrous and ferrous metals raw materials processing, Ural Federal University n.a. the First President of Russia B.N. Yeltsin (UrFU).
https://orcid.org/0000-0001-7705-0864
E-mail: oleg.dizer@yandex.ru

Dmitry I. Golovkin – Cand. Sci. (Eng.), Junior Researcher of the Laboratory of advanced technologies in non-ferrous and ferrous metals raw materials processing, UrFU.
https://orcid.org/0000-0001-6308-4086
E-mail: dmitry.golovkin@urfu.ru

Yuri E. Shklyaev – Research Engineer of the Laboratory of advanced technologies in non-ferrous and ferrous metals raw materials processing, UrFU.
https://orcid.org/0009-0001-4220-4330
E-mail: iushkliaev@urfu.ru

Denis A. Rogozhnikov – Dr. Sci. (Eng.), Head of the Laboratory of advanced technologies in non-ferrous and ferrous metals raw materials processing, UrFU.
https://orcid.org/0000-0002-5940-040X
E-mail: darogozhnikov@urfu.ru

Информация об авторах

Олег Анатольевич Дизер – к.т.н., ст. науч. сотрудник лаборатории перспективных технологий комплексной переработки минерального и техногенного сырья цветных и черных металлов, Уральский федеральный университет имени первого Президента России Б.Н. Ельцина (УрФУ).
https://orcid.org/0000-0001-7705-0864
E-mail: oleg.dizer@yandex.ru

Дмитрий Игоревич Головкин – к.т.н. мл. науч. сотрудник лаборатории перспективных технологий комплексной переработки минерального и техногенного сырья цветных и черных металлов, УрФУ.
https://orcid.org/0000-0001-6308-4086
E-mail: dmitry.golovkin@urfu.ru

Юрий Евгеньевич Шкляев – инженер-исследователь лаборатории перспективных технологий комплексной переработки минерального и техногенного сырья цветных и черных металлов, УрФУ.
https://orcid.org/0009-0001-4220-4330
E-mail: iushkliaev@urfu.ru

Денис Александрович Рогожников – д.т.н., зав. лабораторией перспективных технологий комплексной переработки минерального и техногенного сырья цветных и черных металлов, УрФУ.
https://orcid.org/0000-0002-5940-040X
E-mail: darogozhnikov@urfu.ru

Contribution of the authors

O.A. Dizer – defined research objectives, conducted experiments and analyses, and wrote the manuscript.

D.I. Golovkin – performed chemical analysis, and contributed to the discussion of results.

Yu.E. Shklyaev – conducted experiments and contributed to the discussion of results..

D.A. Rogozhnikov – contributed to the discussion of results and edited the manuscript.

Вклад авторов

О.А. Дизер – определение цели работы, проведение экспериментов и анализов, написание статьи.

Д.И. Головкин – проведение экспериментов, выполнение химического анализа, участие в обсуждении результатов.

Ю.Е. Шкляев – проведение экспериментов, участие в обсуждении результатов.

Д.А. Рогожников – участие в обсуждении результатов, редактирование статьи.

The article was submitted 07.05.2025, revised 20.06.2025, accepted for publication 25.06.2025

Статья поступила в редакцию 07.05.2025, доработана 20.06.2025, подписана в печать 25.06.2025

UDC 669.054.8
https://doi.org/10.17073/0021-3438-2025-3-54-65

Research article
Научная статья

Processing of copper anode slimes by aeration leaching (decopperization) and flotation

S.A. Mastyugin[1,3], **K.L. Timofeev**[1,3], **R.S. Voinkov**[1,3], **S.V. Volkova**[2]

[1] **JSC "Uralelectromed"**
1 Uspenskiy Prosp., Sverdlovsk reg., Verkhnyaya Pyshma 624091, Russia

[2] **JSC "Uralmekhanobr"**
87 Khokhryakova Str., Ekaterinburg 620144, Russia

[3] **Technical University of UMMC**
3 Uspenskiy Prosp., Sverdlovsk reg., Verkhnyaya Pyshma 624091, Russia

✉ Sergey A. Mastyugin (S.Mastugin@uralcopper.com)

Abstract: With the declining quality of feedstock in the copper industry, maintaining metal recovery rates and controlling production costs for non-ferrous and precious metals has become increasingly critical. A key research priority is therefore the development of processing strategies that not only concentrate target metals into flotation products but also recover valuable minor elements previously lost with slags and flue dust. One approach involves designing process flowsheets that integrate hydrometallurgical and beneficiation operations. Previous studies have demonstrated the effectiveness of combining autoclave leaching and flotation for decopperization of copper anode slimes and their concentration in gold, silver, and selenium. However, autoclave leaching requires significant capital and operating expenditures. For this reason, a series of tests was carried out on aeration leaching (decopperization) of copper anode slimes followed by flotation, yielding promising results. This study examined the influence of aeration leaching conditions (temperature, agitation, and specific oxidant consumption—air and oxygen), disintegration of the leached product, and flotation parameters on the selective separation of oxide and chalcogenide phases and the quality of the resulting concentrates. Based on the experimental results, process operations were developed that make it possible to concentrate precious metals in copper anode slimes two- to threefold without the use of autoclave leaching. Optimal conditions and equipment configurations were determined for deep decopperization of slimes (to less than 0.5–0.8 % residual copper). An acceptable degree of separation of precious-metal chalcogenides from lead and antimony oxides was achieved, enabling downstream recovery of marketable products from the respective concentrates. Analytical characterization of the products was performed using scanning electron microscopy (SEM) and energy-dispersive *X*-ray spectroscopy (EDS). The findings contribute to the development of an integrated hydrometallurgical technology for processing copper anode slimes..

Key words: copper anode slimes, aeration leaching (decopperization), flotation processing, bulk concentrate, final tails, precious metals, silver, selenium, tellurium, lead.

For citation: Mastyugin S.A., Timofeev K.L., Voinkov R.S., Volkova S.V. Processing of copper anode slimes by aeration leaching (decopperization) and flotation. *Izvestiya. Non-Ferrous Metallurgy.* 2025;31(3):54–65. https://doi.org/10.17073/0021-3438-2025-3-54-65

Обогащение медеэлектролитных шламов по технологии «аэрационное обезмеживание – флотация»

С.А. Мастюгин[1,3], **К.Л. Тимофеев**[1,3], **Р.С. Воинков**[1,3], **С.В. Волкова**[2]

[1] **АО «Уралэлектромедь»**
Россия, 624091, Свердловская обл., г. Верхняя Пышма, Успенский пр-т, 1

[2] **АО «Уралмеханобр»**
Россия, 620144, г. Екатеринбург, ул. Хохрякова, 87

[3] **Технический университет УГМК**
Россия, 624091, Свердловская обл., г. Верхняя Пышма, Успенский пр-т, 3

✉ Сергей Аркадьевич Мастюгин (S.Mastugin@uralcopper.com)

Аннотация: В условиях ухудшения качества сырья в медной подотрасли проблема сохранения параметров извлечения и себестоимости цветных и благородных металлов становится еще более важной. Поэтому приоритетной задачей для исследователей является разработка технологических приемов, позволяющих не только концентрировать целевые металлы в обогащенные продукты, но и извлекать ранее теряемые со шлаками и пылями ценные элементы-примеси. Одним из способов ее решения является создание технологических схем, сочетающих гидрометаллургические и обогатительные операции. Ранее проведенными исследованиями была показана эффективность применения автоклавных процессов и флотации для обезмеживания медеэлектролитного шлама и его обогащения по золоту, серебру и селену. Однако применение автоклавных процессов требует больших капитальных и текущих затрат. Поэтому был проведен цикл экспериментов по аэрационному обезмеживанию шлама с последующей флотацией и получены соответствующие результаты опытов. В настоящей работе было изучено влияние условий аэрационного выщелачивания (температуры, условий перемешивания, удельного расхода окислителя – воздуха и кислорода), дезинтеграции полученного продукта, а также параметров флотации на селективность разделения оксидной и халькогенидной фаз и качество получаемых при этом концентратов. По результатам экспериментов разработаны технологические операции, позволяющие обогащать медеэлектролитные шламы в 2–3 раза по содержанию драгоценных металлов без использования автоклавных процессов. Определены условия и аппаратурное оформление для глубокого обезмеживания шлама (менее 0,5–0,8 % остаточного содержания меди). Достигнут приемлемый уровень разделения халькогенидов драгоценных металлов и оксидных соединений свинца и сурьмы, что позволит в дальнейшем извлекать при переработке соответствующих концентратов товарные продукты. Приведены результаты анализа получаемых продуктов с использованием методов РЭМ и РСМА. Полученные данные являются вкладом в создание комплексной гидрометаллургической технологии переработки анодных шламов медного производства.

Ключевые слова: медеэлектролитный шлам, аэрационное обезмеживание, флотационное обогащение, концентрат, хвосты флотации, драгоценные металлы, серебро, селен, теллур, свинец.

Для цитирования: Мастюгин С.А., Тимофеев К.Л., Воинков Р.С., Волкова С.В. Обогащение медеэлектролитных шламов по технологии «аэрационное обезмеживание – флотация». *Известия вузов. Цветная металлургия*. 2025;31(3):54–65.
https://doi.org/10.17073/0021-3438-2025-3-54-65

Introduction

Copper anode slimes represent a unique feedstock for recovering not only precious metals but also chalcogens, which worldwide are predominantly extracted from primary copper-bearing raw materials [1—4]. The conventional global practice of slime processing, yielding Doré (silver—gold alloy), enables the separation of precious and base metals as well as selenium and tellurium. During oxidative roasting, selenium transitions into the gas phase as dioxide and is subsequently recovered from wet gas-cleaning solutions. In the smelting of the calcine, tellurium is transferred into soda slags, which are further processed to obtain commercial tellurium, while heavy minor metals such as lead and antimony are distributed into silicate or other slags [1; 5—7].

These processes are characterized by significant fuel and energy consumption and relatively low efficiency due to:

— limited recovery of precious metals, selenium, and tellurium, caused by the large quantities of waste generated—slags, dust, furnace refractories, and off-gases from roasting and smelting units;

— the environmental impact of these wastes (containing substances of hazard classes I—II) and the associated costs of multistage gas cleaning, which can reach up to 10 % of production costs;

— additional losses of lead, antimony, and tin to slags and other by-products.

Therefore, the development of new, as well as the improvement of existing, slime treatment operations and the creation of advanced, high-efficiency technologies for the comprehensive processing of copper anode slimes with maximum recovery of valuable components remain pressing objectives.

Among the most notable international developments, pilot tests, and in some cases industrial implementations, hydrometallurgical technologies for anode slime processing are considered highly promising. They have been applied at enterprises such as Kennecott Utah Copper Magna (USA) [8], Naoshima Smelter and Refinery (Japan) [9], Outokumpu Technology Oy (Finland) [10], and Yunnan Smelter (China) [11]. Recent studies include work on leaching metal chalcogenides from slimes in alkaline solutions [12; 13], sintering slimes to convert minor elements into soluble forms [14], as well as analyses of combined pyro- and hydrometallurgical approaches [15].

Based on the analysis of advantages and limitations of the proposed flowsheets and individual operations [9], as well as our own research and laboratory trials, we developed a technology for slime processing involving autoclave oxidative leaching followed by flotation [16]. Pilot-scale testing produced a flotation concentrate containing more than 80—85 % of Au + Ag + Se. The recovery of gold and silver into the high-grade concentrate reached 96—98 %. The secondary concentrate, with 40 % Pb and 20 % Sb, essentially represents a rich lead—antimony concentrate. Despite the advantages of this technology, decopperization and preparation of slimes for flotation under autoclave conditions requires high capital and operating expenditures.

The aim of this study was to evaluate the feasibility of replacing autoclave leaching of slimes with a less costly alternative based on aeration leaching (decopperization) followed by flotation of the decopperized slime, and to analyze this approach in the context of its use as a preliminary stage in an integrated technology for processing copper anode slimes.

Aeration leaching (decopperization): procedure and results

Aeration treatment of the slime slurry was carried out in a 50-dm^3 "Bourbon" type reactor equipped with gas dispersers[1]. As dispersion (air or oxygen) ensured maximum contact area between the gas phase and the slime pulp by generating bubbles 0.05—0.30 mm in size. In one of the experiments, a mechanochemical activator was tested. The experimental conditions are summarized in Table 1.

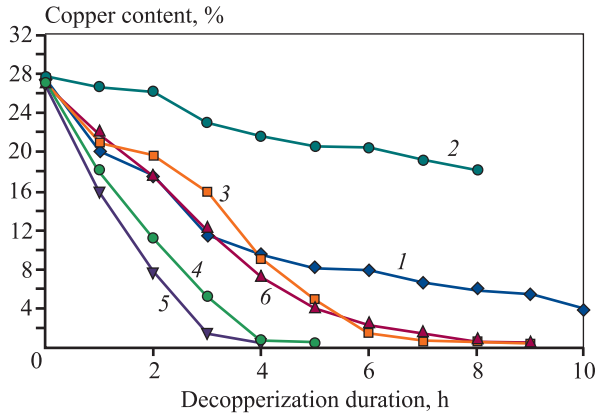

Fig. 1. Change in copper content in slimes over time under different test conditions

The numbering of the curves corresponds to the test number (see Table 1)

Рис. 1. Изменение содержания меди в шламе по времени в зависимости от условий опытов

Нумерация кривых соответствует № опыта (см. табл. 1)

Figure 1 shows the results of the experiments:

— in Test *2*, a mechanochemical activator was used, which blocked the leaching process: the elemental copper present in the slime apparently sealed the reactive surface of the material;

— in Tests *1* and *2*, the required copper content (<3 %) in the solid phase of decopperization was not achieved, indicating that the use of air as an oxidant is ineffective for deep decopperization of copper anode slimes, regardless of flow rate;

— the use of oxygen as an oxidant (Tests *3*—*6*) made it possible to achieve the target copper content in the decopperized residue;

— the duration of decopperization with oxygen depended on its flow rate and the solid—liquid ratio in the slurry.

Based on pilot-scale laboratory trials, the optimal oxygen consumption was determined to be 715 m^3 (31.9 kg) per 1 t of processed slime. Changing the solid—liquid ratio from 1 : 10 to 1 : 5 (Test *6*) increased the decopperization time from 5 to 9 h

[1] Experiments were conducted on equipment and with technical support provided by BFK-Engineering (Moscow).

Table 1. **Experimental conditions for aeration leaching (decopperization)**

Таблица 1. Условия проведенных экспериментов по аэрационному обезмеживанию

Parameter	Test No.					
	1	*2**	*3*	*4*	*5*	*6*
Moisture content of slime, %	25.8	25.8	31	31	26	26
Copper content in slime, %	27.7	27.7	27.1	27.1	27.0	27.0
Slime mass (dry basis), kg	3.9	3.4	4.2	4.2	3.9	9.4
Initial H_2SO_4 concentration, g/dm^3	198.7	204	210	188	196.7	170
Agitation speed, rpm	262	262	315	315	315	315
Solid–liquid ratio (S : L)	1 : 10	1 : 10	1 : 10	1 : 10	1 : 10	1 : 5
Process temperature, °C	94–95	94–95	94–95	94–95	94–95	94–95
Air flow rate, L/min	20	18–19	–	–	–	–
Oxygen flow rate, L/min	–	–	8	10	20	32
Gas consumption, m^3/t of slime	3073.6	2542.6	801.3	715.4	1229.5	1838.5
Duration of leaching, h	10	8	7	5	4	9

* Test involving mechanochemical activation.

and significantly increased oxygen consumption (1839 m^3/t).

Visual inspection and monitoring of the ceramic gas dispersers during decopperization indicated that fluoropolymer-based materials such as PTFE should be used for gas dispersion.

It is known that in unprocessed anode slime, copper is mainly present in elemental form, with a smaller fraction occurring as chalcogenides—primarily copper—silver selenides and tellurides. Previous studies established that during leaching, elemental copper dissolves first, whereas chalcogenides, which require a higher oxidation potential, leach at a later stage. Thus, copper can be oxidized with air down to a residual copper content in the slime of 3—6 %, while deeper decopperization (to 0.5—1.0 %) requires oxygen under elevated pressure, higher initial solution acidity, and efficient gas—slurry contact. It was also established that using a solution containing 200 g/dm^3 sulfuric acid during decopperization reduces tellurium dissolution to 5—8 %, whereas in autoclave treatment tellurium dissolution may reach 25—40 %.

Deep decopperization of slime while maximizing selenium and tellurium retention is important for the effective separation of the chalcogenide and oxide components of decopperized copper anode slimes during flotation processing.

Flotation processing: methodology and results

Phase analysis of copper anode slimes [1; 17] established that in the decopperized slime, gold is mainly present in elemental form, silver occurs as silver selenide, while lead and antimony are present as oxides (sulfates, antimonates, arsenates, etc.). In global practice of sulfide ore processing, flotation methods are widely used to separate oxide minerals from chalcogenides (sulfides, selenides, tellurides). These methods are based on differences in the wettability of minerals in aqueous media, with flotation reagents used to regulate this process.

For the flotation experiments on decopperized slime, samples of the residues obtained after Tests *3—6* were taken. The analysis of these samples for precious metals, lead, and antimony is presented in Table 2.

Bulk flotation of the decopperized slime was carried out at pH = 1.5 and a solid—liquid ratio of 1 : 10. The total consumption of flotation reagents was 450—470 g/t of Aeroflot and 50—65 g/t of MIBK (methyl isobutyl carbinol). The duration of the bulk flotation cycle was 51—62 min. The bulk concentrate was then subjected to regrinding in a bead mill, followed by cleaner flotation stages. Initially, comparative experiments were performed on flotation

Table 2. **Chemical composition of decopperized slime residues (Tests *3–6*)**

Таблица 2. Химический состав проб исходного шлама после опытов *3–6*

Residue (Test No.)	Metal content, %			
	Au	Ag	Pb	Sb
3	0.57	13.44	4.59	14.50
4	0.66	13.78	5.70	15.00
5	0.66	16.13	7.00	15.02
6	0.77	16.36	7.48	14.21

processing of copper anode slime from Test *6* (without regrinding and with regrinding). For concentrate regrinding, a 2.0 L bead mill manufactured by Knelson—Deswik, operating in a circulating mode, was used.

Bead milling of the slime to a particle size of 4—6 μm was previously justified by the need to break down silver selenide spheroids (average size 8—10 μm) that encapsulate oxide compounds of lead, antimony, and arsenic [18—19]. Achieving this particle size increased the transfer of these compounds into the secondary flotation product, thereby improving the quality of the flotation concentrate. As an example, Fig. 2 presents the particle size distribution of the concentrate from decopperization Test *6* after bead milling, measured with a HELOS Particle Size Analyzer (Sympatec).

Comparative flotation results for decopperized copper anode slime processed according to the flowsheet "aeration leaching (decopperization) — flotation — concentrate regrinding", with and without regrinding of the bulk concentrate, are presented in Table 3. Analysis of these data shows that without regrinding, the gold content in the second cleaner concentrate is lower by 22.0 % and the silver content by 10—16 % compared with the second cleaner concentrate obtained after regrinding of the bulk concentrate. Therefore, regrinding of the bulk concentrate prior to cleaner flotation is justified.

The flowsheet for open-circuit flotation tests with concentrate regrinding and 4—5 cleaner stages of the bulk flotation concentrate is shown in Fig. 3. In the first cleaner stage of the reground concentrate, Aeroflot and MIBK were added, except for the slime sample from Test *6*. The highest reagent consumption was 230 g/t of Aeroflot and 60 g/t of MIBK, with a cleaner flotation time of 38 min for the slime sample from Test *5*. Water glass at a dosage of 300 g/t was added in the second, third, fourth, and fifth cleaner stages.

The flotation reagent regimes for copper anode slime samples from Tests *3—6* (see Table 1), along with the duration of the flotation stages, are presented in Table 4.

Technological performance indicators of flotation processing of decopperized copper anode slime according to the flowsheet "flotation — cleaner flotation of the concentrate" are presented in Table 5.

The summarized results of slime flotation are presented in Table 6.

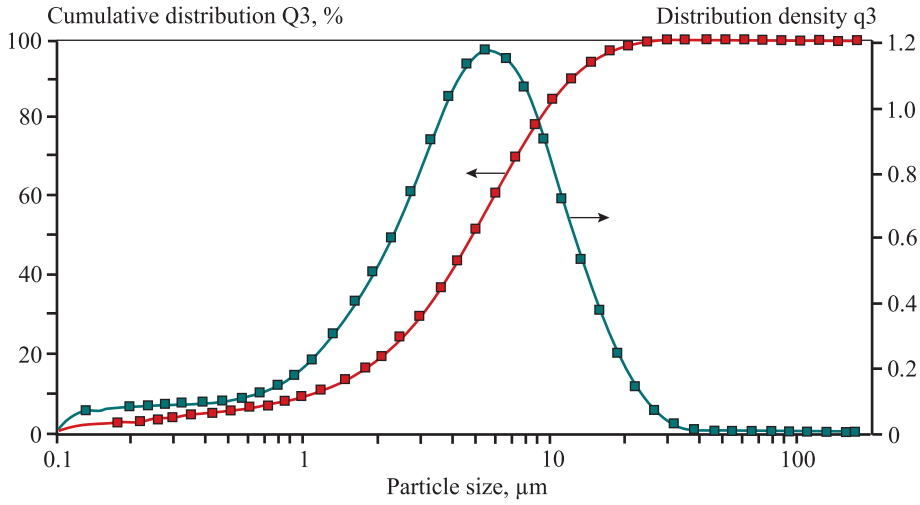

Fig. 2. Particle size distribution of the bulk flotation concentrate of decopperized slime obtained in Test *6* (see Table 2)

Рис. 2. Результаты гранулометрического анализа коллективного концентрата флотации обезмеженного шлама, полученного в опыте *6* (см. табл. 2)

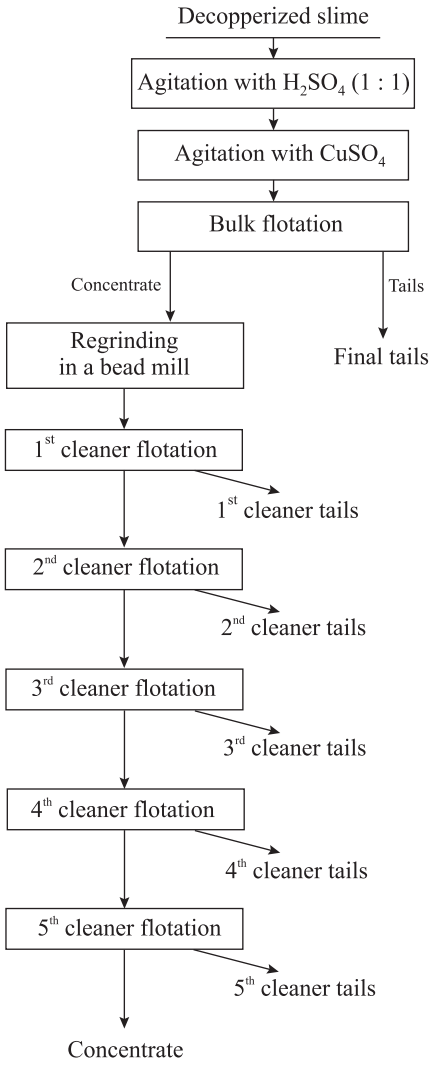

Fig. 3. Flowsheet of open-circuit flotation tests

Рис. 3. Схема проведения флотационных опытов в открытом цикле

Table 3. **Comparative flotation results for anode slime from Test *6* according to the flowsheet "flotation – concentrate regrinding", with and without bulk concentrate regrinding**

Таблица 3. Сравнительные показатели обогащения шлама из опыта *6* по схеме «флотация – доводка концентрата» без измельчения и с доизмельчением коллективного концентрата

Product	Yield, %	Mass fraction, %		Recovery, %	
		Au	Ag	Au	Ag
Without bulk concentrate regrinding					
Concentrate	41.77	1.34	29.8	72.54	76.09
Second cleaner tails	8.80	0.89	20.16	10.15	10.85
First cleaner tails	12.97	0.58	10.46	9.75	8.29
Bulk flotation	**63.54**	–	–	**92.44**	**95.23**
Flotation tails	36.46	0.16	2.14	7.56	4.77
Feed (slime)	100.00	0.77	16.36	100.00	100.00
With bulk concentrate regrinding in a bead mill					
Concentrate	25.76	1.71	35.61	60.14	59.50
Second cleaner tails	5.34	0.97	21.78	7.09	7.54
First cleaner tails	30.31	0.58	14.09	24.06	27.70
Bulk flotation	**61.41**	–	–	**91.29**	**97.74**
Flotation tails	38.59	0.165	2.1	8.71	5.26
Feed (slime)	100.00	0.73	15.42	100.00	100.00

Discussion

The results indicate that through the use of hydrometallurgical operations — namely aeration decopperization and flotation processing — the degree of concentration of copper anode slime can be increased by a factor of 2.5—3.0, with a corresponding rise in gold and silver content. In addition, the flotation tails represent an oxide concentrate rich in lead and antimony.

The concentrate after cleaner flotation and the final tails were examined using a Carl Zeiss EVO MA15 scanning electron microscope with X-Max EDX system (Germany). The results are presented in Fig. 4.

The obtained concentrate of precious metals and chalcogenides requires further upgrading and subsequent separation of gold, silver, and selenium. Its main constituent is refractory silver selenide, and the separation of these components necessitates the application of specialized, potentially unique, technological operations. The recovery of antimony, lead, and other non-ferrous metals present in copper anode slimes has been addressed in a number of publications [20; 21]. For processing flotation tails, which consist mainly of oxide compounds of lead and antimony, a previously developed integrated technology may be applied: in stage 1, leaching of lead sulfate with conventional complexing agents; in stage 2, electrolysis of an antimony — lead anode in an alkaline — glycerate solution, producing commercial antimony while simultaneously precipitating lead from the electrolyte as

Table 4. **Process and reagent regimes for flotation processing of copper anode slime samples (see Table 1) according to the flowsheet "bulk flotation – ultrafine regrinding of the bulk concentrate – cleaner flotation of the bulk concentrate"**

Таблица 4. Технологический и реагентный режимы обогащения образцов шлама (см. табл. 1) по схеме «основная флотация – ультратонкое измельчение концентрата основной флотации–перечистка концентрата основной флотации»

Stage	Slurry pH	Reagent consumption, g/t					Duration, min
		H_2SO_4 (1 :1)	$CuSO_4$	Aeroflot (sodium butyl xanthate)	MIBK (methyl isobutyl carbinol)	Water glass	
Slime sample from Test *3*							
Agitation		25335	66.7	–	–	–	–
Bulk flotation	1.49	–	–	450	50	–	52
Regrinding of bulk concentrate	–	–	–	–	–	–	12
1st cleaner flotation of the bulk concentrate	1.57	–	–	50	10	–	22
2nd cleaner flotation of the bulk concentrate	1.6	–	–	–	–	300	21
3rd cleaner flotation of the bulk concentrate	1.6	–	–	–	–	300	14
4th cleaner flotation of the bulk concentrate	1.7	–	–	–	–	300	13
5th cleaner flotation of the bulk concentrate	1.7	–	–	–	–	300	10
Slime sample from Test *4*							
Agitation	–	22520	66.7	–		–	–
Bulk flotation	1.49	–	–	450	50	–	52
Regrinding of bulk concentrate	–	–	–	–	–	–	12
Agitation	–	16890	–	–	–	–	–
1st cleaner flotation of the bulk concentrate	1.55	–	–	120	30	–	18
2nd cleaner flotation of the bulk concentrate	1.62	–	–	–	–	300	13
3rd cleaner flotation of the bulk concentrate	1.6	–	–	–	–	300	11
4th cleaner flotation of the bulk concentrate	1.7	–	–	–	–	300	10
5th cleaner flotation of the bulk concentrate	1.7	–	–	–	–	–	10
Slime sample from Test *5*							
Agitation	–	22520	66.7	–	–	–	–
Bulk flotation	1.5	–	–	450	50	–	52
Regrinding of bulk concentrate	–	–	–	–	–	–	12
Agitation	–	19705	–	–	–	–	–
1st cleaner flotation of the bulk concentrate	1.64	–	–	230	60	–	38
2nd cleaner flotation of the bulk concentrate	1.57	–	–	100	10	300	24
3rd cleaner flotation of the bulk concentrate	1.6	–	–	–	–	300	20
4th cleaner flotation of the bulk concentrate	1.7	–	–	–	–	300	17
5th cleaner flotation of the bulk concentrate	1.7	–	–	–	–	300	10
Slime sample from Test *6*							
Agitation	–	33780	66.7	–	–	–	–
Bulk flotation	1.5	–	–	470	65	–	61
Regrinding of bulk concentrate	–	–	–	–	–	–	12
Agitation	–	7037	–	–	–	–	–
1st cleaner flotation of the bulk concentrate	1.7	–	–	–	–	–	18
2nd cleaner flotation of the bulk concentrate	1.6	–	–	–	–	300	15
3rd cleaner flotation of the bulk concentrate	1.6	–	–	–	–	300	13
4th cleaner flotation of the bulk concentrate	1.7	–	–	–	–	300	11
Agitation	–	33780	66.7	–	–	–	–
Bulk flotation	1.5	–	–	450	50	–	52
Agitation	–	28150	66.7	–	–	–	–
Bulk flotation	1.5	–	–	450	50	–	52
1st cleaner flotation of the bulk concentrate	1.7	–	–	–	–	300	15
2nd cleaner flotation of the bulk concentrate	1.7	–	–	–	–	–	8

Table 5. **Technological performance indicators of slime flotation processing**

Таблица 5. Технологические показатели флотационного обогащения шлама

Product	Yield, %	Metal content in product, % / metal recovery to product, %			
		Au	Ag	Pb	Sb
Slime sample from Test *3*					
Concentrate	22.59	1.36 / 54.23	35.97 / 60.45	1.63 / 8.03	2.9 / 4.52
5th cleaner tails	7.35	1.22 / 15.83	31.29 / 17.11	3.2 / 5.13	5.3 / 2.69
4th cleaner tails	4.17	0.97 / 7.14	22.7 / 7.04	5.4 / 4.90	7.8 / 2.24
3rd cleaner tails	3.50	0.73 / 4.51	14.98 / 3.90	5.7 / 4.35	13.5 /3.26
2nd cleaner tails	6.80	0.57 /6.84	11.94 / 6.04	6.1 / 9.04	14.2 / 6.66
1st cleaner tails	16.91	0.166 / 4.96	2.44 /3.07	6.7 / 24.7	21.1 /24.61
Bulk flotation stage	**61.32**	**93.51** (recovery)	**97.61** (recovery)	–	–
Final tails	38.68	0.095 / 6.49	0.83 / 2.39	5.2 / 43.85	21.0 / 56.02
Feed (slime)	100.00	0.57 / 100.00	13.44 / 100.00	4.59 / 100.00	14.50 / 100.00
Slime sample from Test *4*					
Concentrate	21.67	1.69 / 55.15	36.31 / 57.12	3.00 / 11.41	2.90 / 4.19
5th cleaner tails	5.18	1.23 / 9.60	31.95 / 12.01	2.9 / 2.64	4.4 / 1.52
4th cleaner tails	3.04	1.06 / 4.85	24.94 / 5.50	4.9 / 2.62	7.5 / 1.52
3rd cleaner tails	4.38	0.90 / 5.94	19.90 / 6.33	6.1 / 4.69	11.5 / 3.36
2nd cleaner tails	8.49	0.70 / 8.95	14.63 / 9.02	6.1 / 9.09	15.2 / 8.60
1st cleaner tails	17.13	0.311 / 8.02	5.27 / 6.55	6.5 / 19.55	20.2 / 23.06
Bulk flotation stage	**59.89**	**92.51** (recovery)	**96.53** (recovery)	–	–
Final tails	40.11	0.124 / 7.49	1.19 / 3.47	7.1 / 50.00	21.6 / 57.75
Feed (slime)	100.00	0.66 / 100.00	13.78 / 100.00	5.70 / 100.00	15.00 / 100.00
Slime sample from Test *5*					
Concentrate	30.75	1.35 / 63,04	36.29 / 69.19	1.68 / 7.38	2.9 / 5.94
5th cleaner tails	1.34	1.01 / 2,06	23.22 / 1.93	6.6 / 1.26	7.8 / 0.70
4th cleaner tails	3.38	1.24 / 6,36	28.68 / 6.01	4.3 / 2.08	7.1 / 1.60
3rd cleaner tails	6.27	1.02 / 9,71	24.31 / 9.45	6.2 / 5.56	10.6 / 4.43
2nd cleaner tails	8.33	0.6 / 7,59	14.4 / 7.44	15.5 / 18.45	15.3 / 8.49
1st cleaner tails	19.25	0.152 / 4,44	2.89 / 3.45	8.9 / 24.49	21.2 / 27.16
Bulk flotation stage	**69.32**	**93.20** (recovery)	**97.47** (recovery)	–	–
Final tails	30.68	0.146 / 6,80	1.33 / 2.53	9.3 / 40.78	25.3 / 51.68
Feed (slime)	100.00	0.66 / 100.00	16.13 / 100.00	7.00 / 100.00	15.02 / 100.00
Slime sample from Test *6*					
Concentrate	64.80	1.09 / 90.85	23.78 / 94.58	–	–
Final tails	35.20	0.202 / 9.15	2.51 / 5.42	–	–
Feed (slime)	100.00	0.78 / 100.00	16.29 / 100.00	–	–
Concentrate	41.77	1.34 / 72.54	29.8 / 76.09	–	–
2nd cleaner tails	8.80	0.89 / 10.15	20.16 / 10.85	–	–
1st cleaner tails	12.97	0.58 / 9.75	10.46 / 8.29	–	–
Bulk flotation stage	**63.54**	**92.44** (recovery)	**95.23** (recovery)	–	–
Final tails	36.46	0.16 / 7.56	2.14 / 4.77	–	–
Feed (slime)	100.00	0.77 / 100.00	16.36 / 100.00	–	–
Concentrate	23.34	1.77 / 56.54	36.9 / 55.86	2.6 / 8.12	2.3 / 3.78
4th cleaner tails	0.94	1.02 / 1.31	20.94 / 1.28	7.1 / 0.89	7.7 / 0.51
3rd cleaner tails	1.48	1.13 / 2.29	24.57 / 2.36	6.6 / 1.31	8.4 / 0.87
2nd cleaner tails	5.34	0.97 / 7.09	21.78 / 7.54	7.1 / 5.07	10.5 / 3.95
1st cleaner tails	30.31	0.58 / 24.06	14.09 / 27.70	10.3 / 41.76	12.7 / 27.08
Bulk flotation stage	**61.41**	**91.29** (recovery)	**97.74** (recovery)	–	–
Final tails	38.59	0.165 / 8.71	2.1 / 5.26	8.3 / 42.85	23.5 / 63.81
Feed (slime)	100.00	0.73 / 100.00	15.42 / 100.00	7.48 / 100.00	14.21 / 100.00

Table 6. **Flotation results for decopperized slime**

Таблица 6. Результаты флотации обезмеженного шлама

Test No.	Metal content in the bulk concentrate, %			Metal recovery to the bulk concentrate, %		Metal content in flotation tails, %		
	Au	Ag	Σ Pb + Sb	Au	Ag	Au	Ag	Σ Pb + Sb
3	1.36	35.97	4.53	93.51	97.61	0.095	0.83	26.2
4	1.69	36.31	5.90	92.51	96.53	0.124	1.19	28.7
5	1.35	36.29	4.58	93.20	97.47	0.146	1.33	34.6
6	1.09	23.70	4.90	91.29	97.75	0.165	2.1	31.8

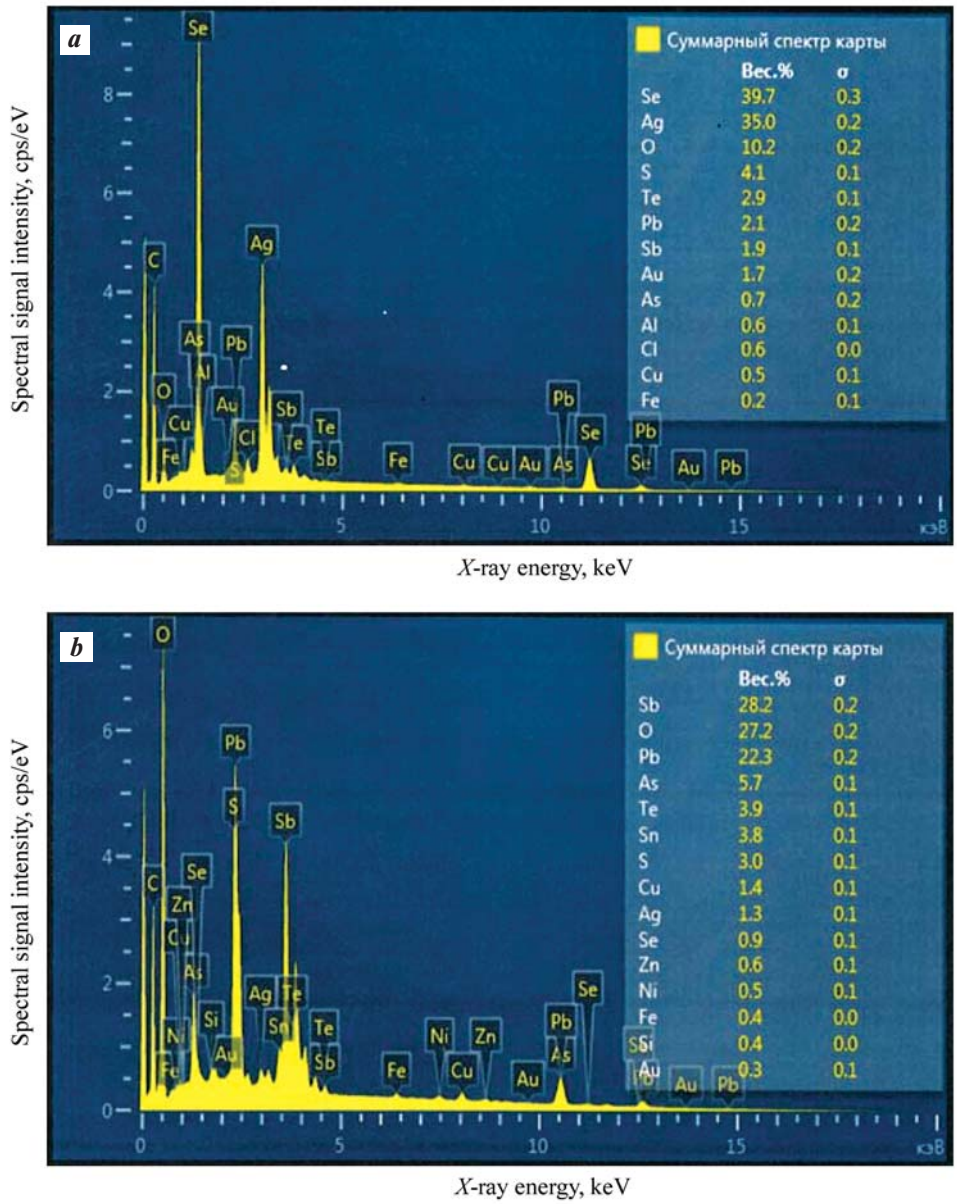

Fig. 4. Results of semi-quantitative chemical analysis of (***a***) the flotation concentrate after cleaner flotation and (***b***) the final flotation tails

Рис. 4. Результаты полуколичественного химического анализа концентрата флотации после перечисток (***a***) и отвальных хвостов обогащения (***b***)

lead sulfide concentrate [22]. Alternatively, integrated pyro- and hydrometallurgical technologies for antimony and lead recovery, developed and implemented at JSC "Uralelektromed" [23], or other established methods [24] may be employed.

Conclusions

1. Technological operations — namely aeration decopperization followed by flotation — have been developed, enabling the processing of copper anode slimes without the use of costly autoclave leaching.

2. The conditions and equipment configuration required for deep decopperization of slime (to less than 0.5—0.8 % residual copper) have been determined.

3. The method of aeration decopperization using oxygen in sulfuric acid solution (200 g/dm^3) is suitable for deep copper removal, while simultaneously suppressing the undesirable dissolution of tellurium. This substantially reduces the formation of slags and dust, thereby minimizing gold and silver losses during Doré smelting.

4. An acceptable degree of separation between chalcogenides of precious metals and oxide compounds of lead and antimony was achieved, allowing for the production of commercial products from the respective concentrates in subsequent processing.

5. The results obtained contribute to the development of an integrated hydrometallurgical technology for processing copper anode slimes.

References

1. Hait J., Jana R.K., Sanyal S.K. Processing of copper electrorefining anode slime: a review. *Mineral Processing and Extractive Metallurgy*. 2009;118(4):240—252. https://doi.org/10.1179/174328509x431463
2. Cooper W.C. The treatment of copper refinery anode slimes. *JOM*. 1990;8:45—49. https://doi.org/10.1007/BF03221054
3. Meyerovich A.S., Meretukov M.A. Technique and technology of processing electrolytic sludge abroad: Review information. Moscow: TsNIITsvetmet of Economics and Information, 1988. 52 p. (In Russ.).
Мейерович А.С., Меретуков М.А. Техника и технология переработки электролитных шламов за рубежом: Обзорная информация. М.: ЦНИИцветмет экономики и информации, 1988. 52 с.
4. Meretukov M.A., Orlov A.M. Metallurgy of precious metals (Foreign experience). Moscow: Metallurgiya, 1990. 416 p. (In Russ.).
Меретуков М.А., Орлов А.М. Металлургия благородных металлов (Зарубежный опыт). М.: Металлургия, 1990. 416 с.
5. Wei Dong Xing, Seong Ho SohnMan Seung Lee. A Review on the recovery of noble metals from anode slimes. *Mineral Processing and Extractive Metallurgy Review*. 2019; 2:1—14. https://doi.org/10.1080/08827508.2019.1575211
6. Lobanov V.G., Polygalov S.E., Mamyachenkov S.V., Khmelev N.B., Melnik F.F. On the problem of intensifying the demineralization of copper electrolyte sludge. *Tsvetnye metally*. 2023;12:35—40. (In Russ.). https://doi.org/ 10.17580/tsm.2023.12.02
Лобанов В.Г., Полыгалов С.Э., Мамяченков С.В., Хмелев Н.Б., Мельник Ф.Ф. К проблеме интенсификации обезмеживания медеэлектролитного шлама. *Цветные металлы*. 2023;12: 35—40. https://doi.org/ 10.17580/tsm.2023.12.02
7. Greiver T.N., Zaitseva I.G., Kosover V.M. Selenium and tellurium. Moscow: Metallurgiya, 1977. 296 p. (In Russ.).
Грейвер Т.Н., Зайцева И.Г., Косовер В.М. Селен и теллур. М.: Металлургия, 1977. 296 с.
8. Hoffman J.E., Sutcliff K.E., Wells B.A., George D.B. Hydrometallurgical processing of kennecott refinery slimes. In: *COPPER 95 — COBRE 95: Electrorefining and Hydrometallurgy of Copper*. Canada. Montreal: Canadian Institute of Mining, Metallurgy and Petroleum, 1995. Vol. 3. P. 41—57.
9. Komori K., Ito S., Okada S., Iwahori S. Hydrometallurgical process of precious metals in naoshima smelter and refinery. *Processing of Copper*. 2010;4:1403—1411.
10. Jarvinen O., Virtanen H. A new hydrometallurgical process for treating copper anode slimes. In: *Proc. of COBRE 2003*. Chili: Santiago, 2003. P. 221—232.
11. Chuanyan Lei, Peihua Zhu. Recovery of precious metals from copper anode slime by combined metallurgy and beneficiation. In: *Mineral processing and extractive metallurgy:* Proc. of Int. Conf. China: Kunming, 1984. P. 699—705.
12. Dong Li, XueyiGuo, Zhipeng Xu, Runze Xu, Qiming Feng. Metal values separation from residue generated in alkali fusion-leaching of copper anode slime. *Hydrometallurgy*. 2016;165(2):290—294. https://doi.org/10.1016/j.hydromet.2016.01.021
13. Yasin K., Guldem K., Servet T. An investigation of copper and selenium recovery from copper anode slimes. *International Journal of Mineral Processing*. 2013;124(11):75—82. https://doi.org/10.1016/j.minpro.2013.04.006
14. Dong Li, XueyiGuo, Zhipeng Xu, Qinghua Tian, Qiming Feng. Leaching behavior of metals from copper anode slime using analkali fusion-leaching process. *Hydrometallurgy*. 2015;157(10):9—12.

15. Chen A., Peng Z., Hwang J-Y., Ma Y., Liu X., Chen X. Recovery of silver and gold from copper anode slimes. *JOM*. 2015;67(2):493—502. https://doi.org/10.1007/s11837-014-1114-9
16. Lastochkina M.A., Greiver T.N., Vergizova T.V., Mastyugin S.A., Ashikhin V.V., Krayukhin S.A., Krestyaninov A.T. Method for processing lead sludge from copper electrorefining (variants): Patent 2451759 (RF). 2012. (In Russ.).
Ласточкина М.А., Грейвер Т.Н., Вергизова Т.В., Мастюгин С.А., Ашихин В.В., Краюхин С.А., Крестьянинов А.Т. Способ переработки свинцовистых шламов электрорафинирования меди (варианты): Патент 2451759 (РФ). 2012.
17. Chen T.T., Dutrizac J.E. Mineralogical characterization of anode slimes. *Canadian Metallurgy Quarterly*. 1993;32(4):267—279.
18. Yanliang Zeng, Chunfa Liao, Fupeng Liu, Xun Zhou. Occurrence behaviors of As/Sb/Bi in copper anode slime and their separation by compound leaching followed by stepwise precipitation. *ACS Omega*. 2023;8: 10022—10029.
19. Mastyugin S.A., Lastochkina M.A., Naboychenko S.S., Voinkov R.S. Use of disintegration techniques in processing copper electrolyte sludge. *Tsvetnye metally*. 2014;(11):35—40. (In Russ.).
Мастюгин С.А., Ласточкина М.А., Набойченко С.С., Воинков Р.С. Использование приемов дезинтеграции при переработке медеэлектролитных шламов. *Цветные металлы*. 2014;(11):35—40.
20. Ugorets M.Z., Glazkova T.I. Hydrometallurgical extraction of lead and antimony from copper electrolyte sludge. In: *Complex use of raw materials of non-ferrous metallurgy*. Sverdlovsk: House of the Ural Scientific Center of the USSR Academy of Sciences, 1980. P. 63–66. (In Russ.).
Угорец М.З., Глазкова Т.И. Гидрометаллургическое извлечение свинца и сурьмы из медеэлектролитных шламов. В кн.: *Комплексное использование сырья цветной металлургии*. Свердловск: УНЦ АН СССР, 1980. С. 63—66.
21. Khlomanskikh Yu.B., Cherkasov G.F., Savin V.M., Lobanov E.N. On the removal of Sb, As and Bi during the processing of copper electrolyte sludge. *Tsvetnye metally*. 1970;(7):30—31. (In Russ.).
Хломанских Ю.Б., Черкасов Г.Ф., Савин В.М., Лобанов Е.Н. О выводе Sb, As и Bi при переработке медеэлектролитных шламов. *Цветные металлы*. 1970;(7):30—31.
22. Voinkov R.S. Complex processing of flotation tailings of copper electrolyte sludge: Abstract of the dissertation of Cand. Sci. (Eng.). Yekaterinburg: UrFU, 2015. (In Russ.).
Воинков Р.С. Комплексная переработка хвостов флотации медеэлектролитных шламов: Автореф. дис. канд. техн. наук. Екатеринбург: УрФУ, 2015.
23. Timofeev K.L., Korolev A.A., Krayukhin S.A., Maltsev G.I., Voinkov R.S., Shunin V.A., Sergeychenko S.V., Kokshin A.A. Development of tin and antimony production at Uralelectromed JSC. In: *Modern technologies for the production of non-ferrous metals:* Proceedings of the International Scientific Conference dedicated to the 80th anniversary of S.S. Naboychenko (March 24, 2022). Yekaterinburg: UrFU, 2022. P. 159–165. (In Russ.).
Тимофеев К.Л., Королев А.А., Краюхин С.А., Мальцев Г.И., Воинков Р.С., Шунин В.А., Сергейченко С.В., Кокшин А.А. Освоение производства олова и сурьмы в АО «Уралэлектромедь». В сб.: *Современные технологии производства цветных металлов*: Материалы междунар. науч. конф., посвященной 80-летию С.С. Набойченко (24 марта 2022 г.). Екатеринбург: УрФУ, 2022. С. 159—165.
24. Baole Li, Juhai Deng, Wenlong Jiang, Guozheng Zha, Bin Yang Removal of arsenic, lead and bismuth from copper anode slime by a one-step sustainable vacuum carbothermal reduction process. *Separation and Purification Technology*. 2023;310:123059. https://doi.org/10.1016/j.seppur.2022.123059

Information about the authors

Sergey A. Mastyugin – Dr. Sci. (Eng.), Chief Technologist of Technical department of engineering and production management of JSC "Uralelectromed"; Associate Professor of the Department of metallurgy, Technical University UMMC.
https://orcid.org/0009-0007-7417-6876
E-mail: S.Mastugin@uralcopper.com

Konstantin L. Timofeev – Dr. Sci. (Eng.), Head of Department of JSC "Uralelectromed"; Associate Professor of the Department of metallurgy, Technical University UMMC.
https://orcid.org/0000-0002-9525-6476
E-mail: K.Timofeev@uralcopper.com

Roman S. Voinkov – Cand. Sci. (Eng.), Head of the Research Center of JSC "Uralelectromed"; Associate Professor of the Department of metallurgy, Technical University UMMC.
https://orcid.org/0000-0001-6697-1596
E-mail: R.Voinkov@uralcopper.com

Svetlana V. Volkova – Senior Researcher of the Laboratory for the enrichment of non-ferrous metal ores and man-made raw materials, JSC "Uralmekhanobr".
https://orcid.org/0009-0008-7545-0125
E-mail: volkova_sv@umbr.ru

Информация об авторах

Сергей Аркадьевич Мастюгин – д.т.н., гл. технолог технического отдела Инженерно-производственного управления АО «Уралэлектромедь»; доцент кафедры металлургии Технического университета УГМК.
https://orcid.org/0009-0007-7417-6876
E-mail: S.Mastugin@uralcopper.com

Константин Леонидович Тимофеев – д.т.н., начальник технического отдела Инженерно-производственного управления АО «Уралэлектромедь»; доцент кафедры металлургии Технического университета УГМК.
https://orcid.org/0000-0002-9525-6476
E-mail: K.Timofeev@uralcopper.com

Роман Сергеевич Воинков – к.т.н., начальник Исследовательского центра АО «Уралэлектромедь»; доцент кафедры металлургии Технического университета УГМК.
https://orcid.org/0000-0001-6697-1596
E-mail: R.Voinkov@uralcopper.com

Светлана Владимировна Волкова – ст. науч. сотрудник лаборатории обогащения руд цветных металлов и техногенного сырья, АО «Уралмеханобр».
https://orcid.org/0009-0008-7545-0125
E-mail: volkova_sv@umbr.ru

Contribution of the authors

S.A. Mastyugin – defined the research objectives and experimental conditions, participated in all tests, prepared the manuscript.

K.L. Timofeev – defined the overall research tasks, ensured fulfillment of contractual obligations between organizations, carried out pilot-scale tests, participated in the discussion of results, revisd the manuscript.

R.S. Voinkov – prepared initial samples, participated in decopperization tests of slimes (at JSC Uralelektromed), performed chemical analyses, contributed to the discussion of experimental results, revised the manuscript.

S.V. Volkova – conducted flotation experiments (at JSC "Uralmekhanobr") on decopperized slime, including bead milling, performed analyses, including scanning electron microscopy.

Вклад авторов

С.А. Мастюгин – определение цели работы и условий проведения экспериментов, участие в проведении всех испытаний, написание статьи.

К.Л. Тимофеев – определение общей задачи работ, обеспечение выполнения договорных обязательств между организациями и проведение укрупненных испытаний, участие в обсуждении результатов, редактирование статьи.

Р.С. Воинков – подготовка исходных образцов, участие в проведении испытаний по обезмеживанию шламов (в АО «Уралэлектромедь»), проведение химических анализов, участие в обсуждении результатов испытаний, редактирование статьи.

С.В. Волкова – проведение экспериментов (в АО «Уралмеханобр») по флотационному обогащению обезмеженного шлама, включая бисерное измельчение, проведение анализов, в том числе на электронном микроскопе.

The article was submitted 05.05.2025, revised 19.05.2025, accepted for publication 23.05.2025

Статья поступила в редакцию 05.05.2025, доработана 19.05.2025, подписана в печать 23.05.2025

UDC 669.213.6
https://doi.org/10.17073/0021-3438-2025-3-66-73

Research article
Научная статья

Combined scheme for conditioning circulating cyanide solutions

A.M. Samofeev[1,2], **V.G. Lobanov**[1], **F.M. Nabiullin**[2], **A.V. Tretyakov**[2]

[1] **Ural Federal University n.a. the First President of Russia B.N. Yeltsin**
19 Mira Str., Ekaterinburg 620002, Russia

[2] **LLC "Berezovsky Rudnik"**
1 Berezovsky Tract, Sverdlovsk Reg., Berezovsky 623700, Russia

✉ Alexander M. Samofeev (alexander.samofeev@gmail.com)

Abstract: Due to the specific features of hydrometallurgical processing, where cyanide solutions are used, the composition of the leaching solution undergoes periodic changes referred to in the literature as "fatigue." This adversely affects the rate of gold recovery and cementation, and therefore the overall efficiency of cyanide leaching technology. One of the most important markers determining the "fatigue" of the solution is copper. This study examined the possibility of applying a combined scheme for the purification of circulating cyanide solutions with high concentrations of copper (1196 mg/dm^3), iron (111 mg/dm^3), arsenic (19 mg/dm^3), and sodium cyanide (0.94 g/dm^3). A two-stage technology (reverse osmosis + chemical precipitation) was developed for the reduction of treated solution volumes and the removal of impurities. At the first stage, the solution was separated in a reverse osmosis unit equipped with LP22-8040 membranes, producing permeate and concentrate in a 1 : 1 ratio. The permeate (12 mg/dm^3 Cu and 0.01 mg/dm^3 Fe, pH = 11.13) was returned to the process cycle. At the second stage, the concentrate, which contained 99 % of the initial impurities, was further purified by the stepwise addition of a $CuSO_4$ solution (70 g/dm^3 Cu) in 1–11 cm^3 doses under stirring (500 rpm, 10 min). The results showed that the optimal $CuSO_4$ dose (11 cm^3) provided removal of more than 86 % of Cu from the initial solution, as well as 100 % of Fe and more than 96 % of As. The precipitate obtained in the process consisted of 68.3 % copper, with CuCN and $Cu(OH)_2$ as the main components.

Keywords: gold, cyanide leaching, Merrill-Crowe, cementation, reverse osmosis, copper, arsenic, surface passivation.

For citation: Samofeev A.M., Lobanov V.G., Nabiullin F.M., Tretyakov A.V. Combined scheme for conditioning circulating cyanide solutions. *Izvestiya. Non-Ferrous Metallurgy.* 2025;31(3):66–73. https://doi.org/10.17073/0021-3438-2025-3-66-73

Комбинированная схема кондиционирования оборотных цианистых растворов

А.М. Самофеев[1,2], **В.Г. Лобанов**[1], **Ф.М. Набиуллин**[2], **А.В. Третьяков**[2]

[1] **Уральский федеральный университет имени первого Президента России Б.Н. Ельцина**
Россия, 620002, г. Екатеринбург, ул. Мира, 19

[2] **ООО «Березовский рудник»**
Россия, 623700, Свердловская обл., г. Березовский, ул. Березовский тракт, 1

✉ Александр Михайлович Самофеев (alexander.samofeev@gmail.com)

Аннотация: Ввиду специфики работы гидрометаллургических переделов, где применяются цианистые растворы, происходит периодическое изменение состава выщелачивающего раствора, получившее в литературе название «утомляемость». Это в не-

гативном ключе влияет на скорость процесса извлечения и цементации золота, а следовательно, в целом на эффективность технологии цианистого выщелачивания. Одним из наиболее важных маркеров, определяющих «утомляемость» раствора, является медь. В работе исследовалась возможность применения комбинированной схемы очистки оборотных цианистых растворов с высоким содержанием примесей меди (1196 мг/дм^3), железа (111 мг/дм^3), мышьяка (19 мг/дм^3) и цианида натрия (0,94 г/дм^3). Разработана 2-этапная технология (обратный осмос + химическое осаждение) для сокращения объемов обрабатываемых растворов и удаления примесей. На первом этапе раствор разделяли на обратноосмотической установке с мембранами LP22-8040, получая пермеат и концентрат в пропорции 1 : 1. Пермеат (12 мг/дм^3 Cu и 0,01 мг/дм^3 Fe, pH = 11,13) возвращали в технологический цикл. А на втором этапе концентрат, содержащий 99 % исходных примесей, доочищали дозированным введением раствора $CuSO_4$ (70 г/дм^3 Cu) с интервалом доз 1–11 см^3 при перемешивании (500 об/мин, 10 мин). Результаты показали, что оптимальная доза $CuSO_4$ (11 см^3) обеспечивает удаление более 86 % Cu из исходного раствора, а также 100 % Fe и более 96 % As. Полученный в процессе осадок на 68,3 % состоит из меди, а основными компонентами являются CuCN и $Cu(OH)_2$.

Ключевые слова: золото, цианистое выщелачивание, Меррилл-Кроу, цементация, обратный осмос, медь, мышьяк, пассивация поверхности.

Для цитирования: Самофеев А.М., Лобанов В.Г., Набиуллин Ф.М., Третьяков А.В. Комбинированная схема кондиционирования оборотных цианистых растворов. *Известия вузов. Цветная металлургия*. 2025;31(3):66–73.
https://doi.org/10.17073/0021-3438-2025-3-66-73

Introduction

In 2010, a cyanide leaching facility for gold extraction from flotation concentrate was established at the concentration plant of LLC “Berezovsky Rudnik”, which processes ore from Russia’s oldest deposit of the same name. Over the years of operation, continuous improvement of the process and equipment enabled mine specialists to achieve 95—97 % gold recovery into the commercial cement product, while reducing the gold content in the leach tailings of the concentrate to as low as 0.2—0.1 g/t. It is noteworthy that comparable results for direct leaching of gold from pyrite concentrate have not been reported in the literature.

In hydrometallurgical processing, where cyanide solutions are employed, the composition of the leaching solution undergoes periodic changes, described in the literature as “fatigue” [1]. This phenomenon has an adverse effect on the rate of gold recovery and cementation, and thus on the overall efficiency of cyanide leaching technology. One of the most important indicators of solution “fatigue” is the copper concentration in circulating solutions. Previous studies have confirmed the negative impact of “fatigued” solutions on the kinetics of gold leaching [2]. According to the theory proposed by M.D. Ivanovsky, elevated copper concentrations in circulating solutions promote the formation of passivating CuCN films on the gold surface:

$$[Cu(CN)_4]^{3-} = CuCN\downarrow + 3CN^-. \qquad (1)$$

The density of these films depends on the copper concentration in the solution. The formation of cop-

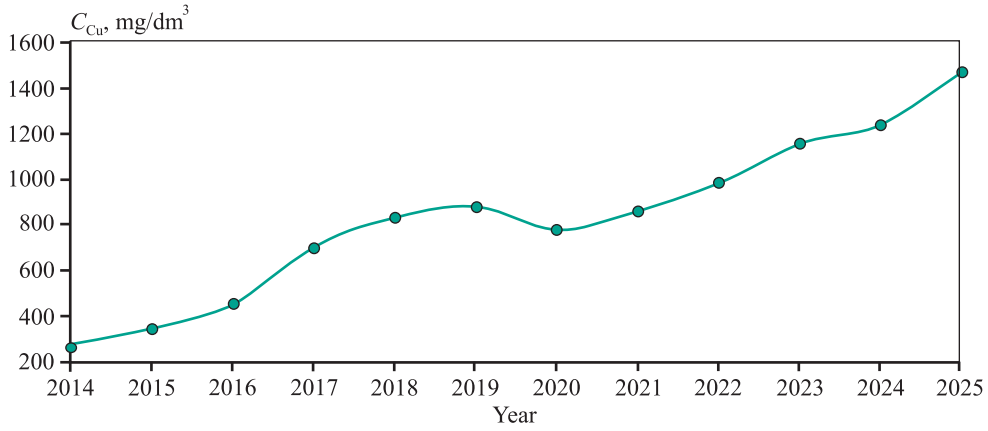

Fig. 1. Average annual copper concentration in the circulating solution

Рис. 1. Среднегодовое содержание меди в оборотном растворе

per (I) cyanide (CuCN) becomes possible when the cyanide concentration in the diffusion layer decreases during the dissolution of gold [1; 3—8].

Over the years of hydrometallurgical operation, the copper content in the circulating solution has shown a steady increase (Fig. 1).

In hydrometallurgical practice, short-term periods (1—2 days) are sometimes observed during which leaching efficiency decreases and the gold content in the leach tailings rises to 1.0—2.5 g/t. After this period, with process parameters maintained within the specified limits, leaching performance returns to the optimal level. Prompt laboratory tests ruled out possible causes such as the periodic presence of coarse gold in the concentrate (which requires longer dissolution time) and deviations from process regulations, including low cyanide concentration or insufficient exposure of metal. At the same time, analysis of the leach tailings confirmed the potential for further recovery of gold to previously achieved levels of 0.1—0.2 g/t. Elevated copper concentrations in circulating solutions were found to adversely affect gold precipitation in the Merrill—Crowe plant (Fig. 2). Possible reasons include increased zinc consumption due to copper reduction and passivation of zinc particle surfaces by a dense copper layer. Additional complications occur during filtration of the cementation product: at higher copper concentrations in the pregnant solution, the hydraulic resistance of the cement layer increases sharply. In any case, cementation of gold becomes more difficult, and plant productivity declines.

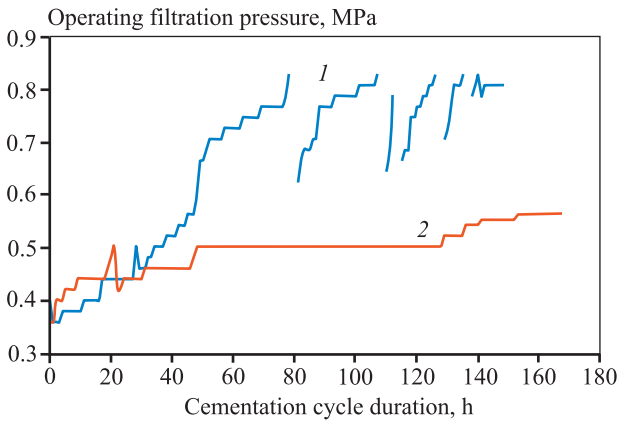

Fig. 2. Change in filter pressure during gold precipitation
1 – cycle with elevated copper content; ***2*** – standard cycle

Рис. 2. Изменение давления на фильтре осадка в процессе осаждения золота
1 – цикл с повышенным содержанием меди;
2 – стандартный цикл

Table 1. **Characteristics of zinc precipitates**
Таблица 1. Особенности цинковых осадков

Cycle No.	Mass of precipitate, kg	C_{Cu}, % (kg)
1 (abnormal)	171	56.0 (96.1)
2 (normal)	80.4	8.9 (7.15)

The discontinuity of curve 1 reflects shutdowns of the Merrill—Crowe unit caused by a sharp increase in filter-press pressure. When the unit stopped, the cement layer partially detached from the vertical filter surface, and after the feed pump was restarted, the pressure temporarily returned to normal. At the end of the cycle, visual inspection of the cement product revealed dense plates resembling metallic copper. Subsequent analysis showed more than a twofold increase in cement product mass and abnormally high copper content (Table 1).

To partially address this problem, it is recommended to add larger amounts of soluble lead salts to the pregnant solution, which suppress copper precipitation [3]. However, practice shows that at elevated copper concentrations, the effectiveness of lead addition decreases.

Another negative effect of copper in circulating solutions is its interference with the analytical determination of cyanide concentration [9], which may lead to potential violation of process regulations and under-recovery of gold.

The literature describes several methods for removing copper from circulating solutions, which can be classified according to the Cu-containing product formed: CuCN — ARV process [1; 10]; Cu_2S — MNR process [11—16]; $Cu(OH)_2$ — treatment with oxidizing agents [17—20]; Cu^0 — cementation with zinc or electrolysis [3].

In this study, a combined conditioning scheme for circulating solutions was investigated, consisting of two stages.

1. Reverse osmosis for concentrating impurities in a reduced volume. Reverse osmosis (RO) is a technology that removes ions, molecules, and impurities from water through membranes under high pressure [21—24]. The feed solution is separated into two streams: concentrate and permeate. The permeate is an impurity-free solution, while the concentrate contains nearly all components of the original solution. The product volumes and separation coefficients depend on the membrane properties and system pressure.

2. Purification of the concentrate through the formation of sparingly soluble copper (I) cyanide. For impurity precipitation, copper sulfate ($CuSO_4$) was proposed. Prototypes of this technological stage include processes involving treatment with iron salts and oxidation with hydrogen peroxide, where soluble copper salts are used as catalysts for cyanide destruction in wastewater [17—20]. The method considered in this study provides for the precipitation of copper as well as several other impurities accumulated during flotation concentrate leaching.

Thus, the aim of this study was to develop a combined two-stage technology (reverse osmosis + + chemical precipitation with $CuSO_4$) for conditioning circulating cyanide solutions with high concentrations of copper, iron, and arsenic. The technology is designed to reduce treatment volumes and restore the functional properties of the solutions for gold cyanide leaching.

Materials and methods

The circulating cyanide solution from the gold leaching circuit of LLC "Berezovsky Rudnik" served as the object of the study.

Sampling of the circulating solution and reverse osmosis products was carried out on a pilot hydrometallurgical unit with a feed capacity of 60 m^3/h. The unit was equipped with LP22-8040 polyamide thin-film composite membranes with a total active surface area of 2040 m^2. Operating parameters were as follows: solution temperature 20 °C, product volume ratio (permeate : concentrate) 1 : 1, and inlet pressure 1.7 MPa. The feed solution and osmosis products were analyzed for metal and sodium cyanide content, with the results presented in Table 2. Once the permeate was purified to the target impurity level, it was returned to the cyanidation circuit. Further impurity removal from the concentrate was performed under laboratory conditions.

Copper precipitation was carried out using a known process [17; 25] based on the formation of sparingly soluble copper (I) cyanide:

$$Cu(CN)_4^{2-} + CuSO_4 = 2CuCN\downarrow + SO_4^{2-} + (CN)_2. \quad (2)$$

Copper precipitation from the concentrate was studied in a series of tests using a $CuSO_4$ solution (C_{Cu} = = 70 g/dm^3), in order to establish the dosage that yields the lowest copper concentration in solution.

For each test, 100 cm^3 of concentrate was placed in a beaker on a magnetic stirrer. A specified volume of $CuSO_4$ solution (C_{Cu} = 70 g/dm^3) was added at once, followed by stirring for 10 min. The resulting suspension was filtered to obtain clarified solution and precipitate. Solution and precipitate analyses were performed by atomic absorption spectroscopy using a Kvant-2 spectrometer (Russia). Sodium cyanide concentration was determined by titration with nickel nitrate, and pH was measured using an Anion 4100 pH meter (Russia).

Results and discussion

Analysis of the reverse osmosis products (Table 2) confirmed that the solution can be separated into two streams with different component concentrations. Impurities were virtually absent in the permeate. As shown in earlier studies [2], the kinetics of gold recovery using permeate are comparable to those obtained with process water. This allows the permeate to be returned to the circuit after fortification with sodium cyanide, thereby reducing the volume of treated solutions by half. More than 99 % of the impurities from the feed solution remained in the concentrate, which was used for further purification tests. The absence of gold and silver separation in the circulating solution is attributed to their low concentrations and the limitations of the pilot unit.

A series of six tests confirmed the expected dependence of copper precipitation on the $CuSO_4$ dosage

Table 2. **Composition of the circulating solution and reverse osmosis products**

Таблица 2. Составы оборотного раствора и продуктов обратного осмоса

Solution	C, mg/dm^3					C_{NaCN}, g/dm^3	pH
	Au	Ag	Cu	Fe	As		
Circulating	0.01	0.01	1196	111	19	0.94	11.13
Permeate	0.01	0.01	12	0.01	0.6	0.1	11.1
Concentrate	0.01	0.01	2379	222	37	1.78	11.1

Table 3. **Change in concentrate composition**

Таблица 3. Изменение состава концентрата

V_{CuSO_4}, cm^3	C, mg/dm^3					C_{NaCN}, g/dm^3	pH
	Au	Ag	Cu	Fe	As		
1	0.01	0.01	2500	128	7.5	0.06	7.86
3	0.01	0.01	2875	0	6.6	0	6.67
5	0.01	0.01	2240	0	5.5	0	6.56
7	0.01	0.01	1137	0	4.5	0	6.46
9	0.01	0.01	367	0	1.9	0	6.22
11	0.01	0.01	302	0	0.6	0	6.20

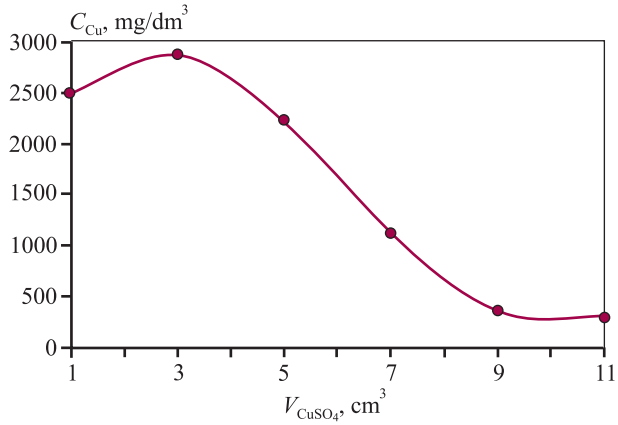

Fig. 3. Change in residual copper concentration in the concentrate with $CuSO_4$ addition

Рис. 3. Изменение остаточного содержания меди в концентрате при добавке $CuSO_4$

(Table 3, Fig. 3). The curve can be divided into two characteristic regions:

1. Increase in copper concentration in the concentrate. At low $CuSO_4$ dosages (1—3 cm^3), Cu^{2+} ions primarily reacted with iron cyanide complexes, free cyanide ions, and hydroxyl ions. This was accompanied by a sharp drop in iron (3) and cyanide ion concentrations (4), a decrease in pH to 6.67, and a rise in copper concentration (4):

$$2Cu^{2+} + [Fe(CN)_6]^{4-} = Cu_2[Fe(CN)_6]\downarrow, \quad (3)$$

$$2Cu^{2+} + 9CN^- + H_3O = $$
$$= 2[Cu(CN)_4]^{3-} + CNO^- + 2H^+. \quad (4)$$

Partial hydrolysis of copper ions also occurred:

$$Cu^{2+} + 2OH^- = Cu(OH)_2\downarrow. \quad (5)$$

2. Decrease in copper concentration in the concentrate. Further addition of $CuSO_4$ initiated reactions of Cu^{2+} with copper cyanide complexes, forming CuCN (1) and $Cu(OH)_2$ (5). Stabilization of pH at this stage is likely due to the buffering capacity of the sulfate ion:

$$SO_4^{2-} + H_2O = HSO_4^- + OH^-. \quad (6)$$

A reduction in arsenic concentration was also observed; however, the mechanism requires further investigation.

The purified concentrate solution can be returned to the circuit after mixing with permeate and reinforcing with caustic soda and sodium cyanide. A comparison of the purified concentrate—permeate mixture with the original circulating solution is shown in Table 4.

At the maximum $CuSO_4$ dosage, a precipitate with a mass of 0.98 g was obtained. Its composition was as follows (wt. %):

Cu 68.3
Fe 4.2
As 0.37
Other 27.13

Table 4. **Comparative analysis of solutions**

Таблица 4. Сравнительный анализ растворов

Solution	C, mg/dm^3				
	Au	Ag	Cu	Fe	As
Circulating solution	0.01	0.01	1196	111	19
Permeate + purified concentrate	0.01	0.01	157	0.005	0.6

The main components of the precipitate were $Cu(OH)_2$ and CuCN. This copper-rich material, after simple processing such as calcination, may be considered a marketable product. Following further chemical treatment, part of the copper in the form of $CuSO_4$ can be reused to condition fresh batches of circulating "fatigued" solutions.

Conclusions

1. Reverse osmosis technology enables a 2—3-fold concentration of impurities that accumulate in circulating cyanide solutions.

2. The study confirmed that soluble copper salts ($CuSO_4$) can be used to remove impurities from "fatigued" solutions in the form of a copper-rich precipitate.

3. Precipitation with copper sulfate achieved removal rates of 86.8 % for Cu, 100 % for Fe, and 96.8 % for As from the circulating solution.

References

1. Plaksin I.N. Metallurgy of Precious Metals. Moscow: Metallurgizdat, 1958. 366 p. (In Russ.).
Плаксин И.Н. Металлургия благородных металлов. М.: Металлургиздат, 1958. 366 с.
2. Samofeev A.M., Abdrakhmanova A.S., Lobanov V.G., Pomortsev V.N. Research on the Features of Gold Leaching from the Flotation Concentrate of LLC "Berezovski rudnik". In: *Scientific foundations and practice of ore and technogenic raw:* Materials of the XXVIII Scientific-Practical Conference (Ekaterinburg, 6–7 April 2023). Yekaterinburg: FortDialog, 2023. P. 277–280. (In Russ.).
Самофеев А.М., Абдрахманова А.С., Лобанов В.Г., Поморцев В.Н. Исследование особенностей выщелачивания золота из флотоконцентрата ООО «Березовский рудник». В сб.: *Научные основы и практика переработки руд и техногенного сырья:* Материалы XXVIII науч.-практ. конф. (Екатеринбург, 6—7 апреля 2023 г.). Екатеринбург: ФортДиалог, 2023. С. 277—280.
3. Maslenitskiy I.N., Chugaev L.V., Borbat V.F. Metallurgy of precious metals (Ed. L.V. Chugaev). 2nd ed., revised and supplemented. Moscow: Metallurgiya, 1987. 432 p. (In Russ.).
Масленицкий И.Н., Чугаев Л.В., Борбат В.Ф. Металлургия благородных металлов. Под ред. Л.В. Чугаева. 2-е изд., перераб. и доп. М.: Металлургия, 1987. 432 с.
4. Sceresini B. Gold-copper ores. In: *Developments in Mineral Processing* (Eds. Mike D., Adams B.A.). Amsterdam: Elsevier, 2005. Vol. 15. P. 789—824.
5. Gonzalo Larrabure J.C., Rodrнguez-Reyes J.C.F. A review on the negative impact of different elements during cyanidation of gold and silver from refractory ores and strategies to optimize the leaching process. *Minerals Engineering.* 2021;173:107194. https://doi.org/10.1016/j.mineng.2021.107194
6. Barchenkov V.V. Mineral processing and hydrometallurgical processes for gold extraction from ores. Vladimir: Transit-IKS, 2022. 544 p. (In Russ.).
Барченков В.В. Обогатительные и гидрометаллургические процессы извлечения золота из руд. Владимир: Транзит-ИКС, 2022. 544 с.
7. Maganga S., Wikedzi A., Budeba M., Manyele S. Overview of the challenges and opportunities in processing complex gold-copper ores. *Mining, Metallurgy & Exploration*. 2023;40:1—18. https://doi.org/10.1007/s42461-023-00854-7
8. Medina D., Anderson C. A review of the cyanidation treatment of copper-gold ores and concentrates. *Metals.* 2020;10(7):897. https://doi.org/10.3390/met10070897
9. Yilmaz E., Ahlatci F., Celep O., Yazэcэ E., Deveci H. Interference of metals with the determination of free cyanide. In: *Proceedings of the 14th International Mineral Processing Symposium* (Kusadasi, Turkey, 15—17 October 2014). 2014. P. 1027—1033. https://doi.org/10.13140/2.1.3302.3682
10. Adams M.D. Advances in gold ore processing. Guildford: Elsevier Science & Technology, 2001. 1076 p.
11. Estay H., Ruby-Figueroa R., Gim-Krumm M., Quilaqueo M., Seriche G., Díaz-Quezada S., Cortés I., Barros L. The SuCy process: A more efficient and safer technology to recover cyanide and copper in cyanidation plants. In: *Proc. of 12th International Conference on Process Hydrometallurgy* (Hydroprocess 2020). 2020. https://doi.org/10.13140/RG.2.2.10213.63208
12. Seriche G., Quilaqueo M., Barros L., Gim-Krumm M., Cortés I., Troncoso E., Ruby-Figueroa R., Estay H. Integrated membrane process coupled with metal sulfide precipitation to recover zinc and cyanide. *Minerals.* 2022;12(2):229. https://doi.org/10.3390/min12020229
13. Parga J.R., Valdés J.V., Valenzuela J.L., Gonzalez G., Pérez L.M.J., Cepeda T.F. New approach for lead, zinc and copper ions elimination in cyanidation process to improve the quality of the precipitate. *Materials Sciences and Applications*. 2015;6:117—129. https://doi.org/10.4236/msa.2015.62015
14. Estay H., Gim-Krumm M., Seriche G., Quilaqueo M., Barros L., Ruby-Figueroa R., Romero J., Troncoso E. Optimizing the SART process: A critical assessment of its design criteria. *Minerals Engineering.* 2020;146:106116. https://doi.org/10.1016/j.mineng.2019.106116

15. Alonso-González O., Nava-Alonso F., Uribe-Salas A. Copper removal from cyanide solutions by acidification. *Minerals Engineering*. 2009;22:324—329. https://doi.org/10.1016/j.mineng.2008.09.004
16. Kassymova D., Sapinov R., Kushakova L., Kulenova N., Shoshay Z., Adylkanova M. Optimization of copper recovery from cyanide leaching solutions used in gold—copper ore processing using probabilistic—deterministic experimental design. *Processes*.2025;13(1):61. https://doi.org/10.3390/pr13010061
17. Meretukov M.A., Orlov A.M. Metallurgy of precious metals: foreign experience. Moscow: Metallurgiya, 1990. 416 p. (In Russ.).
Меретуков М.А., Орлов А.М. Металлургия благородных металлов: Зарубежный опыт. М.: Металлургия, 1990. 416 с.
18. Knorre H., Griffiths A. Cyanide detoxification with hydrogen peroxide using Degussa process. In: *Proc. of Conference on Cyanide and the Environment* (Tucson, Arizona, 1984). Ed. by D. Van Zyl. Colorado State University, 1995. Vol. 2. P. 519—530.
19. Chen F., Zhao X., Liu H., Qu J. Reaction of $Cu(CN)_3^{2-}$ with H_2O_2 in water under alkaline conditions: Cyanide oxidation, Cu^+/Cu^{2+} catalysis and H_2O_2 decomposition. *Applied Catalysis B: Environmental*. 2014;158-159:85—90. https://doi.org/10.1016/j.apcatb.2014.04.010
20. Sarla M., Pandit M., Tyagi D.K., Kapoor J. Oxidation of cyanide in aqueous solution by chemical and photochemical process. *Journal of Hazardous Materials*. 2005;116(1-2):49—56. https://doi.org/10.1016/j.jhazmat.2004.06.035
21. Goyburo-Chávez C., Mendez-Ruiz J.I., Jiménez-Oyola S., Romero-Crespo P., Gutierrez L., Valverde-Armas P.E. Pilot-scale reverse osmosis treatment of gold cyanidation effluent for the removal of cyanide, heavy metal(loid)s, and ionic species. *Case Studies in Chemical and Environmental Engineering*. 2024;9:100688. https://doi.org/10.1016/j.cscee.2024.100688
22. Vásquez Salazar E.E., Hurtado Bolaños F.P. Cyanide compounds removal efficiency in a reverse osmosis system using a water supply from a co-precipitation chemical process. *Desalination and Water Treatment*. 2021;229:235—242. https://doi.org/10.5004/dwt.2021.27390
23. Pabby A.K., Rizvi S.S.H., Sastre A.M. (Eds.) Handbook of membrane separations: Chemical, pharmaceutical, food, and biotechnological applications. 3rd ed. Boca Raton: CRC Press, 2022. 1200 p. https://doi.org/10.1201/9781003285656
24. Samaei S.M., Gato-Trinidad S., Altaee A. Performance evaluation of reverse osmosis process in the post-treatment of mining wastewaters: Case study of Costerfield mining operations, Victoria, Australia. *Journal of Water Process Engineering*. 2020;34:101116. https://doi.org/10.1016/j.jwpe.2019.101116
25. Method for copper recovery from cyanide solutions and cyanide regeneration: Patent Application No. 2024137940 (RF). 2024. (In Russ.).
Способ извлечения меди из цианистых растворов и регенерации цианидов: Заявка № 2024137940 (РФ). 2024.

Information about the authors

Alexandr M. Samofeev – Postgraduate Student of the Department of non-ferrous metallurgy (NFM) of Ural Federal University n.a. the First President of Russia B.N. Yeltsin (UrFU); Deputy General Director for research and science of LLC "Berezovsky Rudnik".
https://orcid.org/0009-0000-0797-0892
E-mail: alexander.samofeev@gmail.com

Vladimir G. Lobanov – Cand. Sci. (Eng.), Associate Professor, Department of NFM, UrFU.
https://orcid.org/0000-0001-6450-8434
E-mail: lobanov-vl@yandex.ru

Farit M. Nabiullin – General Director of LLC "Berezovsky Rudnik".
https://orcid.org/0009-0003-6557-0274
E-mail: info@ooobru.ru

Alexandr V. Tretyakov – Executive Director of LLC "Berezovsky Rudnik".
https://orcid.org/0009-0000-9853-3072
E-mail: info@ooobru.ru

Информация об авторах

Александр Михайлович Самофеев – аспирант кафедры металлургии цветных металлов (МЦМ), Уральский федеральный университет имени первого Президента России Б.Н. Ельцина (УрФУ); зам. ген. директора по исследовательской деятельности и науке, ООО «Березовский рудник».
https://orcid.org/0009-0000-0797-0892
E-mail: alexander.samofeev@gmail.com

Владимир Геннадьевич Лобанов – к.т.н., доцент кафедры МЦМ, УрФУ.
https://orcid.org/0000-0001-6450-8434
E-mail: lobanov-vl@yandex.ru

Фарит Минниахметович Набиуллин – ген. директор ООО «Березовский рудник».
https://orcid.org/0009-0003-6557-0274
E-mail: info@ooobru.ru

Александр Вительевич Третьяков – исп. директор ООО «Березовский рудник».
https://orcid.org/0009-0000-9853-3072
E-mail: info@ooobru.ru

Contribution of the authors

A.M. Samofeev – defined the objectives of the study, developed the main concept, conducted experiments, participated in the discussion of results, and wrote the manuscript.

V.G. Lobanov – provided scientific supervision, defined the objectives of the study, developed the main concept, participated in the discussion of results, and revised the text.

F.M. Nabiullin – formulated the research task, developed the main concept, provided resources, and participated in the discussion of results.

A.V. Tretyakov – defined the objectives of the study, developed the main concept, and participated in the discussion of results.

Вклад авторов

А.М. Самофеев – определение цели работы, формирование основной концепции, проведение экспериментов, участие в обсуждении результатов, написание статьи.

В.Г. Лобанов – научное руководство, определение цели работы, формирование основной концепции, участие в обсуждении результатов, корректировка текста.

Ф.М. Набиуллин – постановка задачи, формирование основной концепции, обеспечение ресурсами, участие в обсуждении результатов.

А.В. Третьяков – определение цели работы, формирование основной концепции, участие в обсуждении результатов.

The article was submitted 10.05.2025, revised 04.08.2025, accepted for publication 06.08.2025

Статья поступила в редакцию 10.05.2025, доработана 04.08.2025, подписана в печать 06.08.2025

METALLURGY OF RARE AND PRECIOUS METALS / МЕТАЛЛУРГИЯ РЕДКИХ И БЛАГОРОДНЫХ МЕТАЛЛОВ

UDC 66.082
https://doi.org/10.17073/0021-3438-2025-3-74-84

Research article
Научная статья

Investigation of the behavior of sodium dichloroisocyanurate in aqueous solutions

R.E. Khabibulina, E.B. Kolmachikhina, V.G. Lobanov, O.B. Kolmachikhina

Ural Federal University n.a. the First President of Russia B.N. Yeltsin
19 Mira Str., Ekaterinburg 620002, Russia

✉ Raisa E. Khabibulina (raisa.khabibulina@urfu.ru)

Abstract: Global gold consumption has steadily increased in recent decades, driven by expanding industrial applications and reserve accumulation by many countries. In parallel, depletion of high-grade deposits has shifted processing toward low-grade and refractory ores. These trends—together with tighter environmental regulations—highlight the need for alternative lixiviants for gold extraction. Although cyanide remains the industry standard, it is highly toxic and often ineffective for refractory sulfide ores. Other systems—thiosulfate (including ammoniacal thiosulfate), thiourea, and bromide/iodide lixiviants—are used far less frequently due to significant disadvantages. Among acidic chloride lixiviants, sodium dichloroisocyanurate (NaDCC) was investigated as a promising candidate. Use of NaDCC requires strongly acidic solutions (pH < 1.0) and an excess of Cl^-, i.e., conditions consistent with the stability domain of the Au(III) chloride complex ($AuCl_4^-$). Using the rotating-disk technique, we examined the effects of temperature, disk rotation rate, and HCl concentration on the specific dissolution rate of the reagent (NaDCC), as well as on solution pH and redox potential (Eh). NaDCC hydrolyzes in water to form hypochlorous acid (HClO)—the primary source of active chlorine—while the concurrent pH decrease arises from formation of weak acids (hypochlorous and cyanuric). Adding HCl to NaDCC solutions generates molecular chlorine (Cl_2), which evolves once its solubility limit is exceeded. Gold-dissolution tests across NaDCC and HCl concentrations identified an optimum at [HCl] = 14.4 g/dm^3 and [NaDCC] = 3.0 g/dm^3, yielding a maximum gold dissolution rate of $\upsilon_{Au} = 0.118$ mg/(cm^2·min).

Keywords: sodium dichloroisocyanurate (NaDCC), cyanuric acid, hydrochloric acid, rotating-disk, gold leaching, dissolution.

Acknowledgments: This research was supported by the Russian Science Foundation grant, Project No. 25-29-00787,No. 25-29-00787, https://rscf.ru/project/25-29-00787/

For citation: Khabibulina R.E., Kolmachikhina E.B., Lobanov V.G., Kolmachikhina O.B. Investigation of the behavior of sodium dichloroisocyanurate in aqueous solutions. *Izvestiya. Non-Ferrous Metallurgy.* 2025;31(3):74–84.
https://doi.org/10.17073/0021-3438-2025-3-74-84

Изучение поведения дихлоризоцианурата натрия в водных растворах

Р.Э. Хабибулина, Э.Б. Колмачихина, В.Г. Лобанов, О.Б. Колмачихина

Уральский федеральный университет имени первого Президента России Б.Н. Ельцина
Россия, 620002, г. Екатеринбург, ул. Мира, 19

✉ Раиса Энверовна Хабибулина (raisa.khabibulina@urfu.ru)

Аннотация: В последние десятилетия мировое потребление золота стабильно повышается, что обусловлено его возрастающей ролью как промышленного металла и стремлением накопления многими странами золотых резервов. Одновременно с этим наблюдается истощение золотосодержащих месторождений, что ведет к вовлечению в переработку бедных и упорных руд. Такое

изменение сырьевой базы и усиление экологических требований к металлургическому производству делает очень актуальной задачей поиск новых реагентов для выщелачивания золота. Традиционно используемые для этой цели цианистые растворы имеют высокую токсичность и низкую эффективность при выщелачивании золота из упорных и сульфидных руд. Прочие растворители – тиосульфатные и аммиачно-тиосульфатные растворы, тиомочевина, бромиды и йодиды, используются гораздо реже, так как имеют целый ряд существенных недостатков. Вариантом эффективного альтернативного реагента для выщелачивания золота из различного сырья могут стать хлоридные растворители, например дихлоризоцианурат натрия (ДЦН). Его использование предполагает кислый характер раствора pH < 1,0 и избыток Cl^--ионов. Поэтому для практического применения ДЦН при гидрометаллургической переработке золотосодержащих материалов необходимо изучение поведения данного реагента в условиях, соответствующих области существования хлоридного комплекса золота (III). Эксперименты проводили методом вращающегося диска. Исследовали влияние температуры, скорости вращения диска, концентрации соляной кислоты на удельную скорость растворения ДЦН, величину pH и окислительно-восстановительный потенциал растворов. Установлено, что при растворении ДЦН в воде происходит его гидролиз с образованием хлорноватистой кислоты (HClO), которая служит основным источником активного хлора. Сопровождающееся при этом снижение pH связано с образованием слабых кислот – хлорноватистой и циануровой. Введение соляной кислоты в водный раствор ДЦН приводит к образованию молекулярного хлора, который при достижении своей предельной растворимости переходит в газообразное состояние. Проведены экспериментальные исследования по определению скорости растворения золота при различных концентрациях ДЦН и соляной кислоты. Установлено, что при C_{HCl} = 14,4 г/дм^3 и $C_{ДЦН}$ = 3,0 г/дм^3 достигается максимальная скорость растворения υ_{Au} = 0,118 мг/(см^2·мин).

Ключевые слова: дихлоризоцианурат натрия (ДЦН), циануровая кислота, соляная кислота, вращающийся диск, растворение, золото.

Благодарности: Исследование выполнено за счет гранта Российского научного фонда № 25-29-00787, https://rscf.ru/project/25-29-00787/

Для цитирования: Хабибулина Р.Э., Колмачихина Э.Б., Лобанов В.Г., Колмачихина О.Б. Изучение поведения дихлоризоцианурата натрия в водных растворах. *Известия вузов. Цветная металлургия*. 2025;31(3):74–84. https://doi.org/10.17073/0021-3438-2025-3-74-84

Introduction

Global gold consumption has risen from about 3500 to nearly 5000 t/year over the past two decades [1], driven by its expanding use in electronics and its role as an investment asset under conditions of economic instability. Approximately 90 % of gold is produced by the cyanidation process, which remains an effective and economical method for extracting the metal from both primary and secondary resources [2]. However, cyanide is associated with severe drawbacks: high biological toxicity, excessively long leaching times, and poor efficiency in the treatment of refractory and sulfide ores. Gold-mining operations have also been implicated in major environmental accidents caused by cyanide spills into surface waters — for example, in Russia (2014, 2019), Canada (2024), Mexico (2018), Papua New Guinea (2000), and Kyrgyzstan (1998, 2021). These risks underscore the urgent need to identify alternative lixiviants for gold in order to minimize the environmental impact of Au-bearing material processing [3].

It is well established that gold leaching requires the simultaneous presence of a complexing agent and an oxidant. Among cyanide-free complexing systems for gold, the most studied are based on inorganic reagents: thiosulfate, ammoniacal thiosulfate, thiourea, chloride, iodide, and bromide solutions [4—6]. In addition, a wide range of organic compounds have been proposed as potential gold lixiviants, including humic substances and amino acids (glycine, alanine, valine, aspartic acid, phenylalanine, asparagine, cysteine, etc.), malononitrile, β-hydroxynitriles, potassium tricyanomethanid, calcium cyanamide, dibromodimethylhydantoin, and dimethyl sulfoxide [7—10].

The use of halogen-based solutions, particularly those containing chlorine, dates back to the Middle Ages [11]. Halogen leaching systems combine the dual functions of oxidant and complexing agent [12]. Table 1 summarizes reported gold dissolution rates in halide media together with the corresponding operating conditions. Chloride systems — including chlorine, hypochlorous acid, hypochlorites, and iron or copper chlorides — have demonstrated high effectiveness for dissolving gold. Thermodynamically, chlorine and hypochlorous acid have relatively high standard potentials (E^0 = 1.36÷1.49 V), compared with iodides (E^0 = 0.54 V) and bromides (E^0 = 1.1 V). The $[AuCl_4]^-$ complex is stable in the presence of excess chloride ions.

Table 1. **Properties of halide-based gold lixiviants**

Таблица 1. Свойства растворителей золота на основе галогенидов

Process type	Gold dissolution rate, mg/(m^2·s)	Conditions	Advantages	Disadvantages	Ref.
Hydrochlorination with OCl^-	36.1	[NaCl] = 100 g/dm^3 [OCl^-] = 10 g/dm^3 pH = 6	• High dissolution rate • Applicable to a variety of feed materials • Wide choice of oxidants	• High corrosivity • Requires maintaining low pH	[13]
Chloride leaching with $FeCl_3$	143.8	[$FeCl_3$] = 27.9 g/dm^3 [NaCl] = 141.8 g/dm^3 pH ≈ 1.0 t = 95 °C	• High dissolution rate • Reagents are readily available	• Requires elevated temperature • Possible $Fe(OH)_3$ formation • Narrow pH range	[14]
Bromide leaching	19.7	[Br^-] = 2 g/dm^3 pH = 4 t = 25 °C	• High dissolution rate • Applicable to a variety of feed materials	• High corrosivity • High lixiviant consumption • Complicated gold recovery from solution • Surface passivation • Process control difficulties	[15]
Iodide leaching	6.6	[NaI] = 1.5 g/dm^3 [I_2] = 1.27 g/dm^3 pH = 4÷6 t = 23 °C	• Effective for refractory and sulfide ores • Lixiviants can be regenerated • Low corrosivity	• High lixiviant consumption • Instability of iodides • Process control difficulties • Solution instability • Impurity sensitivity • Low gold dissolution rate	[16]

Chlorine-containing reagents, unlike bromine and iodine, are inexpensive, widely produced, and less hazardous when handled under standard safety protocols. By contrast, bromide- and iodide-based systems are more demanding in terms of storage and handling and are considerably more costly, which limits their large-scale industrial application.

The chlorination process is highly versatile and enables the recovery of gold from mineral feed of almost any composition [17]. An important advantage of this technology is its suitability for comprehensive processing, allowing not only gold but also other valuable metals, such as the platinum-group metals, to be recovered [18—20].

A key requirement for effective chloride leaching of gold is the presence of an oxidant with high redox potential that remains stable under leaching conditions (pH, temperature, solution composition). The oxidants most commonly employed in hydrochlorination and chloride leaching include chlorine gas, hypochlorous acid (HClO), hypochlorites, ferric iron, and cupric copper [21—23]. To enhance the efficiency of gold

leaching, particular attention has been given to oxidants capable of generating active chlorine directly in solution. Among such reagents are chlorine-containing organic compounds, such as trichloroisocyanuric acid (TCCA, $C_3N_3O_3Cl_3$) and sodium dichloroisocyanurate (NaDCC, $C_3Cl_2N_3O_3Na$). These substances are derivatives of cyanuric acid and act as oxidants and sources of active chlorine widely used in sanitation and water treatment.

Studies [24—27] on the application of TCCA to Au-bearing materials confirm its high effectiveness. NaDCC can likewise serve as a controlled and environmentally safer oxidative medium for gold dissolution in chloride systems. However, NaDCC has been much less studied as a gold lixiviant, even though its dissolution rate is somewhat higher and its working pH range is broader than those of TCCA [28]. Moreover, unlike TCCA, NaDCC is less susceptible to degradation by moisture and elevated temperatures during long-term storage, which is a critical factor for gold-mining operations in remote regions [29].

Our earlier work [30; 31] on hydrochlorination of oxidized Au-bearing ore with NaDCC addition demonstrated higher dissolution rates and more complete gold recovery compared with conventional cyanidation. We also identified process parameters that allow recovery of over 90 % of gold from a gravity concentrate [32]. At present, however, no data are available on how process conditions affect the dissolution rate of NaDCC, its speciation in solution, or changes in solution redox potential (Eh).

The present study addresses the influence of temperature, initial hydrochloric acid concentration, and disk rotation speed on the dissolution rate of NaDCC, as well as the effects of hydrochloric acid and oxidant (NaDCC) concentrations on the rate of gold dissolution.

Experimental procedure

The experiments employed tablets ("Altaykhimia" LLC, Russia) containing 84 % sodium dichloroisocyanurate (NaDCC) and reagent-grade hydrochloric acid. Dissolution tests were carried out using the rotating-disk technique with the setup shown in Fig. 1. A 26-mm-diameter tablet was fixed in a holder made of inert material and mounted on a top-driven stirrer. The reactor was charged with 50 mL of aqueous solution, sealed, and heated to the desired temperature using a heating mantle. The tablet holder was then immersed in the reactor and stirring was initiated. During the experiments,

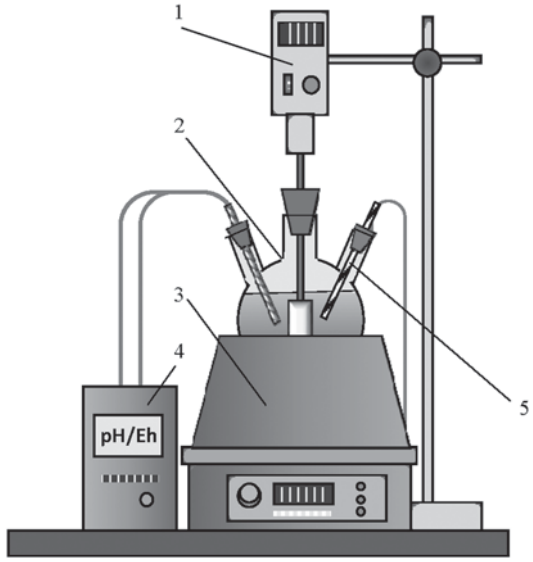

Fig. 1. Experimental setup for studying NaDCC dissolution

1 – top-driven stirrer with disc; ***2*** – three-neck flask with solution; ***3*** – heating mantle; ***4*** – pH meter; ***5*** – temperature probe

Рис. 1. Установка для изучения растворения ДЦН

1 – верхнеприводная мешалка с диском; ***2*** – трехгорлая колба с раствором; ***3*** – колбонагреватель; ***4*** – pH-метр; ***5*** – термодатчик

the temperature was automatically maintained within ±2 °C, and the solution pH and redox potential (Eh) were monitored with a pH-410 meter (Aquilon JSC, Russia). Tablet mass loss was determined by weighing before and after each test.

The effects of temperature (25—70 °C), disk rotation speed (50—900 rpm), and initial HCl concentration ([HCl] = 0.1÷30 g/dm^3) on the specific dissolution rate of NaDCC (υ_{NaDCC}), solution pH, and redox potential (Eh) were investigated. The effect of NaDCC concentration ([NaDCC] = 0.5÷10 g/dm^3) on pH and Eh of aqueous solutions was also determined. The dissolved mass of NaDCC (m_{NaDCC}) was calculated based on its content in the tablet. The specific dissolution rate was determined from equation

$$\upsilon_{NaDCC} = \frac{m_{\tau\,NaDCC}}{\tau S}, \qquad (1)$$

where $m_{\tau NaDCC}$ is the mass of NaDCC dissolved during time τ, mg; τ is the test duration, min; S = 5.31 cm^2 is the disk surface area.

Gold dissolution in NaDCC solutions was studied using the rotating-disk technique. A 10-mm-diameter disk of metallic gold (99.9 %) was mounted in a holder made of inert material. Prior to each experi-

ment, the disk surface was polished with GOI polishing paste (chromium oxide—based), rinsed with ethanol and distilled water, and dried in air. Leaching tests were carried out in 50 mL of solution at 25 °C and 300 rpm. The effects of [NaDCC] (1—5 g/dm^3) and [HCl] (0—21.6 g/dm^3) on the gold dissolution rate were evaluated. After each experiment, the solution was filtered and analyzed by atomic absorption spectrometry (novAA 300, Analytik Jena, Germany) at a wavelength of 242.8 nm. The specific gold dissolution rate was calculated from equation

$$\upsilon_{Au} = \frac{C_{Au}V}{S\tau}, \quad (2)$$

where C_{Au} is the gold concentration in solution, mg/dm^3; V is the solution volume, dm^3; S is the disk surface area, cm^2; τ is the test duration, min.

All experiments were conducted in triplicate under identical conditions, with deviations between parallel measurements not exceeding 5 %.

Results and discussion

Sodium dichloroisocyanurate (NaDCC) undergoes dissociation and hydrolysis upon contact with water, yielding cyanuric acid ($C_3H_3N_3O_3$), hypochlorous acid (HClO), and sodium hydroxide (NaOH). The overall reaction can be represented as:

$$NaC_3Cl_2N_3O_3 + 3H_2O = $$
$$= C_3H_3N_3O_3 + 2\,HClO + NaOH. \quad (3)$$

According to reaction (3), sodium hydroxide is formed as a product. In practice, however, the observed decrease in solution pH (Fig. 2, *a*) is due to the accumulation of weak acids — hypochlorous and cyanuric — which partially dissociate and increase the hydrogen ion concentration. Furthermore, hypochlorous acid may undergo disproportionation with H^+ release, further acidifying the medium.

Owing to the high standard redox potential of hypochlorous acid, NaDCC dissolution resulted in an increase in solution Eh to 1000—1180 mV and a decrease in pH to 3.7—2.7 at [NaDCC] = 1÷10 g/dm^3 (Fig. 2). Cyanuric acid did not directly affect Eh but stabilized Cl-containing species and acted as a buffer.

The high redox potential of aqueous NaDCC solutions suggests that it can be applied for gold dissolution in chloride media. It is well established that gold oxidation in hydrochloric acid solutions begins at solution Eh values above 1000—1200 mV

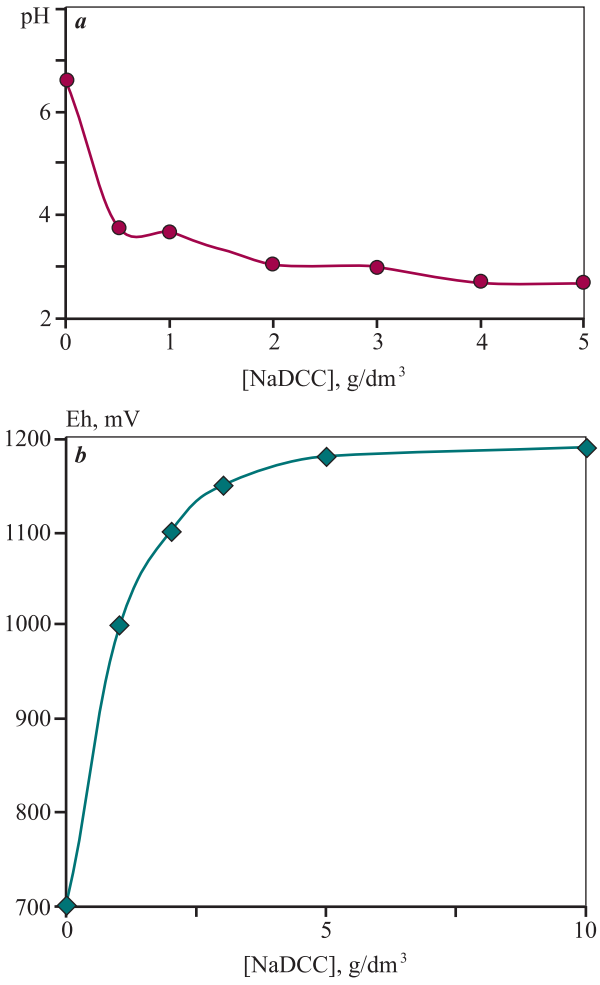

Fig. 2. Effect of sodium dichloroisocyanurate concentration on pH (***a***) and redox potential (Eh) (***b***) of aqueous solution

Рис. 2. Влияние концентрации дихлоризоцианурата натрия на pH (***a***) и ОВП (***b***) водного раствора

(Fig. 3). In chlorine-chloride systems, NaDCC serves as a source of active chlorine, thereby acting as the oxidant.

NaDCC dissolution with the release of active chlorine in water and weakly acidic solutions occurs slowly, что хорошо синхронизируется с растворением золота. The gold chloride complex $[AuCl_4]^-$ is less stable than the cyanide complex $[Au(CN)_2]^-$, with stability constants (lgβ) of 26 and 38.3, respectively [1]. To ensure the stability of the gold chloride complex, pH values below 1.0 and an excess of chloride ions are required [1]. Therefore, for practical application of NaDCC in hydrometallurgical processing of Au-bearing materials, it is necessary to study the behavior of this oxidant under conditions corresponding to the stability region of the Au(III) chloride complex.

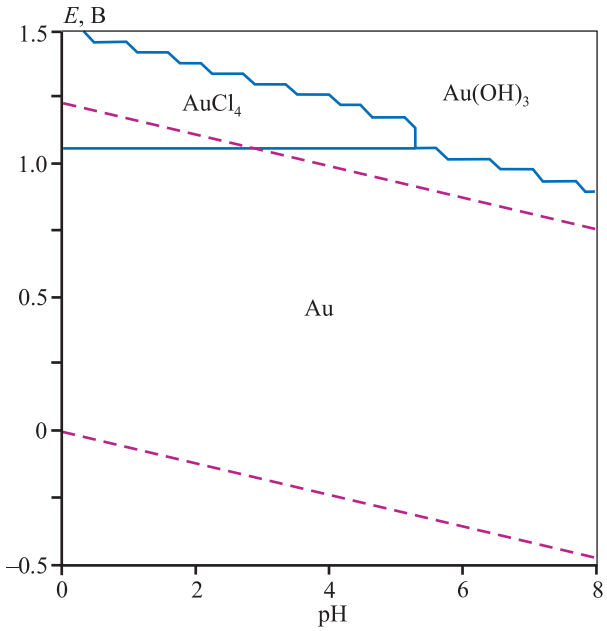

Fig. 3. Pourbaix diagram for the Au–Cl–H_2O system
[Cl] = 0.5 M, [Au] = $1 \cdot 10^{-5}$ M, ionic strength – 0.5 M,
t = 25 °C
Diagram generated using the Medusa–Hydra software

Рис. 3. Диаграмма Пурбе для системы Au–Cl–H_2O
[Cl] = 0,5 М, [Au] = $1 \cdot 10^{-5}$ М, ионная сила раствора – 0,5 М,
t = 25 °C
Диаграмма построена с применением программы
Medusa-Hydra

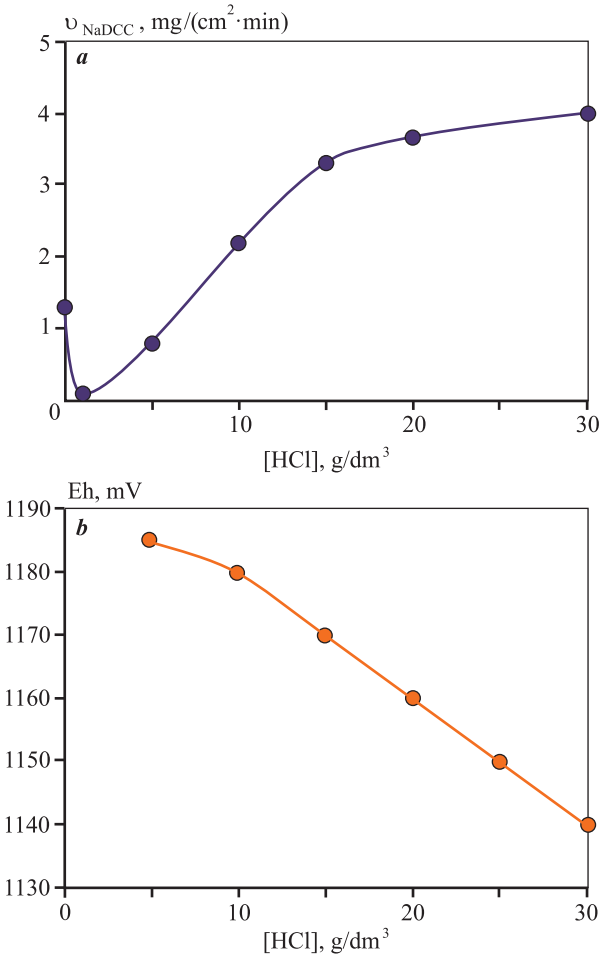

Fig. 4. Effect of hydrochloric acid concentration on the dissolution rate of NaDCC (***a***) and solution redox potential (Eh) (***b***) at [NaDCC] = 3 g/dm^3, t = 25 °C

Рис. 4. Влияние концентрации соляной кислоты на скорость растворения ДЦН (***a***) и величину ОВП водных растворов (***b***) при $C_{ДЦН}$ = 3 г/дм^3, t = 25 °C

Under such conditions, reactions involving NaDCC and hypochlorous acid occur with the release of chlorine gas:

$$NaC_3Cl_2N_3O_3 + 3HCl = C_3H_3N_3O_3 + 2Cl_2\uparrow + NaCl, \quad (4)$$

$$HClO + HCl = Cl_2\uparrow + H_2O. \quad (5)$$

Molecular chlorine is readily soluble in aqueous solutions (0.63 g/100 g water at 25 °C [33]). Once the solubility limit is reached, chlorine escapes to the atmosphere.

As seen from the data (Fig. 4, *a*), the dissolution rate of NaDCC initially decreased with the addition of small amounts of HCl, but began to rise again once [HCl] reached 1 g/dm^3. Notably, at [HCl] = = 1÷5 g/dm^3 the dissolution rate was lower than in pure water, amounting to 0.1—0.8 mg/(cm^2·min), while a further increase in [HCl] up to 30 g/dm^3 enhanced the rate to 4 mg/(cm^2·min). The most probable explanation for this behavior is diffusion limitation. It has been reported [34] that trichloroisocyanuric acid has low solubility (0.7 %), and during NaDCC dissolution it can precipitate on the tablet surface, forming a diffusion barrier. The subsequent increase in υ_{NaDCC} at higher [HCl] (>5—10 g/dm^3) is associated with the decomposition of trichloroisocyanuric acid, accompanied by intensive release of gaseous chlorine and formation of cyanuric acid.

The key parameter of this system in relation to gold dissolution is the solution redox potential. Adding HCl to an aqueous NaDCC solution ([NaDCC] = = 3 g/dm^3) increased Eh from 1150 mV at [HCl] = = 0 to 1185 mV at [HCl] = 5 g/dm^3 (Fig. 4, *b*). Across the full [HCl] range studied, further acid addition led to a gradual decrease in Eh to 1140 mV at [HCl] = = 30 g/dm^3. Although thermodynamically, an increase

in proton concentration should raise the Eh of the HClO/Cl^- couple, the excess hydrochloric acid promotes decomposition of NaDCC and hypochlorous acid according to reactions (4) and (5), producing molecular chlorine. Since Cl_2 has a lower redox potential ($E^0_{Cl_2/Cl^-}$ = +1.36 V) than hypochlorous acid (E^0_{HClO/Cl^-} = +1.49 V) the overall result is a reduction in the concentration of active oxidants and a corresponding decrease in solution Eh.

At [HCl] = 15 g/dm^3, the dissolution rate of NaDCC increased exponentially with temperature from 2.81 to 13.61 mg/(cm^2·min) over the range 25—70 °C (Fig. 5 , *a*). The $\upsilon_{NaDCC} = f(t)$ curve can be divided into two regions: the first between 25—45 °C, and the second between 45—70 °C. In the lower range, the dissolution rate increased by 0.133 mg/(cm^2·min) per °C, while in the higher range the increment was 0.326 mg/(cm^2·min) per °C. The acceleration of NaDCC dissolution at elevated temperatures can be attributed to several factors:

— enhanced decomposition of hypochlorous acid with Cl_2 formation and reduced solubility of Cl_2, shifting reactions (4) and (5) to the right;

— increased solubility of cyanuric acid, which at moderate temperatures tends to passivate the reactive surface [7].

When the disk rotation speed was increased from 50 to 900 rpm, the dissolution rate of NaDCC rose from 0.8 to 5.3 mg/(cm^2·min) at [HCl] = 15 g/dm^3 (Fig. 5, *b*), consistent with enhanced mass transfer at the solid—liquid interface. Thus, NaDCC solutions in the presence of hydrochloric acid exhibit high Eh values, confirming their potential as alternative oxidants for gold leaching.

The next stage examined the effect of [HCl] and [NaDCC] on the gold dissolution rate (υ_{Au}). The results are given in Table 2. In pure aqueous NaDCC solutions, only a small amount of gold entered solution at [NaDCC] = 3÷5 g/dm^3, with υ_{Au} = 0.001÷÷0.051 mg/(cm^2·min). Increasing [HCl] from 1.44 to 14.4 g/dm^3 at constant [NaDCC] enhanced gold dissolution. For instance, at [HCl] = 1.44 g/dm^3, υ_{Au} increased from 0.018 to 0.052 mg/(cm^2·min) as [NaDCC] rose from 1 to 5 g/dm^3, respectively. At higher acid concentration ([HCl] = 21.6 g/dm^3), the gold dissolution rate declined to 0.05—0.08 mg/(cm^2·min). The

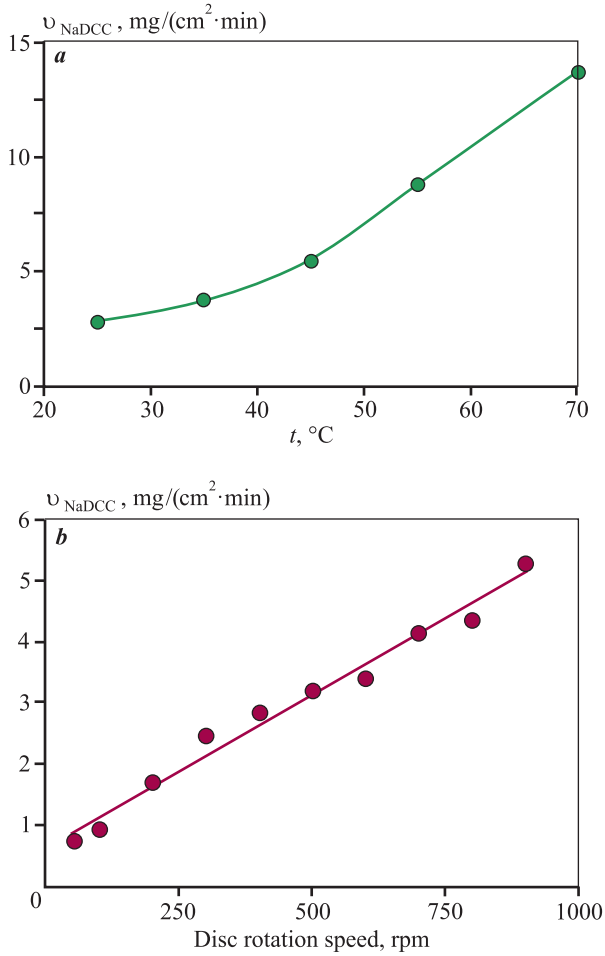

Fig. 5. Effect of temperature (***a***) and disc rotation speed (***b***) on the dissolution rate of NaDCC in hydrochloric acid solutions ([HCl] = 15 g/dm^3)

Рис. 5. Влияние температуры (***a***) и скорости вращения диска (***b***) на скорость растворения ДЦН в растворах соляной кислоты (C_{HCl} = 15 г/дм^3)

Table 2. **Effect of HCl and NaDCC concentrations on the gold dissolution rate (*n* = 300 rpm, *t* = 25 °C, *r* = 5 mm)**

Таблица 2. Влияние концентраций HCl и ДЦН на скорость растворения золотого диска (*n* = 300 об/мин, *t* = 25 °C, *r* = 5 мм)

[HCl], g/dm^3	υ_{Au}, mg/(cm^2·min) at [NaDCC], g/dm^3		
	1	*3*	*5*
0	0.000	0.001	0.051
1.44	0.018	0.022	0.052
7.2	0.034	0.062	0.079
14.4	0.108	0.118	0.101
21.6	0.049	0.085	0.083

maximum rate was achieved at [HCl] = 14.4 g/dm^3 and [NaDCC] = 3 g/dm^3.

We attribute the intensification of gold dissolution at [HCl] = 1.44÷14.4 g/dm^3 to the increased concentration of chloride ions, which act as complexing agents. The subsequent decline in dissolution rate at [HCl] > > 14.4 g/dm^3 may indicate reduced stability of HClO and its non-productive decomposition to Cl_2 with volatilization, as well as surface passivation by intermediate species.

Conclusions

It was established that aqueous NaDCC solutions exhibit high redox potential due to the release of hypochlorous acid during dissolution, while the addition of hydrochloric acid accelerates NaDCC dissolution and promotes the evolution of gaseous chlorine.

1. At [HCl] = 1÷5 g/dm^3, the NaDCC dissolution rate is lower than in pure water, which is attributed to the formation of dichloroisocyanuric acid.

2. Increasing the hydrochloric acid concentration enhances the NaDCC dissolution rate, reaching ~4 mg/(cm^2·min) at [HCl] = 30 g/dm^3.

3. Adding HCl to aqueous NaDCC raises solution Eh from 1150 mV at [HCl] = 0 to 1185 mV at [HCl] = = 5 g/dm^3; however, a further increase to 30 g/dm^3 decreases Eh to 1140 mV, owing to decomposition of both NaDCC and hypochlorous acid.

4. At [HCl] = 15 g/dm^3 and T = 25÷70 °C, the NaDCC dissolution rate increased exponentially from 2.81 to 13.61 mg/(cm^2·min).

5. Raising disk rotation speed from 50 to 900 rpm resulted in a linear increase in NaDCC dissolution rate, reflecting enhanced mass transfer at the reaction surface.

6. The maximum gold dissolution rate (υ_{Au} = = 0.118 mg/(cm^2·min)) was observed at [NaDCC] = = 3 g/dm^3 and [HCl] = 14.4 g/dm^3. At higher HCl concentrations, however, dissolution efficiency declined, requiring further investigation.

7. The findings confirm the potential of sodium dichloroisocyanurate combined with hydrochloric acid as an environmentally safer alternative to cyanide systems for processing Au-bearing materials.

References

1. Filippov A.P., Nesterov Yu.V. Redox processes and intensification of metal leaching. Moscow: Publishing house “Ruda i Metally”, 2009. 543 p. (In Russ.).
Филиппов А.П., Нестеров Ю.В. Редокс-процессы и интенсификация выщелачивания металлов. М.: ИД «Руда и Металлы», 2009. 543 с.
2. Barani K., Kogani Y., Nazarian F. Leaching of complex gold ore using a cyanide-glycine solution. *Minerals Engineering.* 2022;180:107475. https://doi.org/10.1016/j.mineng.2022.107475
3. Logsdon M.J., Hagelstein K., Mudder, T.I. The Management of cyanide in gold extraction. Ottawa: International Council on Metals and the Environment, 1999. 40 p.
4. Birich A., Stopic S., Friedrich B. Kinetic investigation and dissolution behavior of cyanide alternative gold leaching reagents. *Scientific Reports.* 2019;9(1):7191. https://doi.org/10.1038/s41598-019-43383-4
5. Hilson G., Monhemius A.J. Alternatives to cyanide in the gold mining industry: what prospects for the future? *Journal of Cleaner Production*. 2006; 14(12-13):1158—1167. https://doi.org/10.1016/j.jclepro.2004.09.005
6. Kholov Kh.I., Sharifboev N.T., Samikhov Sh.R., Dzhurakulov Sh.R., Zarifova M.S. Gold leaching by various solutions, alternative of cyanide and their prospects in the future. *Zhurnal Sibirskogo federal’nogo universiteta. Seriya: Tekhnika i tekhnologii.* 2021;14(4):433—447. (In Russ.). https://doi.org/10.17516/1999-494X-0324
Холов Х. И., Шарифбоев Н. Т., Самихов Ш. Р., Джуракулов Ш.Р., Зарифова М.С. Выщелачивание золота различными растворами, заменители цианида и их перспективы в будущем. *Журнал Сибирского федерального университета. Серия: Техника и технологии.* 2021;14(4):433—447. https://doi.org/10.17516/1999-494X-0324
7. Merck I., O’Neil, Ann Smith. The Merck index: An encyclopedia of chemicals, drugs, and biologicals. 13th ed. NJ: Whitehouse Station, 2001. 2564 p.
8. Vlassopoulos D., Wood S.A., Mucci A. Gold speciation in natural waters: II. The importance of organic complexing—experiments with some simple model ligands. *Geochimica et Cosmochimica Acta.* 1990;54(6):1575—1586. https://doi.org/10.1016/0016-7037(90)90392-X
9. Perea C.G., Restrepo O.J. Use of amino acids for gold dissolution. *Hydrometallurgy.* 2018;177:79—85. https://doi.org/10.1016/j.hydromet.2018.03.002
10. Brown D.H., Smith W.E., Fox P., Sturrock R.D. The reactions of gold (0) with amino acids and the significance

of these reactions in the biochemistry of gold. *Inorganica Chimica Acta*. 1982;67:27—30. https://doi.org/10.1016/S0020-1693(00)85035-5

11. Marsden J., House I. The chemistry of gold extraction. 2nd ed. Littleton, Colorado, USA: Society for Mining, Metallurgy, and Exploration, 2006. 138 p. https://doi.org/10.1007/BF03215543
12. Sadia Ilyas, Jae-chun Lee. Gold metallurgy and the environment. 1st ed. Boca Raton, FL: Environmental Science, Geology, 2018. 232 p.
13. Nam K.S., Jung B.H., An J.W., Ha T.J., Tran T., Kim M.J. Use of chloride—hypochlorite leachants to recover gold from tailing. *International Journal of Mineral Processing*. 2008;86(1-4):131—140. https://doi.org/10.1016/j.minpro.2007.12.003
14. Seisko S., Lampinen M., Aromaa J., Laari A., Koiranen T., Lundström M. Kinetics and mechanisms of gold dissolution by ferric chloride leaching. *Minerals Engineering*. 2018;115:131—141. https://doi.org/10.1016/j.mineng.2017.10.017
15. Pesic B., Sergent R.H. A rotating disk study of gold dissolution by bromine. *JOM*. 1991;43(12):35—37. https://doi.org/10.1007/BF03223146
16. Qi P.H., Hiskey J.B. Dissolution kinetics of gold in iodide solutions. *Hydrometallurgy*. 1991;27(1):47—62. https://doi.org/10.1016/0304-386X(91)90077-Y
17. Ojeda M.W., Perino E., Ruiz M.C. Gold extraction by chlorination using a pyrometallurgical process. *Minerals Engineering*. 2009;22(4):409—411. https://doi.org/10.1016/j.mineng.2008.09.002
18. Dosmukhamedov N., Kaplan V., Zholdasbay E., Argyn A., Kuldeyev E., Koishina G., Tazhiev Y. Chlorination treatment for gold extraction from refractory gold-copper-arsenic-bearing concentrates. *Sustainability*. 2022; 14(17):11019. https://doi.org/10.3390/su141711019
19. Yakoumis I., Panou M., Moschovi A.M., Panias D. Recovery of platinum group metals from spent automotive catalysts: A review. *Cleaner Engineering and Technology*. 2021;3:100112. https://doi.org/10.1016/j.clet.2021.100112
20. Puvvada G.V.K., Sridhar R., Lakshmanan V.I. Chloride metallurgy: PGM recovery and titanium dioxide production. *JOM*. 2003;55(8):38—41. https://doi.org/10.1007/s11837-003-0103-1
21. Baghalha M. Leaching of an oxide gold ore with chloride/hypochlorite solutions. *International Journal of Mineral Processing*. 2007;82(4):178—186. https://doi.org/10.1016/j.minpro.2006.09.001
22. Rinne M., Elomaa H., Seisko S., Lundstrom M. Direct cupric chloride leaching of gold from refractory sulfide ore: process simulation and life cycle assessment. *Mineral Processing and Extractive Metallurgy Review*. 2022;43(5):598—609. https://doi.org/10.1080/08827508.2021.1910510
23. Karppinen A., Seisko S., Nevatalo L., Wilson B.P., Yliniemi K., Lundström M. Gold recovery from cyanidation residue by chloride leaching and carbon adsorption — preliminary results from CICL process. *Hydrometallurgy*. 2024;226:106304. https://doi.org/10.1016/j.hydromet.2024.106304
24. Niu H., Yang H., Tong L. Research on gold leaching of carbonaceous pressure-oxidized gold ore via a highly effective, green and low toxic agent trichloroisocyanuric acid. *Journal of Cleaner Production*. 2023;419: 138062. https://doi.org/10.1016/j.jclepro.2023.138062
25. Feng F., Sun Y., Rui J., Yu L., Liu J., Zhang N., Zhao M., Wei L., Lu C., Zhao J., Zhang Q., Li X. Study of the "oxidation-complexation" coordination composite ionic liquid system for dissolving precious metals. *Applied Sciences*. 2020;10(10):3625. https://doi.org/10.3390/app10103625
26. Kenzhaliyev B., Koizhanova A., Surkova T., Fischer D., Azlan M.N., Atanova O., Magomedov D., Yerdenova M., Abdyldayev N. Extraction of gold from gravity-flotation concentrates via surfactant and oxidation reagents. *Discover Applied Sciences*. 2024;6(11):598. https://doi.org/10.1007/s42452-024-06281-7
27. Kenzhaliyev B.K., Tussupbayev N.K., Abdykirova G.Z., Koizhanova A.K., Fischer D.Y., Baltabekova Z.A., Samenova N.O. Evaluation of the efficiency of using an oxidizer in the leaching process of gold-containing concentrate. *Processes*. 2024;12(5):973. https://doi.org/10.3390/pr12050973
28. Zhang G., Huang Y., Xiong Z., Ge F., Li Y., Tan J., Zha R. Gold recovery from WPCB gold finger using water-soluble organic leaching agent sodium dichloroisocyanurate. *Sustainability*. 2025;17(6):2415. https://doi.org/10.3390/su17062415
29. Wahman D.G., Alexander M.T., Dugan A.G. Chlori-

nated cyanurates in drinking water: Measurement bias, stability, and disinfectant byproduct formation. *AWWA Water Science*. 2019;1(2):e1133. https://doi.org/10.1002/aws2.1133

30. Lobanov V.G., Naumov K.D., Kolmachikhina O.B., Makovskaya O.Yu., Khabibullina R.E., Kolmachikhina E.B. Method of extracting gold from gold-containing raw materials: Patent 2758915 (RF). 2021.
Лобанов В.Г., Наумов К.Д., Колмачихина О.Б., Маковская О.Ю., Хабибулина Р.Э., Колмачихина Э.Б. Способ извлечения золота из золотосодержащего сырья: Патент 2758915 (РФ). 2021.
31. Lobanov V.G., Khabibulina R.E., Kolmachikhina O.B., Makovskaia O.I. Selection of a leaching system for extraction gold from the Byngovskoe deposits ore. *iPolytech Journal*. 2022; 26(4):688—696. (In Russ.). https://doi.org/ 10.21285/1814-3520-2022-4-688-696
Лобанов В. Г., Хабибулина Р. Э., Колмачихина О. Б., Маковская О. Ю. Выбор выщелачивающей системы для извлечения золота из руды месторождения «Быньговское». *iPolytech Journal*. 2022; 26(4):688—696. https://doi.org/ 10.21285/1814-3520-2022-4-688-696
32. Khabibullina R. E., Lobanov V. G. Environmentally friendly technology of gold leaching from man-made raw materials. In: Actual problems of the development of technical sciences. Ekaterinburg: Ministry of Education and Youth Policy of the Sverdlovsk Region, 2021. P. 31–35. (In Russ.).
Хабибулина Р. Э., Лобанов В. Г. Экологически чистая технология выщелачивания золота из техногенного сырья. В сб: *Актуальные проблемы развития технических наук*. Екатеринбург: Министерство образования и молодежной политики Свердловской обл., 2021. С. 31—35
33. Whitney R.P., Vivian J.E. Solubility of chlorine in Water. *Industrial & Engineering Chemistry*. 1941;33(6):741—744. https://doi.org/10.1021/ie50378a014
34. Jacqueline I. Kroschwitz Kirk-Othmer encyclopedia of chemical technology. 5th ed. Wiley-Interscience, 2004. 896 p.

Information about the authors

Raisa E. Khabibulina – Graduate Student, Department of non-ferrous metallurgy, Ural Federal University n.a. the First President of Russia B.N. Yeltsin (UrFU).
https://orcid.org/0000-0002-2764-4434
E-mail: raisa.khabibulina@urfu.ru

Elvira B. Kolmachikhina – Cand. Sci. (Eng.), Department of non-ferrous metallurgy, UrFU.
https://orcid.org/0000-0002-6007-498X
E-mail: e.b.khazieva@urfu.ru

Vladimir G. Lobanov – Cand. Sci. (Eng.), Associate Professor, Department of non-ferrous metallurgy, UrFU.
https://orcid.org/0000-0001-6450-8434
E-mail: lobanov-vl@yandex.ru

Olga B. Kolmachikhina – Cand. Sci. (Eng.), Department of non-ferrous metallurgy, UrFU.
https://orcid.org/0000-0002-7879-8791
E-mail: o.b.kolmachikhina@urfu.ru

Информация об авторах

Раиса Энверовна Хабибулина – аспирант кафедры металлургии цветных металлов (МЦМ), Уральский федеральный университет имени первого Президента России Б.Н. Ельцина (УрФУ).
https://orcid.org/0000-0002-2764-4434
E-mail: raisa.khabibulina@urfu.ru

Эльвира Барыевна Колмачихина – к.т.н., доцент кафедры МЦМ, УрФУ.
https://orcid.org/0000-0002-6007-498X
E-mail: e.b.khazieva@urfu.ru

Владимир Геннадьевич Лобанов – к.т.н., доцент кафедры МЦМ, УрФУ.
https://orcid.org/0000-0001-6450-8434
E-mail: lobanov-vl@yandex.ru

Ольга Борисовна Колмачихина – к.т.н., доцент кафедры МЦМ, УрФУ.
https://orcid.org/0000-0002-7879-8791
E-mail: o.b.kolmachikhina@urfu.ru

Contribution of the authors

R.E. Khabibulina – conducted experiments, participated in the discussion of the results, prepared the manuscript.

E.B. Kolmachikhina – summarized experimental results, prepared the manuscript.

V.G. Lobanov – defined the aim of the work, summarized experimental results, prepared the manuscript.

O.B. Kolmachikhina – participated in the discussion of results, prepared the manuscript.

Вклад авторов

Р.Э. Хабибулина – проведение экспериментов, участие в обсуждении результатов, написание статьи.

Э.Б. Колмачихина – обобщение результатов экспериментов, написание статьи.

В.Г. Лобанов – определение цели работы, обобщение результатов экспериментов, написание статьи.

О.Б. Колмачихина – участие в обсуждении результатов, написание статьи.

The article was submitted 21.04.2025, revised 01.05.2025, accepted for publication 12.05.2025

Статья поступила в редакцию 21.04.2025, доработана 01.05.2025, подписана в печать 12.05.2025